Effective design of marine reserves: Incorporating alongshore currents, size structure, and uncertainty

Jody Reimer

Merton College

University of Oxford

A thesis submitted for the degree of

MSc by Research

Trinity 2013

This thesis is dedicated to
Wes and Sherril Reimer
for their careful selection of my childhood wallpaper.
Thank-you for starting me young.

Acknowledgements

I would like to express my gratitude to my advisors, Prof. Philip Maini and Dr. Michael Bonsall, for their support during this study and for achieving that elusive balance between fostering my independence as a researcher and ensuring that I didn't go too far awry. Thanks also to Mark Kot for his helpful correspondance on his foundational work. I also could not have completed this work without the financial support of the Rhodes Trust, and the Natural Sciences and Engineering Research Council of Canada.

Abstract

Effective design of marine reserves: Incorporating alongshore currents, size structure, and uncertainty

Jody Reimer, Merton College
MSc by Research, Trinity 2013

Marine populations worldwide are in decline due to anthropogenic effects [42, 119]. Spatial management via marine reserves may be an effective conservation method for many species, but the requisite theory is still underdeveloped [36]. Integrodifference equation (IDE) models can be used to determine the critical domain size required for persistence and provide a modelling framework suitable for many marine populations. Here, we develop a novel spatially implicit approximation for the proportion of individuals lost outside the reserve areas which consistently outperforms the most common approximation [113]. We examine how results using this approximation compare to the existing IDE results on the critical domain size for populations in a single reserve, in a network of reserves, in the presence of alongshore currents, and in structured populations. We find that the approximation consistently provides results which are in close agreement with those of an IDE model with the advantage of being simpler to convey to a biological audience while providing insights into the significance of certain model components.

We also design a stochastic individual based model (IBM) to explore the probability of extinction for a population within a reserve area. We use our spatially implicit approximation to estimate the proportion of individuals which disperse outside the reserve area. We then use this approximation to obtain results on extinction using two different approaches, which we can compare to the baseline IBM; the first approach is based on the Central Limit Theorem and provides efficient simulation results, and the second modifies a simple Galton-Watson branching process to include loss outside the reserve area. We find that this spatially implicit approximation is also effective in obtaining results similar to those produced by the IBM in the presence of both demographic and environmental variability. Overall, this provides a set of complimentary methods for predicting the reserve area required to sustain a population in the presence of strong fishing pressure in the surrounding waters.

Contents

Chapter 1

Introduction and establishment of an IDE framework

1.1 Ecological motivation

Marine ecosystems around the world are in crisis, as can be observed through the collapse of fisheries and severely depleted fish stocks [42]. A decade ago, it was estimated that at least half of the world's fishery stocks were either over-fished or fished to capacity, and the situation has not improved [86]. Industrialization of the fishing process has allowed for ever-increasing amounts of aquatic life to be harvested and the effects of this have been devastating for many species of commercial interest [79]. Extrapolating from past and present fisheries data, Worm et al. (2006) made a highly controversial prediction that by the year 2048, *all* taxa currently being fished will be extinct. If management of our oceans continues along the present path, there will be severe environmental, economic, and societal consequences for ecosystem stability, coastal water quality, and global food security [119].

Attempts to change or regulate human impact on fish stocks have taken many forms.

One management strategy is to implement a catch quota. The aim of this has typically been to allow fishermen to harvest only the *maximum sustainable yield* (MSY), which is defined as the largest yield that can be sustainably taken from a population. Other methods have included limiting the number of fishing vessels, placing restrictions on the type of equipment permitted, and implementing seasonal or regional fishing bans during important times in a key species' life history (for example, not allowing fishing that may interfere with spawning). Unfortunately, many of these efforts have seen low success rates, due to faulty estimations of what is a "sustainable" harvest, and the disregard of catch quotas by fishermen [8].

A conservation method for marine populations growing in popularity is that of marine protected areas (MPAs). Similar to terrestrial protected areas, MPAs can be divided into several broad classifications: those concerned with fisheries enhancement, ecosystem diversity, or special features such as cultural importance, a species' breeding ground, or the habitat of rare species [86]. Marine reserves, on which we will focus here, fall under the broader category of MPAs. While some MPAs may allow for seasonal fishing, recreational fishing, tourism, scientific research, or resource extraction, marine reserve restrictions are the most severe. Also known as "no-take zones", they are left completely without anthropogenic impact in order to allow the ecosystem to function as naturally as possible. These areas allow resident species to increase in both abundance and fecundity [43]. In the past few decades, reserves have become a popular management tool and data suggest that reserves achieve both conservation and fishery management goals [36].

While scientific reports on the effects of marine reserve creation offer a wide variety of results, nearly all of these results are positive [90]. Worm et al.'s study found that fishery closures and the creation of reserves resulted in increased species diversity

of both target and non-target species averaging a 23% increase in species richness. They also noted a fourfold average increase in catch per unit effort in fished areas around the reserves [119]. A comprehensive study carried out by the Partnership for Interdisciplinary Studies of Coastal Oceans has found that, as of 2010, there have been studies done on more than 150 marine reserves in over 60 countries. These studies monitored biological changes within the reserves and found that, on average, biomass increased 466%, density increased 166%, body size increased 28%, and the number of species increased an average of 21% inside a reserve [90]. Some studies found results as high as a 1000% increase in biomass inside reserves, generally where there had previously been very heavy fishing [90]. It is also interesting to note that, in general, biomass increases more than abundance inside reserves [86]. While much work remains to be done on quantifying the effects of marine reserves on previously exploited populations, it seems that reserves will play a large part in the future of fishery and marine ecosystem management.

There are several key design questions which are fundamental to the successful utilization of reserves as a conservation and management tool. Previously, reserves have often been designated on a somewhat *ad hoc* basis, and much remains to be explored in order to be able to use this tool most effectively. Where should reserves be placed? How big should individual reserves be? Is it more effective to have one large reserve or several small ones in a reserve network (in terrestrial systems, this is known as the "single large or several small" (SLOSS) problem)? How much area should a reserve network cover [36]?

Several studies have looked at qualitative methods of selecting which areas should be designated as marine reserves [29, 31, 91, 95, 96, 98], but this work will focus on the quantitative questions of sizing and spacing. Many useful terms and abbreviations

Benthic	Individuals who reside near the ocean floor
Pelagic	Individuals who reside in open water, near the surface
Recruit	Individual that has passed from the larval stage into reproductive maturity
Settlement	Process by which larvae leave the water column for the benthos in order to become juveniles
IDEs	Integrodifference equations
Critical domain size	Minimum habitat size required for species persistence
IMP models	Integrodifference matrix population models (an extension of IDEs to include size structure)
FNLS	Fraction of natural larval settlement
PDF	Probability density function
MGF	Moment-generating function
MVP	Minimum viable population
IBM	Individual-based model
iid random variables	Independent and identically distributed random variables
BPRE	Branching process in a random environment

Table 1.1: Useful terms and abbreviations used throughout this work, in the order in which they occur in the text.

used throughout this text can be found in Table 1.1.

Many fish and benthic (bottom-dwelling) invertebrates are relatively sedentary as adults but spend their time as larvae dispersing long distances during a pelagic (open water) phase. A dominant fraction, over 70%, of marine species have dispersing, planktonic larvae, with many of those species having comparatively sedentary adult lives [30, 56]. Species falling under this category include, among others, coral reef fish, most shellfish (e.g. abalone, scallops, and clams), the spiny lobster and many bottom dwelling fish [89]. It is species with these general life history characteristics which will be the target species of this work.

1.2 Modelling approaches

Attempts to model various aspects of marine reserve design have ranged from metapopulation models (examining distinct populations spatially separated but with degrees of connectivity between them) [35, 65, 115], bioeconomic models [37, 89, 100, 107], integrodifferential models [62], models using delay-differential equations [7] and, quite recently, even to individual-based models [72] and network structures [115]. The majority of modelling efforts have, however, been developed using systems of partial differential equations (PDEs) to represent populations changing in both space and time [63]. The earliest attempts to account for dispersal were modelled after diffusion processes using PDEs. A significant attempt came with the introduction of the nonlinear reaction-diffusion equation known as the Fisher-Kolmogoroff equation [26],

$$\frac{\partial u}{\partial t} = ru(1-u) + D\frac{\partial^2 u}{\partial x^2} \tag{1.2.1}$$

where $u(x,t)$ is the population density at location x and time t, and $r > 0$ and $D > 0$ are the population growth rate and diffusion coefficient, respectively [76]. This is the natural extension of the logistic growth model to a situation where a population disperses via linear diffusion.

For the purposes of looking at marine populations of the type considered here, we have chosen to use integrodifference equations (IDEs) instead of any of the above methods. While reaction-diffusion equations have shed much light on spatial population models, they assume that population growth happens simultaneously with diffusion, which is not the case for many marine species who spend their adult life in the benthic zone and only disperse during their pelagic stage, as larvae. IDEs use probability density functions to describe the movement of individuals during their dispersal phase. Reaction-diffusion models assume dispersal via diffusion, even for very

short time-scales, which may not be true of larval dispersal patterns which are often found to have more leptokurtic distributions over short sampling periods, with fatter tails and a more pronounced peak. Reaction-diffusion models also assume continuous reproduction and dispersal, whereas IDEs take into account the typically seasonal reproductive strategies of the species of interest [93]. A downside to several of the other model types mentioned is that these models are often no longer analytically tractable, so the results and sensitivity analyses are difficult to standardize, and provide little intuitive understanding of any mechanistic underpinnings or sensitivity to various factors [45].

1.3 Aims and objectives

In this work, we will use IDEs as our primary means of modelling the populations of interest. In the rest of this chapter, we provide the reader with a review of many of the main results on the critical domain size problem for IDEs. We take a comprehensive look at established results on the critical domain size of an IDE for a single reserve area, a network of reserves connected by larval dispersal, a population subject to alongshore currents, and finally to size- or stage-structured models. Unfortunately, many of these results can only be obtained in specific cases with very well-behaved dispersal patterns, and so we turn our attention to developing a more broadly applicable approximation in order to avoid the otherwise necessary computationally intensive numerics which prevent an understanding of the population's dependence on key parameters or comparison between kernels and growth functions.

In Chapter 2, we propose a spatially implicit approximation to an IDE, building on the ideas of Van Kirk and Lewis (1997) and their average dispersal success function. Unlike their approximation, we do not assume that the population is evenly

distributed throughout the reserve area, and thus obtain a modified dispersal success approximation to the proportion of individuals lost outside the reserve area to fishing pressure. In Sections 2.2 through 2.5, we compare the critical domain size predicted by this new approximation to that provided by an IDE, again for a single large reserve, then for a reserve network, for a population subject to a unidirectional current, and finally to structured populations. We find that the approximation consistently results in a critical domain size very similar to that of the IDE, and best outperforms the existing approximation of Van Kirk and Lewis (1997) for parameter values where their approximation performs most poorly. In the case where an alongshore current is present, we observe an interesting inability of our approximation to capture the "wash-out" behaviour of the IDE, and suggest some possible reasons for this.

In Chapter 3, we develop a series of stochastic models to examine the probability of extinction of the population, as we are dealing with populations initially at low density and well below the environmental carrying capacity. We first develop an intuitive stochastic analogue to an IDE in the form of an individual-based model (IBM). However, IBM simulations are computationally expensive, due to each individual's explicit spatial movement patterns, and so we again aim to create a spatially implicit approximation. The first attempt at this is to scale the model up to the level of the whole population using the Central Limit Theorem to obtain the average demographic and dispersal rates. This is computationally more efficient, but does not yield the kind of analytic understanding we are interested in. We thus turn to a Galton-Watson type branching process and modify it to include spatially implicit loss by dispersing individuals outside the reserve area where there is strong fishing pressure. We use this three-part approach first for models with only demographic stochasticity and then incorporate random environmental states. We again consistently find that the novel approximation for the proportion of individuals lost during the dispersal period

from Chapter 2 closely predicts the critical domain size as found by the baseline IBM model. We begin all of this by familiarizing the reader with IDEs and some resulting dynamical behaviours.

1.4 Integrodifference equations

A model based on IDEs assumes that population growth does not happen simultaneously with dispersal, which is appropriate for the populations represented here. We have chosen to use a discrete model, as many marine populations can best be described as having separate generations, with seasonally coordinated reproduction and development [93]. Thus in our model, one time step will typically represent one year. Due to the different spatial scales of movement of the pelagic larvae and sedentary adults, the continuous space and discrete time of IDEs provides a realistic modelling framework from which to explore the behaviour of the populations in question.

In the simplest instances, IDEs behave like reaction-diffusion equations. Indeed, the travelling wave speed of a simple IDE can be made identical to that of the Fisher-Kolmogoroff equation [26] if the IDE uses a Gaussian distribution for its dispersal kernel and a logistic growth function. In the event that the growth dynamics are over-compensatory (e.g. the Ricker growth model, see (A.0.2) in Appendix A), IDEs can exhibit behaviour far more complicated than Fisher-Kolmogoroff type models, such as periodic solutions or chaotic dynamics [48].

Initially used to model the propagation of gene alleles [104, 105], IDEs were first applied to population biology by Kot and Shaffer (1986). Since then, they have been studied for properties such as travelling wave solutions [41, 48, 49, 82, 116], dispersal-driven instability in predator-prey interactions [81], and the effects of differ-

ent dispersal strategies in both spatially and temporally varying habitats [39]. They have also been used to model shifting species ranges under climate change [120]. Much of this work has been done with regards to plant growth and dispersal [3, 13] and for marine populations [11]. Building on these results, Botsford et al. (2001) were the first to use IDEs specifically to address questions related to marine reserves and we will present some of their work in Section 2.1.

1.4.0.1 The basic IDE framework

Here we outline the conventional IDE framework (though see Lutscher (2008) for other possible formulations) in order to familiarize the reader with the basic assumptions and notation. We first consider the growth of a *non-spatial* population according to a function $f(N_t)$ where N_t is the density of the population at time $t \geq 0$. This will typically be a nonlinear function, and can often be written as $f(N_t) = N_t g(N_t)$, where $g(N_t)$ is the per capita growth rate. For a population modelled in discrete time with no movement,

$$N_{t+1} = f(N_t) = N_t g(N_t), \tag{1.4.1}$$

given an initial condition $N_{t_0} = N_0$ for some $t_0 \geq 0$ and $N_0 \geq 0$. Many marine populations experience density dependent growth of this nature, which is often due to filial cannibalism [67]. A short list of commonly used growth functions is included for reference in Appendix A. Note that, for the duration of this work, our modelling efforts will focus solely on females, which corresponds to the assumption that the entire population reproduces according to the chosen growth function.

Determining the maximum reproductive rate of a population (usually this rate is assumed to be realized only at very low population densities in the absence of an Allee effect) is a central question in marine biology. In an extensive study, Myers and colleagues (1999) examined a database of over 700 spawner-recruitment series (i.e.

the number of offspring of a mature individual which successfully survive to reproductive maturity) [78]. They found that each individual typically has a maximum reprodutive rate of 1 to 7 individuals per year, with most species having between 3 and 5 recruits. For our purposes, since we are here modelling only females, we assume a roughly even sex ratio and so will typically parameterize our growth functions with a maximum reproductive rate (this is $g'(0)$ in (1.4.1)) between 1 and 4 in order to obtain general, though not species specific, results.

IDEs incorporate a spatial component via a *dispersal kernel*. This is a probability density function (PDF), here denoted $k(x, y)$, which is the probability that an individual starting at point y will settle at point x over the next time step. Thus $k(x, y)dy$ is the probability that the individual will have moved during the dispersal stage from $[y, y + dy)$ to x in the next time step [51]. In this work, we will only consider a one-dimensional domain, mainly for simplicity. This is not biologically unreasonable, as many species live in the shallower waters near the coast, and the scale of any successful dispersal will be much greater along the coast than out towards open water, since any individuals who disperse too far away from the favourable coastal environment will not survive to recruitment. Note that the approximation which we will use in Chapter 2 allows for easy extension of the domain to include more dimensions, but for now we will work with this one-dimensional domain.

Using these dispersal kernels allows us to explicitly choose the type of dispersal rather than assuming diffusion as in reaction-diffusion equations. By integrating the dispersal kernel over the domain of interest, the number of individuals which move to point x over the subsequent time step can be determined. Assuming that no individuals

are lost during the dispersal phase, we have by definition that

$$\int_{-\infty}^{\infty} k(x,y)dy = 1. \tag{1.4.2}$$

Since we are interested in populations on a finite domain, we will rather tend to have

$$\int_{\Omega} k(x,y)dy < 1, \tag{1.4.3}$$

where Ω is the spatial domain relevant to the question of interest. To begin with, we will be looking at the question of the critical domain size. The idea of a critical domain size is a common notion in population ecology and it addresses the question of how large a domain needs to be in order to sustain a population in the absence of immigration and given hostile conditions outside the domain (in this case, strong fishing pressure). In the context of marine reserves, the critical domain size is the minimal size that a reserve needs to be in order to independently sustain a population. This foundational concept in ecology was first considered by Kierstead and Slobodkin (1953) for reaction-diffusion models [44, 47]. We will initially here be looking at the critical domain size of a single reserve, L, so Ω will be $[-L/2, L/2]$. Combining the original growth model (and now allowing for spatial dependence of the growth function) with this spatial movement results in

$$N_{t+1}(x) = \int_{\Omega} k(x,y) f(N_t(y); y)dy, \tag{1.4.4}$$

which is the typical form of an IDE [58]. In reality, it is not biologically reasonable for many of the populations of interest to first all reproduce and then all disperse. We begin with this model formulation which does not incorporate any structure into the population in order to gain insight into the qualitative nature of the results and to develop the requisite mathematical techniques, but we will expand further on this

in Section 1.8.

1.4.1 Larval behaviour and dispersal kernels

The first attempts to model marine populations often depicted the larval stage as a common larval pool, with larvae evenly redistributed over the population regardless of where they originated. Another approach was a "stepping-stone" model, where adults lived in discrete populations and larvae dispersed to adjacent populations [28]. An improvement was made with the introduction of the aforementioned reaction-diffusion models, where dispersal is modelled via diffusion (i.e. following a Gaussian probability distribution).

Empirical research on dispersal patterns has resulted in the realization that dispersal events may take a range of probability distributions and it is unrealistic to assume that simple isotropic diffusion captures the wide range of dispersal behaviour displayed by marine organisms. From the study of invasion dynamics, it has been observed that many organisms have a relatively large proportion of long-distance dispersers [49]. In contrast, others have found several organisms with very short dispersal distances [2]. Thus it is wise to consider a range of dispersal behaviour by allowing for flexibility in the dispersal component of the model.

There are many unsolved questions related to whether larvae are subject to passive dispersal or whether they undergo an active dispersal process. Some studies have found significant positive correlation between the duration of the larval stage and dispersal distance but the relation is, in general, poorly understood [15, 102]. The possible existence of this correlation influences how much significance lies with the length of the pelagic stage (which can range from minutes to months). In addition, fish are generally extremely fecund and produce many more eggs than those which

end up surviving to recruitment, and the rate of those individuals that settle out of their planktonic stage and reach adulthood is unknown. Estimates are generally very low, ranging from 1 in 10,000 [12] to approximately 10% [102] depending on species, location, and various other factors. Thus to obtain the maximum reproductive rate between 1 and 4 previously mentioned, individuals may produce up to 40,000 eggs in order to have only 4 survive to recruitment. Dispersal is also influenced by complex ocean currents, and the scales of these currents compared to those of larval dispersal are not fully understood, with cross-shelf dynamics and geographic features further complicating any predictions of dispersal distances [56]. All of these factors add considerable uncertainty to any modelling results and, for this reason, conservative estimates are generally the most prudent.

Collecting data on larval dispersal patterns in the open ocean is a logistically complicated task. What is currently known has been collected from the creation of biophysical models of circulation and larval behaviour, studies of genetic variation over space [109], direct observations of the time and place of settlement, and elemental fingerprinting. Elemental fingerprinting is the chemical marking of hard body parts on larvae and is arguably the most direct way to estimate dispersal patterns [10]. A good review of the insights gained from physical modelling, chemical tracking and genetic approaches can be found in Levin (2006).

More recently, there have been some more sophisticated dispersal models based on oceanographic circulation patterns. These newer methods have led to the realization that more recruitment may be of local origin than was previously thought, with estimates ranging from 37 - 80 % [10, 86, 88], though successful cases of long-distance disperal (e.g. from the coast of Africa to North and South America) have also been documented [102]. Measurements are complicated by the fact that larval dispersal

behaviour is far from constant, varying with season and tidal phase [55]. Unfortunately for our present purposes, an accurate description of dispersal distances for most species of commercial or conservation interest remains elusive. For most of these species, we do not even know their dispersal distances to within one to three orders of magnitude [109]. As our understanding of the dispersal process is poor, we will focus on approximations like those described in this section [51, 56].

A possible simplification of the description of larval transport can be made from first principles (i.e. basic transport processes and larval behaviour) to describe larval dispersal as a mechanistically derived PDF [35]. The first attempt to incorporate spatial movement of this type was via "contact distributions", which are PDFs for the distance that a dispersing individual moves and are now also known as *dispersal kernels* [73].

Given an isotropic environment with no spatial variation in dispersal behaviour, the kernel will depend on relative distance as opposed to absolute location. We can then rewrite (1.4.4) as

$$N_{t+1}(x) = \int_{\Omega} k(|x-y|) f(N_t(y); y) dy. \tag{1.4.5}$$

Several dispersal kernels are given in Table 1.2 and Figure 1.1. To scale these distributions, we will use the mean of the strictly positive distribution (i.e. the mean of $k(x)$ for $x \geq 0$), which is conventionally called the *effective mean*. This will allow us to scale the kernels in order to isolate the shape of the distributions and compare the population dynamics of an IDE with different kernels.

Dispersal kernels can either be phenomenological (derived from statistical analysis of data) or mechanistic (derived from underlying assumptions about the biological process). Phenomenological models can be very useful in simulation, as most soft-

Common Dispersal Kernels		
Gaussian / normal	$k(x) = \frac{\exp(-x^2/2\sigma^2)}{\sigma\sqrt{2\pi}}$	mean: $\sigma\sqrt{2/\pi}$, *mesokurtic* [56]
log-normal	$k(x) = \frac{\exp\left(\frac{-(\ln(\lvert x\rvert))^2}{2\sigma^2}\right)}{2\sigma\lvert x\rvert\sqrt{2\pi}}$	mean: $e^{\sigma^2/2}$, phenomenological, has been used to model seed dispersal in terrestrial systems [56]
Laplace / double exponential	$k(x) = \sqrt{\frac{\alpha}{4D}}\exp\left(-\lvert x\rvert\sqrt{\frac{\alpha}{D}}\right)$	mean: $\sqrt{\frac{D}{\alpha}}$, *leptokurtic* [48, 56]
double Weibull / Fréchet	$k(x) = \frac{\alpha}{2\beta}\left\lvert\frac{x}{\beta}\right\rvert^{\alpha-1} e^{-\lvert(x)/\beta\rvert^\alpha}$	mean: $\beta\Gamma(\frac{\alpha+1}{\alpha})$, *platykurtic*, suggested by numerous seed shadow studies [56] and wind speed data [13]
double Gamma	$k(x) = \frac{\lvert x/\beta\rvert^{\alpha-1}e^{-\lvert x/\beta\rvert}}{2\beta\Gamma(\alpha)}$	mean: $\alpha\beta$, *leptokurtic*, provides tractable range of shapes for leptokurtic behaviours, suggested by numerous seed shadow studies [56]
Cauchy	$k(x) = \left\{\pi b\left(1+\left[\frac{x}{b}\right]^2\right)\right\}^{-1}$	mean: undefined, fat-tailed, for scaling purposes, conventionally $b = 1$, *leptokurtic* [45]
fat-tailed (as denoted in [62])	$k(x) = \theta\Re\left\{\mathrm{E}_1(\imath\theta x)\exp(\imath\theta x)\right\}/\pi$	mean: undefined, $\theta = \alpha/\rho$ and E_1 is the exponential integral. See (B.0.6) [62].
finite radius	$k(x) = \left(\frac{\pi}{4R}\right)\cos\left[\frac{\pi}{2R}x\right]$ if $-R < x < R$, else $k(x) = 0$	mean: $(R/2)\sin(\pi/2) + \ldots$ $(R/\pi)(\cos(\pi/2) - 1)$, approximates dispersal of organisms with a finite radius of dispersal, R [51]

Table 1.2: Commonly used dispersal kernels and some key properties. See Figure 1.1 to compare their shapes.

ware allows random numbers to be drawn from well-known distributions. However, when environmental factors (e.g. seasonal currents) may strongly affect dispersal distances, mechanistic models will better aid in the prediction of dispersal distances [45].

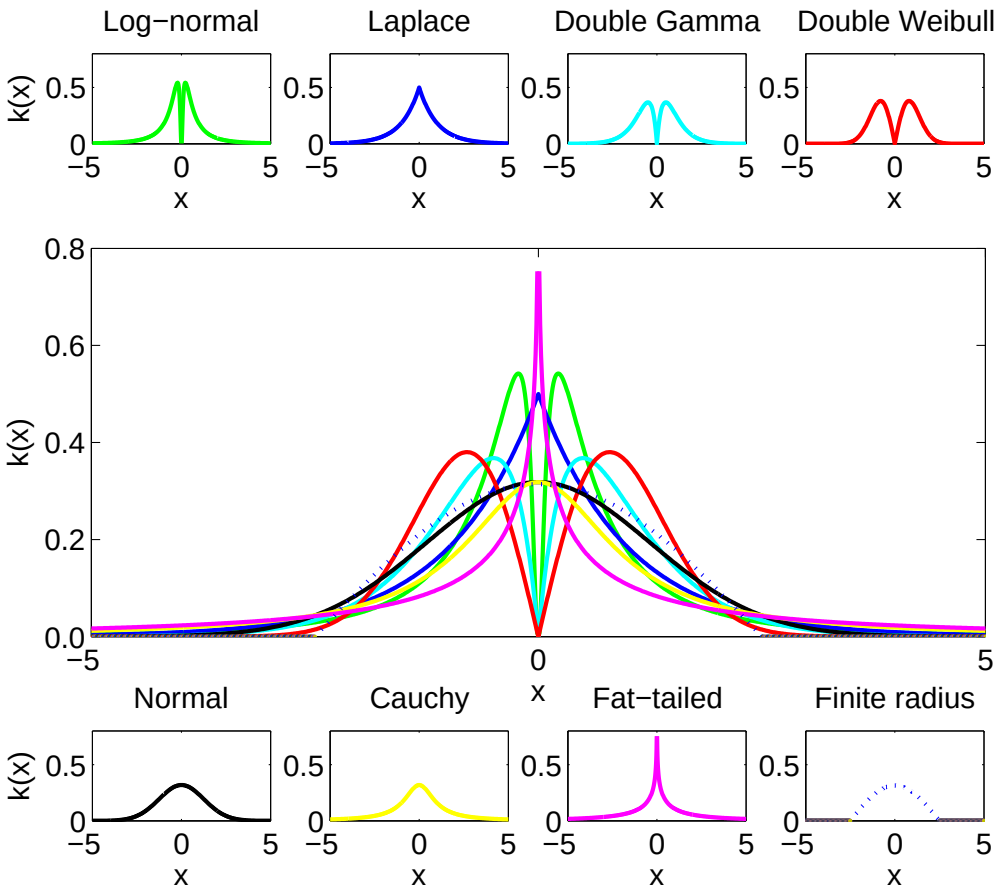

Figure 1.1: Comparison of the shapes of the dispersal kernels from Table 1.2. Parameter values are set so that all but the finite radius, Cauchy and fat-tailed distributions have an effective mean value of 1. Parameters for log-normal are $\sigma = 1$, $\mu = -1/2$, for Laplace, $\alpha = D = 1$, for double Gamma, $\beta = 0.5$, $\alpha = 2$, for double Weibull, $\alpha = 2$, $\beta = 2/\sqrt{\pi}$, for the normal distribution, $\sigma = \sqrt{\pi/2}$, for Cauchy, $b = 1$, for the fat-tailed kernel, $\alpha = 1$, $\rho = 2$, and for the finite radius distribution, the radius is $R = 2.5$.

Several dispersal kernels have been derived based on various mechanistic assumptions. See Appendix B for a summary of the derivation process. Simple models with synchronous settling lead to the Gaussian (or normal) and Cauchy distributions [45, 81]. The Laplace distribution (also known as the double exponential distribu-

tion) arises when organisms disperse via diffusion with a constant settling rate. If the settling rate increases or decreases as a power of time, we obtain the double Weibull distribution, and if the settling rate tends monotonically towards a constant (a very special case), we get the double Gamma distribution (see Neubert (1995) for details). Dispersal can also be density dependent (see [58]), where the individual dispersal probability is a monotone increasing function of local density, though we do not consider this further here.

With these tools in hand, we turn now to consider the necessary conditions for population persistence, exploring some existing results on the behaviour of IDEs in the simplest case, for a single population in a homogeneous isotropic habitat.

1.5 Critical domain size for persistence

While marine reserves may be designed with a variety of motives including fishery management, conservation, and maintenance of biodiversity, population persistence is necessary in order to achieve any of these goals. Here we will look at some established methods for determining the necessary conditions for single population persistence on a homogeneous domain. These methods will use linearization techniques to determine the *critical domain size* necessary to sustain a population, thus setting the lower bound on the size of a single reserve.

Here, we will recapitulate some of the results and methods of Kot and Schaffer (1986) and provide a simple example and some results that will be used in the following chapters. Assuming that the growth function is the same everywhere, independent of location, i.e. $f(N_t(y); y) = f(N_t(y))$, Kot and Schaffer examined the fixed points of a scalar, nonlinear IDE on a closed domain $\Omega = [-L/2, L/2]$. Following the standard

method for discrete models (see [51]), they attempted to find $N^*(x)$ satisfying

$$N^*(x) = \int_{-L/2}^{L/2} k(x,y) f(N^*(y)) dy. \tag{1.5.1}$$

They pointed out the similarities between studying difference equations with no spatial component and the IDEs considered here by introducing a nonlinear operator $\mathcal{F}$ so that $N_{t+1}(x) = \mathcal{F}N_t(x)$. Thus

$$N_{t+1}(x) = \mathcal{F}N_t(x) = \int_{-L/2}^{L/2} k(x,y) f(N_t(y)) dy \tag{1.5.2}$$

and equation (1.5.1) can be rewritten as $N^*(x) = \mathcal{F}N^*(x)$ [51]. As previously stated, for our purposes $f(N(x))$ can typically be expressed as $f(N(x)) = N(x)g(N(x))$ (see (1.4.1)), where $g(N(x))$ is a well-behaved function describing the per capita growth rate. We can assume $N^*(x) = 0$ is always a trivial solution. Obtaining analytic expressions for any non-trivial equilibria will, of course, depend on the kernel and growth function employed.

To determine the linear stability of an equilibrium, Kot and Schaffer (1986) considered a small perturbation $\xi_t(x)$ away from the equilibrium, so that $N_t(x) = N^*(x) + \xi_t(x)$. For sufficiently small $\xi_t(x)$, this is equivalent to studying the linearization of the IDE around the steady state. Considering the nonlinear operator $\mathcal{F}$, this is its Fréchet differential, where

$$\xi_{t+1}(x) = (\mathcal{F}'N^*(x))(\xi_t(x)) = \int_{-L/2}^{L/2} k(x,y) \left[\left. \frac{\partial f(N(y))}{\partial N(y)} \right|_{N^*} \right] \xi_t(y) dy. \tag{1.5.3}$$

Now we can see that the asymptotic stability of the equilibrium $N^*(x)$ is determined by the Fréchet derivative $\mathcal{F}'N^*(x)$. For finite limits of integration and continuous kernels (which are likely, given the question of critical domain size and realistic dispersal

behaviour within the population), this Fréchet derivative is a compact operator [51]. As such, its spectrum consists of, at most, the point zero and a countable number of non-zero eigenvalues [18, 51].

The stability of the equilibrium is determined by examining the magnitude of these eigenvalues. Kot and Schaffer (1986) assumed that $\xi_t(x)$ is of the form

$$\xi_t(x) = \lambda^t \mu(x),$$

where λ represents the eigenvalues and $\mu(x)$ the non-zero eigenvectors. They arrived at this form by analogy with the seperation of variables method commonly used with linear partial differential equations. Assuming this form for $\xi_t(x)$ leads, along with equation (1.5.3), to

$$\lambda\mu(x) = (\mathcal{F}'N^*)\mu(x) = \int_{-L/2}^{L/2} k(x,y) \left[\left. \frac{\partial f(N(y))}{\partial N(y)} \right|_{N^*} \right] \mu(y) dy. \tag{1.5.4}$$

If all eigenvalues λ lie within the unit circle of the complex plane (i.e. $|\lambda| < 1$), then $N^*(x)$ is locally asymptotically stable. Kot and Schaffer (1986) have shown that, given certain conditions of non-negativity and symmetry in the kernel, as well as non-negativity of $f'(N^*(x))$, there exists a positive non-zero dominant eigenvalue, so stability of the trivial steady state will be lost when $\lambda = 1$. Furthermore, Hardin (1990) has shown that for monotonically increasing and bounded growth functions (e.g. Beverton-Holt (A.0.3)), the trivial equilibrium solution is globally stable when its dominant eigenvalue is less than 1 and the non-trivial equilibrium solution is globally stable otherwise [39]. Note that in the event that stability is lost through $\lambda = -1$ (this can happen if $f'(N^*)$ is strictly negative [51]), IDEs can display loss of stability via a Hopf bifurcation, followed by period doubling bifurcations leading to chaos [51].

We will now consider a simple, carefully chosen example in order to illustrate the above. We begin by choosing the Laplace dispersal kernel (see Table 1.2) as it displays convenient properties allowing for analytic tractability, as was noted by Kot and Schaffer (1986). Assuming that growth does not depend explicitly on location, this results in the following IDE

$$N_{t+1}(x) = \sqrt{\frac{\alpha}{4D}} \int_{-L/2}^{L/2} \exp\left(-|x-y|\sqrt{\frac{\alpha}{D}}\right) f(N_t(y))dy. \tag{1.5.5}$$

Any fixed points are the solutions to

$$N^*(x) = \sqrt{\frac{\alpha}{4D}} \int_{-L/2}^{L/2} \exp\left(-|x-y|\sqrt{\frac{\alpha}{D}}\right) f(N^*(y))dy. \tag{1.5.6}$$

Omitting the $*$ for notational convenience, we continue to follow Kot and Schaffer (1986) and differentiate the above with respect to x, which yields

$$\begin{aligned} N'(x) =& \frac{\alpha}{2D}\Big[-\int_{-L/2}^{x} \exp\left((y-x)\sqrt{\frac{\alpha}{D}}\right) f(N(y))dy + \\ & \int_{x}^{L/2} \exp\left((x-y)\sqrt{\frac{\alpha}{D}}\right) f(N(y))dy\Big]. \end{aligned} \tag{1.5.7}$$

Differentiating once more yields

$$\begin{aligned} N''(x) = &-\left(\frac{\alpha}{D}\right) f(N(x)) + \left(\frac{\alpha}{D}\right)\sqrt{\frac{\alpha}{4D}} \mathrm{e}^{(-x\sqrt{\frac{\alpha}{D}})} \int_{-L/2}^{x} \mathrm{e}^{y\sqrt{\frac{\alpha}{D}}} f(N(y))dy + \\ & \left(\frac{\alpha}{D}\right)\sqrt{\frac{\alpha}{4D}} \mathrm{e}^{(x\sqrt{\frac{\alpha}{D}})} \int_{x}^{L/2} \mathrm{e}^{-y\sqrt{\frac{\alpha}{D}}} f(N(y))dy, \end{aligned} \tag{1.5.8}$$

and simplifying results in

$$N''(x) + \frac{\alpha}{D}[f(N(x)) - N(x)] = 0. \tag{1.5.9a}$$

This nice "trick" of using the Laplace dispersal kernel and differentiating twice in order to obtain a second order ordinary differential equation, is the reason for selecting the Laplace dispersal kernel in many of the examples throughout this work. By looking at $x = \pm L/2$ in (1.5.7), we acquire the relevant boundary conditions

$$\begin{aligned} N'(x) &= \sqrt{\tfrac{\alpha}{D}} N(x) \quad \text{at} \quad x = -L/2, \\ N'(x) &= -\sqrt{\tfrac{\alpha}{D}} N(x) \quad \text{at} \quad x = L/2. \end{aligned} \tag{1.5.9b}$$

We can clearly see that $N^*(x) = 0$ is a solution for any growth functions of the form $f(N(x)) = N(x)g(N(x))$. For example, if we use the Ricker equation $f(N(x)) = N(x)\exp\left(r(1 - N(x)/K)\right)$ with carrying capacity $K = 1$, we get

$$N''(x) + N(x)\left(\frac{\alpha}{D}\right)\left[\exp\left(r(1 - N(x))\right) - 1\right] = 0, \tag{1.5.10}$$

with the same boundary conditions as above. $N^*(x) = 0$ is clearly a solution of (1.5.10) and we will now look for any non-trivial equilibrium solutions. Following the method set out by Kot and Schaffer (1986), the most illuminating way to proceed is to turn (1.5.10) into a system of two ODEs by setting $u(x) = N(x)$ and $v(x) = N'(x)$. This results in

$$u'(x) = v(x), \tag{1.5.11a}$$

$$v'(x) = -u(x)\left(\frac{\alpha}{D}\right)\left[\exp\left(r(1 - u(x))\right) - 1\right], \tag{1.5.11b}$$

with boundary conditions

$$\begin{aligned} v(x) &= \sqrt{\tfrac{\alpha}{D}} u(x) \quad \text{at} \quad x = -L/2, \\ v(x) &= -\sqrt{\tfrac{\alpha}{D}} u(x) \quad \text{at} \quad x = L/2. \end{aligned} \tag{1.5.11c}$$

There are two equilibrium solutions (u^*, v^*) at $(0, 0)$ and $(1, 0)$ to the corresponding non-spatial system,

$$u' = v, \tag{1.5.12}$$

$$v' = -u\left(\frac{\alpha}{D}\right)[\exp(r(1-u)) - 1]. \tag{1.5.13}$$

If we look at the phase plane in Figure 1.2, we can see equilibrium solutions for the original system that are periodic in space. Solutions corresponding to our boundary conditions are orbits beginning on $v = u\sqrt{\alpha/D}$ at $x = -L/2$ and ending on $v = -u\sqrt{\alpha/D}$ at $x = L/2$. Because of the dependence of the boundary conditions on L, for a fixed α, D and r, choosing from the possible orbits is, in essence, specifying the length of the domain, L. For a large domain size, L, the solutions will be "slow-

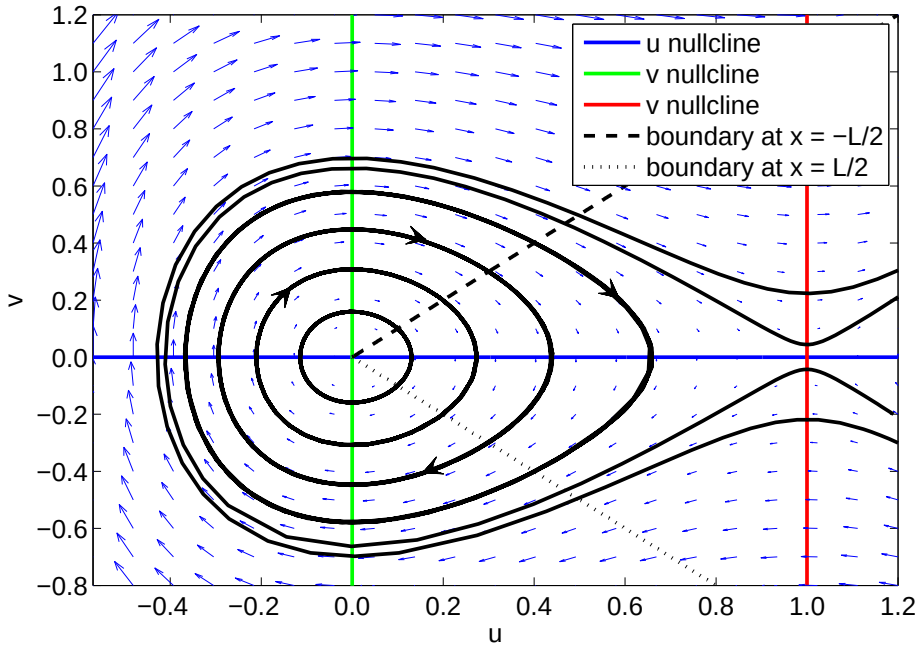

Figure 1.2: Phase plane of system (1.5.11a)-(1.5.11b) with $D = 1$, $\alpha = 1$ and $r = 1$. Solutions were plotted using ode45, a MATLAB ODE solver, which is based on Runge-Kutta methods.

moving", with more values around the saddle point $(1, 0)$ [51]. Biologically, this means

that large viable habitats should lead to larger equilibria, falling off only at the edges of the habitat where individuals are lost via dispersal to fished areas. As the habitat size decreases, a greater portion of the population is lost to the unfavourable habitat. See Figure 1.3 for solutions of (1.5.11).

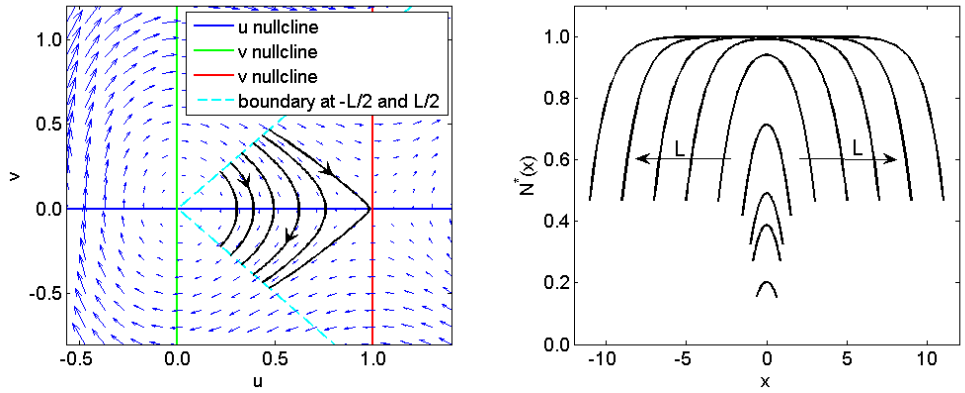

Figure 1.3: Following Kot and Schaffer (1986), the trajectories of system (1.5.11) subject to boundary conditions (1.5.11c) for several values of L. Here $\alpha = 1$, $D = 1$ and $r = 1$ and solutions were plotted in MATLAB using bvp4c, which is a built-in solver for ODE boundary value problems. As we will see in (1.5.20), for these parameter values, the critical domain length is $L^* = 0.99$, and so there will be no nonzero solution between $x = \pm 0.5$. Initial conditions were here determined by the MATLAB function bvpinit, though any nonzero initial condition with compact support yields the same solutions.

Now we address the question of interest: what is the critical domain size? There is a domain threshold size which we will denote as L^* at which reproduction is exactly sufficient to balance the cost of individuals dispersing to the hostile environment outside the reserve. L^* is the bifurcation value for L at which stability switches from the trivial steady state $N^* = 0$ to a non-trivial steady state. If $L < L^*$, the population will go extinct, and if $L > L^*$, we will achieve our goal of persistence. To find L^*, we will look at where the trivial solution loses stability and, from above, recall that the trivial solution is asymptotically stable if all of the eigenvalues λ of (1.5.4) lie within the unit circle of the complex plane. For the chosen kernel, which is continuous,

symmetric, and non-negative, all eigenvalues are real and positive, and stability will be lost through $\lambda = 1$ [51]. For the Laplace kernel chosen in this example, (1.5.4) becomes

$$\lambda\mu(x) = e^r\sqrt{\frac{\alpha}{4D}}\int_{-L/2}^{L/2}\exp\left(-|x-y|\sqrt{\alpha/D}\right)\mu(y)dy. \tag{1.5.14}$$

Differentiating twice, we find

$$\mu''(x) + \left(\frac{\alpha}{D}\right)\frac{e^r-\lambda}{\lambda}\mu(x) = 0, \tag{1.5.15a}$$

with boundary conditions

$$\begin{aligned} \mu'(x) &= \mu(x)\sqrt{\tfrac{\alpha}{D}} \quad \text{at} \quad x = -L/2, \\ \mu'(x) &= -\mu(x)\sqrt{\tfrac{\alpha}{D}} \quad \text{at} \quad x = L/2. \end{aligned} \tag{1.5.15b}$$

Letting

$$\gamma^2 = \frac{e^r-\lambda}{\lambda},$$

we have

$$\mu''(x) + \left(\gamma\sqrt{\frac{\alpha}{D}}\right)^2\mu(x) = 0,$$

and so we can assume a solution of the form

$$\mu(x) = A\cos\left(\gamma\sqrt{\frac{\alpha}{D}}x\right) + B\sin\left(\gamma\sqrt{\frac{\alpha}{D}}x\right),$$

for some A and B constant. In order to satisfy the boundary conditions,

$$\begin{aligned} \mu'(-L/2) &= -A\gamma\sqrt{\frac{\alpha}{D}}\sin\left(-\gamma\sqrt{\frac{\alpha}{D}}\frac{L}{2}\right) + B\gamma\sqrt{\frac{\alpha}{D}}\cos\left(-\gamma\sqrt{\alpha}D\frac{L}{2}\right) \\ &= A\sqrt{\frac{\alpha}{D}}\cos\left(-\gamma\sqrt{\alpha}D\frac{L}{2}\right) + B\sqrt{\frac{\alpha}{D}}\sin\left(-\gamma\sqrt{\frac{\alpha}{D}}\frac{L}{2}\right) \\ &= \sqrt{\frac{\alpha}{D}}\mu(-L/2) \end{aligned}$$

and

$$\begin{aligned}\mu'(L/2) &= -A\gamma\sqrt{\frac{\alpha}{D}}\sin\left(\gamma\sqrt{\frac{\alpha}{D}}\frac{L}{2}\right) + B\gamma\sqrt{\frac{\alpha}{D}}\cos\left(\gamma\sqrt{\frac{\alpha}{D}}\frac{L}{2}\right) \\ &= -A\sqrt{\frac{\alpha}{D}}\cos\left(\gamma\sqrt{\frac{\alpha}{D}}\frac{L}{2}\right) - B\sqrt{\frac{\alpha}{D}}\sin\left(\gamma\sqrt{\frac{\alpha}{D}}\frac{L}{2}\right) \\ &= -\sqrt{\frac{\alpha}{D}}\mu(L/2).\end{aligned}$$

Rearranging yields two equations in two variables,

$$\begin{aligned}A\left[1 - \gamma\tan\left(\gamma\sqrt{\frac{\alpha}{D}}\frac{L}{2}\right)\right] - B\left[\tan\left(\gamma\sqrt{\frac{\alpha}{D}}\frac{L}{2}\right) + \gamma\right] &= 0 \\ A\left[1 - \gamma\tan\left(\gamma\sqrt{\frac{\alpha}{D}}\frac{L}{2}\right)\right] + B\left[\tan\left(\gamma\sqrt{\frac{\alpha}{D}}\frac{L}{2}\right) + \gamma\right] &= 0,\end{aligned}$$

and so the eigenvalues λ (recall $\gamma = \gamma(\lambda)$) will satisfy either the transcendental equation

$$\tan\left(\frac{\gamma L}{2}\sqrt{\frac{\alpha}{D}}\right) = \frac{1}{\gamma} \tag{1.5.16}$$

or

$$\tan\left(\frac{\gamma L}{2}\sqrt{\frac{\alpha}{D}}\right) = -\frac{1}{\gamma}. \tag{1.5.17}$$

There are an infinite number of roots to these equations, hence an infinite number of eigenvalues. When the eigenvalues associated with this root (γ) reach the unit circle at $\lambda = 1$ (i.e. when the stability of the trivial solution is lost), $\gamma = \sqrt{e^r - 1}$ and the critical threshold L^* must satisfy either

$$\tan\left(\frac{\sqrt{e^r - 1}\,L^*}{2}\sqrt{\frac{\alpha}{D}}\right) = \frac{1}{\sqrt{e^r - 1}} \tag{1.5.18}$$

or

$$\tan\left(\frac{\sqrt{e^r - 1}\,L^*}{2}\sqrt{\frac{\alpha}{D}}\right) = -\frac{1}{\sqrt{e^r - 1}}. \tag{1.5.19}$$

Since the second transcendental equation results in a negative value of L^*, which is

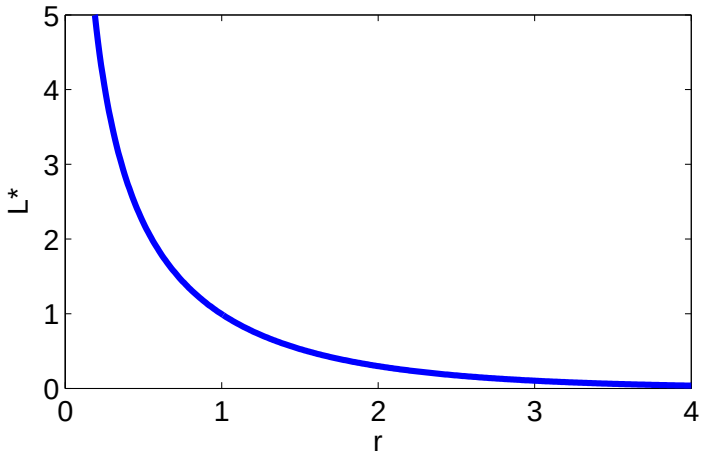

Figure 1.4: Plot of (1.5.20), the critical domain size for an IDE with Ricker growth and a Laplace dispersal kernel. For small growth rates, r, the population cannot persist on a domain of any size, and L^* tends asymptotically to infinity. For large r values, the domain need not be very large to retain enough recruits for persistence.

not relevant to our present problem, the critical domain size for this example is

$$L^* = \frac{2}{\sqrt{e^r - 1}} \sqrt{\frac{D}{\alpha}} \tan^{-1}\left(\frac{1}{\sqrt{e^r - 1}}\right), \tag{1.5.20}$$

seen in Figure 1.4. In addition to the bifurcation through L^* giving rise to the non-trivial equilibrium, Kot and Schaffer (1986) also showed that the solution will bifurcate from the trivial steady state as we increase the population's intrinsic rate of growth $f'(0)$, resulting in a cascade of period doubling bifurcations, similar to what occurs in the related non-spatial growth models (see Figure 2.8 for an example.)

We will use many of the ideas and strategies which we have discussed in this section throughout the rest of this work. For many of the illustrating examples, the Laplace kernel will be used and again we will differentiate the steady state equation twice in order to determine the necessary conditions on reserve size and growth rates for the existence of a non-zero steady state. In the next section, we will look at some results on multiple equally sized and spaced reserves using these same methods.

1.6 Networks of reserves

It is commonly thought to be more beneficial to have multiple smaller reserves than one large one, as together, a reserve network is arguably more than the sum of its parts [29, 83, 86, 96]. A network of marine reserves is a set of reserves connected chiefly by larval dispersal [57] and one way to model this is to create an idealized structure, with an infinite network of reserves of all the same size (having width w) and equally spaced (with periodicity L), as seen in Figure 1.5.

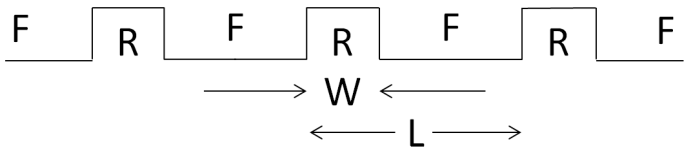

Figure 1.5: An idealized reserve network consisting of infinitely many reserves, here denoted by R, of width w and spacing L surrounded by fished areas, denoted by F.

A simple mathematical interpretation allowing for some analysis is to have "good" and "bad" habitat patches, as first conceived of by Shigesada et al. (1986). The goal is then to find a threshold value for the percentage of hostile habitat beyond which the population cannot persist at all. We here model this spatially periodic growth function as

$$f(N(x);x) = \begin{cases} \text{growth function 1}, & x \in [nL,\, nL+w],\ n \in \mathbb{Z} \\ \text{growth function 2}, & x \in (nL+w,\, (n+1)L),\ n \in \mathbb{Z} \end{cases}$$

assuming that $[nL, nL+w]$, $n \in \mathbb{Z}$, are the reserves, and that $(nL+w, (n+1)L)$, $n \in \mathbb{Z}$, are the fished areas [58, 103]. Under assumptions of strong fishing pressure, we will often set "growth function 2" $= 0$, assuming that all area not in a reserve is completely hostile. As before, we will suppose $f(N(x);x)$ is of the form $f(N(x);x) = N(x)g(N(x);x)$ where $g(\cdot;x)$ is now periodic in x with period L. For

an analytically tractable illustrative example, we choose the Laplace kernel, now following the method outlined by Van Kirk and Lewis (1997). We begin by non-dimensionalizing the problem by dividing the spatial variables by the period L, setting

$$\tilde{x} = \frac{x}{L} \quad \text{and} \quad \tilde{y} = \frac{y}{L}. \tag{1.6.1}$$

This results in the following IDE

$$N_{t+1}(L\tilde{x}) = \int_{-\infty}^{\infty} \frac{L}{2b} \exp\left(-\frac{L}{b}|\tilde{x} - \tilde{y}|\right) f(N_t(L\tilde{y}); L\tilde{y})\, d\tilde{y}, \tag{1.6.2}$$

where $b = \sqrt{D/\alpha}$. If we then let $\hat{L} = L/b$ (i.e. it is the measure of the effective spatial scale of habitat fragmentation, the period length divided by the mean dispersal distance), and $\tilde{N}_t(y) = N_t(L\tilde{y})$ we obtain the dimensionless IDE (dropping the tildes and hats for convenience)

$$N_{t+1}(x) = \int_{-\infty}^{\infty} \frac{L}{2} \exp\left(-L|x - y|\right) f(N_t(y); y)\, dy, \tag{1.6.3}$$

with equilibrium solutions satisfying

$$N^*(x) = \int_{-\infty}^{\infty} \frac{L}{2} \exp\left(-L|x - y|\right) f(N^*(y); y)\, dy. \tag{1.6.4}$$

If we differentiate this twice with respect to x (and drop the $*$ for convenience), we obtain the second order differential equation

$$-\frac{1}{L^2} N''(x) + N(x) - N(x) g(N(x); x) = 0. \tag{1.6.5}$$

Note that $g(\cdot; x)$ and its first derivative now have period 1, so the boundary conditions are $N(0) = N(1)$ and $N'(0) = N'(1)$. If we make a small perturbation around the zero steady state and assume that perturbation to be of the form $\xi_t(x) = \lambda^t \mu(x)$,

where λ represents the eigenvalues and $\mu(x)$ the non-zero eigenvectors, we obtain the eigenvalue problem

$$-\frac{1}{L^2}\mu_{xx}(x) + \mu(x) = \frac{1}{\lambda}g(0;x)\mu(x), \tag{1.6.6}$$

again with boundary conditions $\mu(0) = \mu(1)$ and $\mu'(0) = \mu'(1)$. Van Kirk and Lewis (1997) have shown that for operators like the one employed here, a single positive dominant eigenvalue λ_1 exists and corresponds to a positive eigenfunction, $\mu_1(x)$. Now in order to solve the problem explicitly, we need to specify the form of the periodic growth function $g(0;x)$. We will here consider alternating patches of "bad" and "good" habitat, where $g(0;x) = 0$ in the bad patches (the most extreme, conservative case) and $g(0;x) = r$ in the good patches. Now we will let R be the fraction of coastline in a reserve and this results in a growth function, at low densities, of the form

$$g(0;x) = \begin{cases} 0, & 0 < x < 1 - R \\ r, & 1 - R \leq x \leq 1. \end{cases} \tag{1.6.7}$$

The eigenvalue problem (1.6.6) is now given by

$$\mu_{xx} = \begin{cases} L^2\mu, & \text{bad patches,} \\ -L^2(\frac{1}{\lambda_1}r - 1)\mu, & \text{good patches} \end{cases} \tag{1.6.8}$$

with the same boundary conditions as before. Because the IDE and its first derivative are continuous with respect to x, the eigenfunction $\mu(x)$ and its first derivative must be continuous at the discontinuity $x = 1 - R$ of $g(0;x)$. We now search for a relationship between the length of the period (now a single variable L scaled to the mean dispersal distance) and the width of the reserve area as a fraction R of L. We are interested in this relationship exactly at the bifurcation value $\lambda_1 = 1$, where the zero steady state loses stability.

Setting $\lambda_1 = 1$ and substituting $G^2 = r - 1$, we have eigenfunctions of the form

$$\mu(x) = \begin{cases} c_1 \exp(Lx) + c_2 \exp(-Lx), & x \in (0, 1-R) \\ c_3 \sin(GLx) + c_4 \cos(GLx), & x \in [1-R, 1]. \end{cases} \tag{1.6.9}$$

We now take (1.6.9) and apply both the boundary conditions and the continuity of the eigenfunction and its first derivative at $x = 1 - R$, i.e.

$$\begin{aligned} \mu(0) &= \mu(1) \\ \mu'(0) &= \mu'(1) \\ \mu(1-R)_- &= \mu(1-R)_+ \\ \mu'(1-R)_- &= \mu'(1-R)_+ \end{aligned}$$

where $-$ denotes the limit from below and $+$ the limit from above. From this, we obtain four equations in four variables,

$$\begin{aligned} c_1 + c_2 &= c_3 \sin(LG) + c_4 \cos(LG) \\ c_1 L - c_2 L &= c_3 LG \cos(LG) - c_4 LG \sin(LG) \\ c_1 \exp(L(1-R)) + c_2 \exp(-L(1-R)) &= c_3 \sin(LG(1-R)) + c_4 \cos(LG(1-R)) \\ c_1 L \exp(L(1-R)) - c_2 L \exp(-L(1-R)) &= c_3 LG \cos(LG(1-R)) \\ &\quad - c_4 LG \sin(LG(1-R)). \end{aligned}$$

This can be written as the matrix equation

$$\mathbf{Ac} = \mathbf{0}$$

where $\mathbf{A}$ is the augmented matrix

$$A = \begin{bmatrix} 1 & 1 & -\sin(LG) & -\cos(LG) \\ 1 & -1 & -G\cos(LG) & G\sin(LG) \\ \exp(L(1-R)) & \exp(-L(1-R)) & -\sin(LG(1-R)) & -\cos(LG(1-R)) \\ \exp(L(1-R)) & -\exp(-L(1-R)) & -G\cos(LG(1-R)) & G\sin(LG(1-R)) \end{bmatrix},$$

$\mathbf{c}$ is the column vector $[c_1, \ldots, c_4]^T$ and $\mathbf{0}$ is the zero column vector. In order for there to exist a non-trivial solution to this system of equations, the relationship between the scaled periodicity Ł and the fraction of coastline in reserves R must satisfy $\det(\mathbf{A}) = 0$,

$$\begin{aligned} \det(A) = {} & 4G - \exp(L - LR)\sin(GLR) + \exp(LR - L)\sin(GLR) \\ & - G^2\exp(LR - L)\sin(GLR) - 2G\exp(L - LR)\cos(GLR) \\ & - 2G\exp(LR - L)\cos(GLR) + G^2\exp(L - LR)\sin(GLR) = 0, \end{aligned} \tag{1.6.10}$$

which can be seen in Figure 1.6. In order for this non-trivial solution to exist, r must be greater than 1, so that G is real and positive and the population must be doing more than just replenishing itself in the good patches. Furthermore, (1.6.10) is dependent not only on the fraction of coastline in reserves R, but on how far apart the reserve areas are L. This has important management implications, as it is not only the overall fraction of coastline in reserves that determines population persistence, but how the protected waters are distributed.

Observe in Figure 1.6 that as L tends to infinity, the relationship between R and L becomes inverse linear, tending asymptotically to the critical domain size for a single reserve divided by the periodicity. For small periodicities, connectivity between reserve areas is important for population survival, but once the reserves get too far apart, each individual reserve must retain sufficient larvae produced by its own pop-

ulation in order to persist. For those attempting to implement a reserve network, there is obviously immediate economic benefit to having the smallest proportion of coastline closed to fishing, but determining whether this minimum amount of coastline results from a single reserve or from a reserve network is not immediately clear from this model. It is difficult to compare the relative impact of a single reserve on a coastline to an infinite network of reserves. An infinite network of connected reserves is a mathematical simplification of what, in reality, would be a large but finite number of connected reserves. Thus in order to determine the proportion of a designated coastline required to be in reserves, the model would need to be modified to allow for the loss of dispersing larvae at the ends of the reserve network, where there is no connectivity beyond the most outreaching reserve areas. Even in cases where a single reserve requires less total coastline for persistence, reserve managers will also need to consider other benefits of a reserve network, such as lower risk of catastrophes and the maintenance of genetic diversity.

1.7 Incorporating alongshore currents

One very important aspect of marine reserve design which is often neglected is theory involving advective currents. Many coastal or reef populations experience unidirectional drift either due to alongshore currents created by wind and waves, or larger ocean currents. The speed of this movement can be measured using a variety of methods, and one of the simplest is to drop fluorescent dye into the water and track its movement. Alongshore currents caused by wind and waves tend to be measured in terms of speed, with rates of 2.5 metres per second being achieved in strong storms [66]. Larger ocean currents tend to be measured in Sverdrups (one Sverdrup is equal to one million cubic meters of water per second), with currents such as the Gulf Stream ranging from 30 to 150 Sverdrups depending on latitude and season [21].

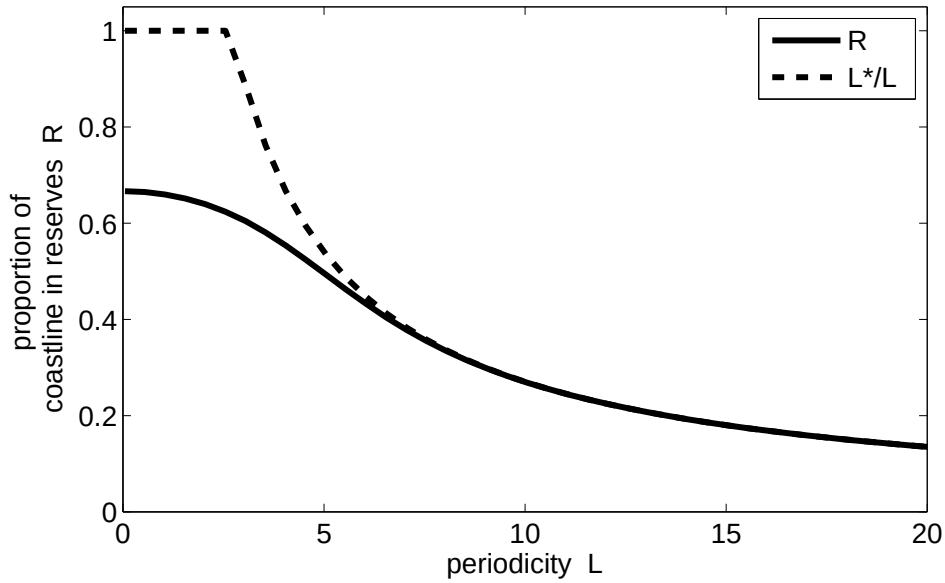

Figure 1.6: Relationship between periodicity (scaled to the mean dispersal distance) and the proportion of coastline R required to be in reserves in order to satisfy $\lambda_1 = 1$ for an IDE on a reserve network, as in (1.6.10). The length of a single reserve L^* required for persistence, given the same parameter values, is shown as a proportion of the periodicity in order to illustrate the benefits of dispersal between reserve areas. These benefits are greatest for small L values, where connectivity between reserve areas contributes heavily to population persistence.

Unidirectional currents can create sink-source dynamics and inevitable extinction of upstream populations if insufficient upstream recruitment occurs [110]. A question related to the one we will look at here, of how advection affects critical domain size, is the basic question of persistence in advective media. This has wide ranging applicability, from insects in streams and rivers, to terrestrial species under the influence of climate change, plants with wind born seeds, and gut-dwelling bacteria [61, 62]. First dubbed the "drift paradox" by Müller (1954), it is an area that has received considerable attention and we will briefly recapitulate a summary of that work here [74].

As in the case without advection, much of the existing work in this area has been

done using PDE models, here with both a diffusive term and an advective term [28, 30, 59, 84, 92, 110]. In this section, we will look at the established ways to incorporate advection into an IDE framework, specifically through modifying the dispersal kernels.

Some have attempted to incorporate advection into the dispersal kernel by simply shifting the mode of the kernel downstream by some advective factor [56, 61, 81]. This is, however, not a biologically reasonable assumption for many of the kernels which are derived from the important assumption that not all larvae settle at the same time. It is an oversight to assume that an advective current will affect kernels of this sort by simply shifting them. We will here draw heavily from the work of Lutscher et al. (2005) who derived modified dispersal kernels to be used in an integrodifferential approach to modelling organisms in river systems. See Appendix B and Figure 1.7 for an overview of their derivation procedure and the resulting dispersal kernels.

1.7.1 The relationship between upstream spread and persistence

Two common approaches to analysis in spatial ecological models are travelling wave theory and bifurcation theory. Here we will briefly discuss how these two approaches are linked when the model contains advection [62]. Let us consider, for a moment, the travelling wave behaviour that can be displayed by IDEs. A travelling wave is a solution which maintains its shape while being propagated through space. Mathematically, this can be written as $N(x,t) = N(x-ct)$, where c is the speed of propagation [75]. We will not go into details here, for the sake of brevity, but will simply state the well-known fact that IDEs can, and often do, display travelling wave behaviour given a set of fairly reasonable assumptions on their initial conditions and dispersal behaviour [41, 48, 49]. As one can imagine, with the addition of advection into a

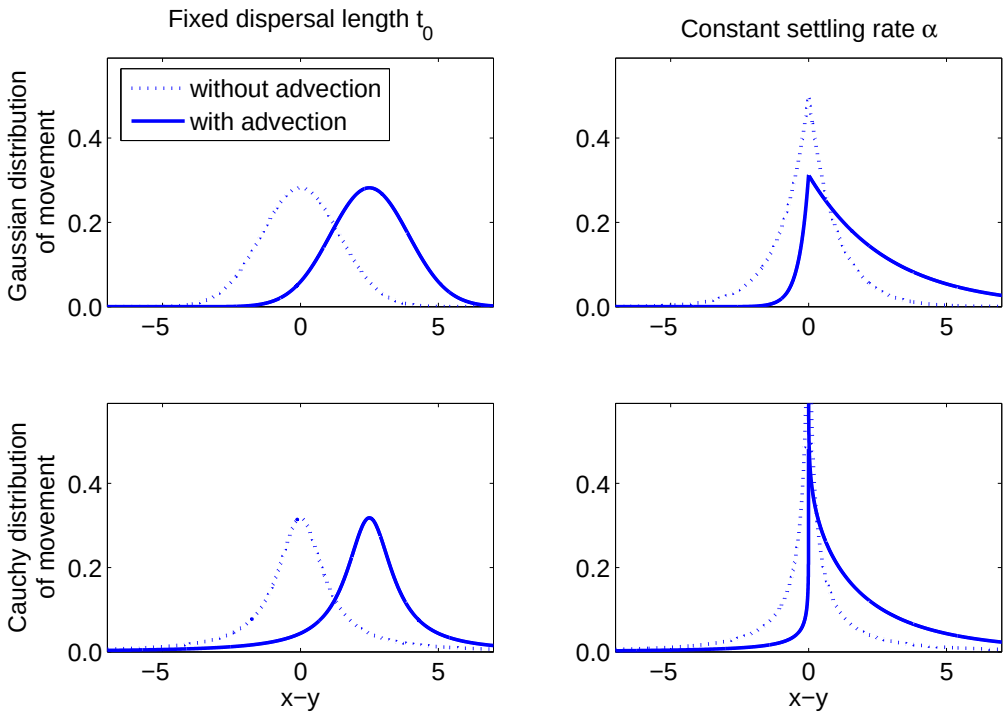

Figure 1.7: Comparison of standard Kernels to those subject to advection, from Table B.1 in Appendix B. Observe that when the assumption is that the larvae all settle at the same time t_0 (as in the left column), advection simply shifts the kernel vt_0 downstream, where v is the strength of advection. If we assume that the population settles at a constant rate α (as in the right column), the shape of the kernel changes to become asymmetrical. Here $\rho = D = t_0 = \mu = 1$ and $v = 2.5$ in the relevant equations in Appendix B.

system, the spreading speed in both directions is no longer equal, and indeed there are conceivably situations in which the downstream flow is too strong (say for some advection value v_i) for any upstream spread at all. As we can also imagine, the critical domain size increases with increased advection as more individuals are lost from the downstream edge and a larger domain is required to retain enough individuals for each generation to persist. This continues until, for some critical advective speed, v_p, there is no finite domain large enough to allow for persistence [61].

This leads us to mention an important result about upstream spread and persistence in environments with unidirectional flow; it has been found that these two critical

advection speeds, v_i and v_p, are the same. It turns out that a species that cannot invade upstream is also incapable of persisting in any finite environment, no matter how large the domain size [61, 62, 84, 110]. Thus the critical persistence condition occurs exactly when the upstream speed is zero. The main advantage of this finding is that it is usually much simpler to calculate the spreading speed of a population than a critical domain size.

For our present purposes, we will consider a linearized IDE, since it has been shown that when population growth is monotone (and also for a wide class of non-monotone growth functions [41]), the linear model has the same invasion speed as the nonlinear model [117]. For kernels with exponentially bounded tails (e.g. Laplace, Weibull, Gamma, and Gaussian), we can find a moment generating function (MGF),

$$M(s) = \int_{-\infty}^{\infty} k(x) \exp(sx) dx \tag{1.7.1}$$

which exists for all s in some interval around zero. Kot et al. (1996) have shown that all IDEs with dispersal kernels with MGFs have a finite, constant-speed travelling wave solution. If the tails of the dispersal kernel are *not* exponentially bounded (e.g. the Cauchy kernel), then the model may exhibit accelerating wavefronts [49]. Lutscher et al. (2005) looked at fat-tailed kernels of this sort in their integrodifferential model and found numerically that populations with this dispersal pattern can persist in bounded domains even for very high advection speeds because of their rare long distance dispersal events. It is tempting to extend this and conjecture that populations with accelerating wavefronts can persist in the face of arbitrarily fast advection. Lutscher et al. (2010) warn, however, about the differences due to the rarity of the long distance events, between persistence on a bounded domain and invasions on an infinite one [61], though to the best of our knowledge, this area has not been explored

further. For our purposes, all of the above simply serves to place a lower bound r^* on the demographic parameter, r, and an upper bound v^* on advection speed, v. For any $r < r^*$ or any $v > v^*$, the population will not be able to persist, no matter the size of a reserve area, so any search for a critical domain size is futile.

1.7.2 Critical domain size for populations subject to alongshore currents

Assuming that the aforementioned two conditions on r and v hold, our goal here is to find similar conditions on the domain size for population persistence as in Section 1.5, this time taking advection into account. As before, we will look at a specific example involving the Laplace dispersal kernel and we will use the standard method to find the critical domain size [51, 61, 62, 84]. We will once more attempt to find the dominant eigenvalue of the nonlinear integral operator and then use its bifurcation behaviour to determine the critical domain size. We again define persistence as occurring when the zero solution is an unstable steady state and there exists a stable non-trivial positive equilibrium.

Following the same method as in the previous sections, we will look at the linearization around the trivial steady state which results in the following eigenvalue problem

$$\lambda\mu(x) = \int_{-L/2}^{L/2} k(x,y) \left[\left. \frac{\partial f(N(y))}{\partial N(y)} \right|_{N\equiv 0} \right] \mu(y) dy. \tag{1.7.2}$$

Note that if we are using logistic growth (A.0.1) or the Beverton-Holt mapping (A.0.3), $f'(0) = r$, and if we are using the Ricker map (A.0.2), $f'(0) = e^r$ and thus we would simply replace r by e^r in the following. Assuming $f'(0) = r$ and looking at

the linearized IDE, we have

$$\lambda\mu(x) = r\int_{-L/2}^{L/2} k(x,y)\mu(y)dy. \tag{1.7.3}$$

Recall that the population can persist if the dominant eigenvalue λ of (1.7.3) is greater than 1. For a given r, the critical domain size is then the value of L for which $\lambda = 1$ and the trivial solution loses its stability. As can be seen in Appendix B, adding advection into the mechanistic derivation of the Laplace kernel results in an asymmetric Laplace kernel,

$$k(x) = \begin{cases} A\exp(a_1 x), & x \leq 0 \\ A\exp(a_2 x), & x \geq 0 \end{cases}, \tag{1.7.4a}$$

where

$$A = \frac{a_1 a_2}{a_2 - a_1} = \frac{\alpha}{\sqrt{v^2 + 4\alpha D}}, \tag{1.7.4b}$$

and

$$a_{1,2} = \frac{v}{2D} \pm \sqrt{\frac{v^2}{4D^2} + \frac{\alpha}{D}}, \tag{1.7.4c}$$

where D is the diffusion coefficient and v is the force of advection. In this carefully chosen example, we follow Lutscher et al. (2010) and differentiate (1.7.3) twice to obtain a second order ordinary differential equation with boundary conditions, as we did in Section 1.5. Then, using the characteristic equation and letting $\lambda = 1$, we calculate the critical domain size L^* as

$$L^* = \frac{4\arctan\left(\sqrt{\frac{4ra_1|a_2|}{(a_1-a_2)^2} - 1}\right)^{-1}}{(a_1 - a_2)\sqrt{\frac{4ra_1|a_2|}{(a_1-a_2)^2} - 1}}. \tag{1.7.5}$$

Note that this is a decreasing function in r, which we would expect, since the more fecund a species is, the smaller the proportion of individuals which need to be retained

inside the reserve area for persistence. The critical domain size $L^* \to \infty$ as

$$r \to \frac{(a_1 - a_2)^2}{4a_1|a_2|},$$

so the persistence threshold is

$$r^* = \frac{(a_1 - a_2)^2}{4a_1|a_2|}.$$

For any $r > r^*$, the population will persist on a domain of length $L > L^*$ [61]. Keep in mind that an explicit critical domain size can only be found in very specific cases and for very few nonlinear models, and the above again serves simply to illustrate an idealized situation and to show the continued dependence of the critical domain size on the demographic parameter r.

1.8 Size-structured models

While IDEs capture the fact that many marine species reproduce and disperse during separate times, it is not biologically accurate to assume that first *all* of the individuals reproduce and then *all* of the individuals, both old and young, disperse in the same way. Indeed, we know that for many marine species of interest, only the juveniles disperse and only those that have been recruited can reproduce. Matrix population models are a well-established tool in population biology, and size-structured models are especially appropriate for marine populations, where fecundity is often not dependent on age, but rather on size. Neubert and Caswell (2000) first combined matrix population models with the idea of integrodifference equations to create *integrodifference matrix population* models (IMP models). Like IDEs, IMPs are based on the assumption that individuals do not reproduce and disperse simultaneously.

IMP models are formulated by combining population growth dynamics (now for a population with m stages) with the dispersal behaviour of each stage. Here $\mathbf{N}_t$ denotes an $(m \times 1)$ population density vector and the growth dynamics are governed by

$$\mathbf{N}_{t+1}(x) = \mathbf{R}(\mathbf{N}_t(x))\mathbf{N}_t(x). \tag{1.8.1}$$

$\mathbf{R}$ is an $(m \times m)$ transition matrix where entry r_{ij} denotes the rate at which individuals at stage j at time t produce individuals of stage i by time $t+1$ [17]. If we wish to account for varying conditions in the domain, we can also allow these entries to depend on space, i.e. $\mathbf{R}(\mathbf{N}_t(y); y)$ (for a comprehensive look at matrix population models, see Caswell (2006)). Dispersal is included by integrating an $(m \times m)$ matrix $\mathbf{K}$ of dispersal kernels over the domain. Each entry $k_{ij}(x, y)$ of $\mathbf{K}$ denotes the probability that an individual who makes the transition from stage j to stage i during the time step, also moves from location y to location x in that time step [80]. As before, dispersal behaviour will often (except in the case with advection) depend solely on the distance between points. Note that in order to maintain our assumption of sedentary adults, k_{ij} will simply be the Dirac delta function

$$\delta(x) = \begin{cases} +\infty, & x = 0 \\ 0, & x \neq 0 \end{cases} \tag{1.8.2}$$

for all non-larval stages. Combining these two components results in the IMP model

$$\mathbf{N}_{t+1}(x) = \mathcal{F}(\mathbf{N}_t(x)) = \int_\Omega [\mathbf{K}(x, y) \circ \mathbf{R}(\mathbf{N}_t(y); y)]\mathbf{N}_t(y)dy \tag{1.8.3}$$

where $\circ$ represents element by element multiplication rather than standard matrix multiplication [80]. Just like an IDE with overcompensatory dynamics, these models can exhibit a wide range of behaviour including periodic cycles and chaos if elements

of the transition matrix include nonlinearities. Extending IDEs to IMP models is surprisingly analytically simple, as any analysis now just requires finding the eigenvalue of matrices, rather than of the IDE integral operator [82]. Lutscher and Lewis (2004) and, more recently, Robertson and Cushing (2012) have analyzed the critical domain size problem for these models. We will here recapitulate some of their framework and main results and later, in Section 2.5 we will compare a novel approximation with the one currently available [60, 97].

The critical domain size for IMP models is determined much as it was in the case of IDEs without stage-structure. We will look for where the stable steady state solution bifurcates from the zero solution to a non-trivial solution, which will be determined by looking at the leading eigenvalue of the nonlinear integral operator $\mathcal{F}$ in (1.8.3). To do so, we will linearize around zero, and we will here draw from the results on the existence and uniqueness of solutions of Lutscher and Lewis (2004). They have shown that under certain assumptions of compactness and differentiability, the nonlinear integral operator is positive, completely continuous, and strongly Fréchet differentiable at $\mathbf{N} = 0$ as given by

$$\mathcal{F}'(0)\boldsymbol{\phi}(x) = \int_{\Omega} [\mathbf{K}(x, y) \circ \mathbf{R}(0, y)]\boldsymbol{\phi}(y)dy. \tag{1.8.4}$$

Given certain conditions on the primitivity of $\mathbf{R}(0, y)$, they then establish the existence of a unique positive eigenvalue of the linear operator $\mathcal{F}'(0)$ with a corresponding positive eigenfunction. They obtain the superpositivity of $\mathcal{F}'(0)$ under further assumptions and so the dominant positive eigenvalue will determine the stability of the zero steady state. The stability of the zero steady state will be lost as the dominant eigenvalue, dependent on both the growth parameters and the domain length, passes through $\lambda = 1$. Note that the required compactness assumption will not hold in the

case of sedentary stages modelled using the Dirac delta function, so for our chosen populations we will need to use the results of Lutscher and Lewis (2004) to guarantee the superpositivity of some power of $\mathcal{F}'(0)$ rather than of $\mathcal{F}'(0)$ itself.

In the event that individuals only disperse during a pelagic larval stage, the dispersal matrix takes the form

$$\mathbf{K}(x,y) = \begin{bmatrix} k_1(x,y) & k_2(x,y) & \dots & k_m(x,y) \\ \delta(x,y) & \delta(x,y) & \dots & \delta(x,y) \\ \vdots & \vdots & \ddots & \vdots \\ \delta(x,y) & \delta(x,y) & \dots & \delta(x,y) \end{bmatrix}, \tag{1.8.5}$$

and the resulting IMP model no longer has the compactness properties needed to use much of the theory of Lutscher and Lewis (2004). Now we could either approximate the delta function by a different dispersal kernel with very small variance, as was done by Hardin (1990) or we could use the results of Lutscher and Lewis (2004). Biologically, their general idea is that every individual disperses at some time in its life cycle, and so we will consider, for some n, $\mathcal{F}^n$. Lutscher and Lewis first look at the linear case, where they split up the linear operator $\mathcal{F}'(0) = \mathcal{D}$ into $\mathcal{D}_1$ and $\mathcal{D}_2$, where $\mathcal{D}_1$ contains all entries where, for every non-zero r_{ij} we have that $k_{ij}(x,y) \in (L^2(\Omega))^2$ and is zero everywhere else, and $\mathcal{D}_2$ contains the function r_{ij} where $k_{ij} = \delta(x,y)$ and is zero otherwise. Now $\mathcal{D}_1$ is compact and $\mathcal{D}_2$ is bounded. By Lemma 7 in Lutscher and Lewis (2004), if $\mathcal{D}_2$ is nilpotent of order n_0, $\forall y \in \Omega$, then $\mathcal{D}^n$ is compact for all $n \geq n_0$. Furthermore, if assumptions A_1, A_3, and A_4 from Lutscher and Lewis (2004) hold, then $\mathcal{D}^n$ is superpositive for some $n \geq n_0$ and we have that the stability of the zero solution is determined by whether the spectral radius of $\mathcal{D}$ is greater than 1.

Lutscher and Lewis turn next to consider the nonlinear case, here splitting the non-

linear operator $\mathcal{F}$ up into the two operators $\mathcal{F}_1$ and $\mathcal{F}_2$, so that $\mathcal{F}_1$ contains all entries where, for every non-zero r_{ij} we have that $k_{ij}(x,y) \in (L^2(\Omega))^2$ and is zero everywhere else, and $\mathcal{F}_2$ contains the function r_{ij} where $k_{ij} = \delta(x,y)$ and is zero otherwise. Now $\mathcal{F}_1$ is compact and $\mathcal{F}_2$ is bounded, as in the linear case, and by Lemma 8 in Lutscher and Lewis (2004), if $\mathcal{F}_2$ is nilpotent of order n, $\forall y \in \Omega$, then $\mathcal{F}^n$ is completely continuous and this allows us to study the existence of fixed points of $\mathcal{F}^n$ with the same theory as before. Note that a fixed point of $\mathcal{F}^n$ corresponds to a periodic solution, but if there exists a solution which is both a fixed point of $\mathcal{F}^n$ and $\mathcal{F}^{n+1}$, then it is the unique fixed point of $\mathcal{F}$ [60].

It is worth mentioning that grouping individuals by size rather than by age, as is more suitable for most marine populations, will often result in there being non-zero entries on the diagonal of $\mathbf{R}$. If there is no dispersal during these stages, then the condition of nilpotency above will not be satisfied. However, as addressed by Lutscher and Lewis (2004), this seems just to be a product of the grouping, and if the population was instead divided so that an individual could not remain in a stage past one time step, then the diagonal would once again contain only zeros and the above theory would hold.

Lutscher and Lewis (2004) have also shown the existence of a positive fixed point stemming from a transcritical bifurcation at a critical domain length or growth rate, under the assumptions that the spectral radius of $\mathcal{F}'(\infty) < 1$ and that the dominant eigenvalue of $\mathcal{F}'(0)$ is greater than 1. The positive fixed point is unique if $\mathbf{R}(\mathbf{N}(y))$ is monotonic increasing (i.e. for Beverton Holt type functions, but not Ricker or logistic) and is density dependent with diminishing returns for all values of $\mathbf{N}$ (i.e. no Allee effects). In the event that the concavity condition above is not met, we may see periodic solutions or even chaotic ones [60].

We will here introduce an example to illustrate the above theory. We have chosen a size-structured population with two stages, as in Figure 1.8,

$$\mathbf{N}(x) = \begin{bmatrix} N_1(x) \\ N_2(x) \end{bmatrix}. \tag{1.8.6}$$

We will consider N_1 as describing the larval population and N_2 any individuals which have been recruited after settling. Only the second stage reproduces, and reproduction is density dependent, with the growth rate monotonically decreasing as a function of N_2 density. This could be due to filial cannibalism, or competition for nutrients amongst larvae [67]. We assume that individuals in stage N_1 either grow from stage

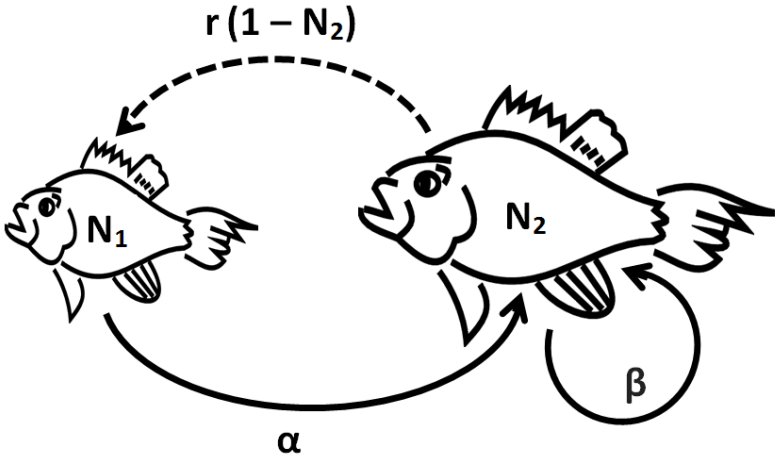

Figure 1.8: Sample fish species life history diagram.

N_1 to stage N_2 at rate α or they die. Individuals in stage N_2 have survivorship β. This results in the transition matrix

$$\mathbf{R}(\mathbf{N}(x)) = \begin{bmatrix} 0 & r(1 - N_2(x)) \\ \alpha & \beta \end{bmatrix}. \tag{1.8.7}$$

The resulting non-spatial model is the simple matrix population model of form

$$\mathbf{N}_{t+1} = \mathbf{R}(\mathbf{N}_t)\mathbf{N}_t, \tag{1.8.8}$$

for which the zero steady state is unstable provided $r > (1-\beta)/\alpha$. If this were not the case, it would be futile to consider the critical domain size of the spatial model, as the population could not persist on a domain of any size. We assume that the population disperses only during reproduction (for our purposes, we will assume a Laplace dispersal kernel in k_{12} and $\delta(x,y)$ elsewhere) and so obtain

$$\mathbf{N}_{t+1}(x) = \int_{-L/2}^{L/2} \left(\begin{bmatrix} \delta(x,y) & k_{12} \\ \delta(x,y) & \delta(x,y) \end{bmatrix} \circ \mathbf{R}(\mathbf{N}(x)) \right) \mathbf{N}_t(y)dy. \tag{1.8.9}$$

We will now study the bifurcation structure of this example by looking at the linearization around the trivial zero steady state. This results in the eigenvalue problem

$$\lambda\boldsymbol{\phi}(x) = \int_{-L/2}^{L/2} \left(\begin{bmatrix} \delta(x,y) & \frac{1}{2b}e^{-\frac{1}{b}|x-y|} \\ \delta(x,y) & \delta(x,y) \end{bmatrix} \circ \begin{bmatrix} 0 & r \\ \alpha & \beta \end{bmatrix} \right) \begin{bmatrix} \phi_1(y) \\ \phi_2(y) \end{bmatrix} dy, \tag{1.8.10}$$

where $b = \sqrt{D/\alpha}$. Continuing to follow the ideas of Lutscher and Lewis (2004) and building on the scalar case presented by Kot and Schaffer (1986), we differentiate twice and examine the relationship between the demographic parameters and the domain length. Differentiating (1.8.10) with respect to x yields

$$\begin{aligned} \phi_1'(x) = &-\left(\frac{r}{2\lambda b^2}\right) e^{-x/b} \int_{-L/2}^{x} e^{y/b}\phi_2(y)dy \\ &+ \left(\frac{r}{2\lambda b^2}\right) e^{x/b} \int_{x}^{L/2} e^{-y/b}\phi_2(y)dy \end{aligned} \tag{1.8.11a}$$

$$\phi_2'(x) = \left(\frac{\alpha}{\lambda-\beta}\right)\phi_1'(x), \tag{1.8.11b}$$

and differentiating again results in

$$\phi_1''(x) = \frac{-r}{\lambda b^2}\phi_2(x) + \frac{1}{b^2}\phi_1(x) \tag{1.8.12a}$$

$$\phi_2''(x) = \frac{\alpha}{\lambda - \beta}\phi_1''(x), \tag{1.8.12b}$$

with boundary conditions

$$\boldsymbol{\phi}'(x) = \frac{1}{b}\boldsymbol{\phi}(x), \qquad x = -L/2, \tag{1.8.12c}$$

$$\boldsymbol{\phi}'(x) = -\frac{1}{b}\boldsymbol{\phi}(x), \qquad x = L/2. \tag{1.8.12d}$$

To begin to find a solution to this boundary value problem, let us assume $\phi_1(x) = A_1 e^{\sigma x}$ and $\phi_2(x) = A_2 e^{\sigma x}$. This results in the system of equations

$$A_1\sigma^2 = \frac{-r}{\lambda b^2}A_2 + \frac{1}{b^2}A_1 \tag{1.8.13a}$$

$$A_2\sigma^2 = \frac{\alpha}{\lambda - \beta}A_1\sigma^2. \tag{1.8.13b}$$

In the event that $\sigma^2 = 0$, we have the relationship

$$A_2 = \left(\frac{\lambda}{r}\right) A_1, \tag{1.8.14}$$

and so our first set of solutions is

$$\phi_1 = A_1 \tag{1.8.15a}$$

$$\phi_2 = \left(\frac{\lambda}{r}\right) A_1. \tag{1.8.15b}$$

If $\sigma^2 \neq 0$, we obtain another relationship between the constants, namely

$$A_2 = \left(\frac{\alpha}{\lambda - \beta}\right) A_1, \tag{1.8.16}$$

and using this (and the assumption that $A_1 \neq 0$), we find,

$$\sigma = \pm\sqrt{\left(\frac{1}{b^2}\right)\left(1 - \frac{r\alpha}{\lambda(\lambda-\beta)}\right)}. \tag{1.8.17}$$

In this way, we obtain two more solutions

$$\phi_1 = A_+ e^{\sigma_+ x} + A_- e^{\sigma_- x} \tag{1.8.18a}$$

$$\phi_2 = \left(\frac{\alpha}{\lambda-\beta}\right) A_+ e^{\sigma_+ x} + \left(\frac{\alpha}{\lambda-\beta}\right) A_- e^{\sigma_- x}. \tag{1.8.18b}$$

We look now for a fourth solution. We assume that $\phi_1(x) = B_1 x$ and $\phi_2(x) = B_2 x$. Since now $\phi_1'' = \phi_2'' = 0$, we obtain the relationship

$$B_2 = \left(\frac{\lambda b^2}{r}\right) B_1, \tag{1.8.19}$$

which results in our fourth set of solutions,

$$\phi_1 = B_1 x \tag{1.8.20a}$$

$$\phi_2 = \left(\frac{\lambda b^2}{r}\right) B_1 x. \tag{1.8.20b}$$

Now any linear combination of these is also a solution, and so putting these together results in a general set of solutions of the form

$$\phi_1 = A_1 + B_1 x + A_+ e^{\sigma_+ x} + A_- e^{\sigma_- x} \tag{1.8.21a}$$

$$\phi_2 = \left(\frac{\lambda}{r}\right) A_1 + \left(\frac{\lambda b^2}{r}\right) B_1 x + \left(\frac{\alpha}{\lambda-\beta}\right) A_+ e^{\sigma_+ x} + \left(\frac{\alpha}{\lambda-\beta}\right) A_- e^{\sigma_- x}, \tag{1.8.21b}$$

and we can now solve for the four unknowns, A_1, B_1, A_+, and A_-, by using the four boundary conditions on $\phi_1'(x)$ and $\phi_2'(x)$ at $x = \pm L/2$. In order for there to exist a non-trivial solution to this system of equations, the following condition must be

satisfied:

$$\left(\frac{2}{b}\right)\left(1+\frac{L}{2b}\right)\left[\left(\frac{1}{b}-s\right)^2 e^{-sL}-e^{sL}\left(\frac{1}{b}+s\right)^2\right] \text{ x}$$
$$\left(\frac{\lambda b^2}{r}-\frac{\alpha}{\lambda-\beta}\right)\left(\frac{\alpha}{\lambda-\beta}-\frac{\lambda}{r}\right)=0$$

where

$$s=\sqrt{\left(\frac{1}{b^2}\right)\left(1-\frac{r\alpha}{\lambda(\lambda-\beta)}\right)}. \tag{1.8.22}$$

We lose the linear stability of the zero steady state as the dominant eigenvalue λ passes through $\lambda=1$, and this leaves us with either

$$\left[\left(\frac{1}{b}-s\right)^2 e^{-sL}-e^{sL}\left(\frac{1}{b}+s\right)^2\right]=0, \tag{1.8.23}$$

$$\left(\frac{b^2}{r}-\frac{\alpha}{1-\beta}\right)=0, \tag{1.8.24}$$

or

$$\left(\frac{\alpha}{1-\beta}-\frac{1}{r}\right)=0, \tag{1.8.25}$$

where s is now given by

$$s=\sqrt{\left(\frac{1}{b^2}\right)\left(1-\frac{r\alpha}{1-\beta}\right)}. \tag{1.8.26}$$

If (1.8.23) holds, then we need to consider two different cases pertaining to the value of s. If

$$1-\frac{r\alpha}{1-\beta}>0, \tag{1.8.27}$$

then s is real and $0<s<1/b$ in which case

$$e^{sL}=\frac{\left(\frac{1}{b}-s\right)}{\left(\frac{1}{b}+s\right)}<1, \tag{1.8.28}$$

and so L must be negative, which is not possible. The other possibility is that s is

complex (we will address the case when $s = 0$ later), i.e. that

$$1 - \frac{r\alpha}{1-\beta} < 0. \tag{1.8.29}$$

In this case, s is of the form $s = ai/b$, where

$$a = \sqrt{\frac{r\alpha}{1-\beta} - 1}, \tag{1.8.30}$$

and

$$e^{\frac{2aiL}{b}} = \frac{\left(\frac{1}{b} - \frac{ai}{b}\right)^2}{\left(\frac{1}{b} + \frac{ai}{b}\right)^2} \tag{1.8.31a}$$

$$= \frac{1 - 6a^2 + a^4}{(1+a^2)^2} + \frac{4a(a^2-1)}{(1+a^2)^2}i \tag{1.8.31b}$$

$$= \cos A + i \sin A. \tag{1.8.31c}$$

So

$$\cos A = \frac{1 - 6a^2 + a^4}{(1+a^2)^2}, \tag{1.8.32}$$

and

$$\sin A = \frac{4a(a^2-1)}{(1+a^2)^2}, \tag{1.8.33}$$

and so

$$A = \arctan\left(\frac{4a(a^2-1)}{1-6a^2+a^4}\right). \tag{1.8.34}$$

It is important to note that in the event that either $\cos A < 0$ or $\sin A < 0$, we need to add π on to the calculation of arctan in order to ensure that we obtain a value for A in the correct quadrant, i.e.

$$A = \arctan\left(\frac{4a(a^2-1)}{1-6a^2+a^4}\right) + \pi. \tag{1.8.35}$$

Now we have that

$$e^{\frac{2aiL}{b}} = e^{Ai}, \tag{1.8.36}$$

and so the critical domain size L^* is

$$L^* = (A + 2n\pi)\frac{b}{2a}. \tag{1.8.37}$$

If we take the parameter values from Figure 1.9, the critical L^* values of (1.8.37) closely match the bifurcation value predicted from the numerical simulations. If we look now to the special case where $s = 0$ when $\lambda = 1$, observe that (1.8.25) is satisfied, and in this way we have infinitely many solutions for the critical domain length. In order to avoid this, we assume a different form for our solutions ϕ_1 and ϕ_2, namely

$$\phi_1 = A_1 + B_1 x + C_1 x^2 + D_1 x^3 \tag{1.8.38a}$$

$$\phi_2 = A_2 + B_2 x + C_2 x^2 + D_2 x^3. \tag{1.8.38b}$$

By putting the above two equations into the system of second order ODEs, we obtain

$$A_2 = \left(\frac{1}{r}\right) A_1 - \left(\frac{2b^2}{r}\right) C_1 \tag{1.8.39a}$$

$$B_2 = \left(\frac{1}{r}\right) B_1 - \left(\frac{3b^2}{r}\right) D_1 \tag{1.8.39b}$$

$$C_2 = \frac{\alpha}{1-\beta} C_1 \tag{1.8.39c}$$

$$D_2 = \frac{\alpha}{1-\beta} D_1, \tag{1.8.39d}$$

so that the solutions in this special case are of the form

$$\phi_1 = A_1 + B_1 x + C_1 x^2 + D_1 x^3 \tag{1.8.40a}$$

$$\phi_2 = \left(\frac{1}{r}\right) A_1 - \left(\frac{2b^2}{r}\right) C_1 + \left[\left(\frac{1}{r}\right) B_1 - \left(\frac{3b^2}{r}\right) D_1\right] x + \left[\frac{\alpha}{1-\beta} C_1\right] x^2 + \left[\frac{\alpha}{1-\beta} D_1\right] x^3. \tag{1.8.40b}$$

Applying the four boundary conditions, we obtain four equations in four variables, A_1, B_1, C_1, and D_1, and in order for there to exist a unique solution, either

$$\left(\frac{L^2}{4b} + L\right)\left(\frac{\alpha}{1-\beta} - \frac{1}{r}\right) - \frac{2b}{r} = 0 \tag{1.8.41}$$

which requires $-2b/r = 0$, which means the population must have a mean dispersal distance of $b = 0$, which is not relevant, or

$$\frac{3b}{r}\left(b + \frac{L}{2}\right) + \left(\frac{1}{r} - \frac{\alpha}{1-\beta}\right)\left(\frac{L^3}{8b} + \frac{3L^2}{4}\right) = 0 \tag{1.8.42}$$

which requires L to be negative and so this solution is not biologically relevant.

As in the scalar case, for certain parameter regimes, a bifurcation from the trivial steady state to a positive non-zero one is possible and dependent on both the demographic parameters and the domain size. Recall that all of the examples we have used in this chapter have employed the Laplace dispersal kernel. This is mainly due to the convenient properties of its derivative but also because of its simple mechanistic description of dispersing individuals simply diffusing and settling at a constant rate. In the event that this process does not describe the dispersal of individuals in a population, analytic results for the critical domain size, like those obtained above, will likely not be possible and the long time solution will need to be found via numerical integration. The next chapter will deal with approximation techniques in order to

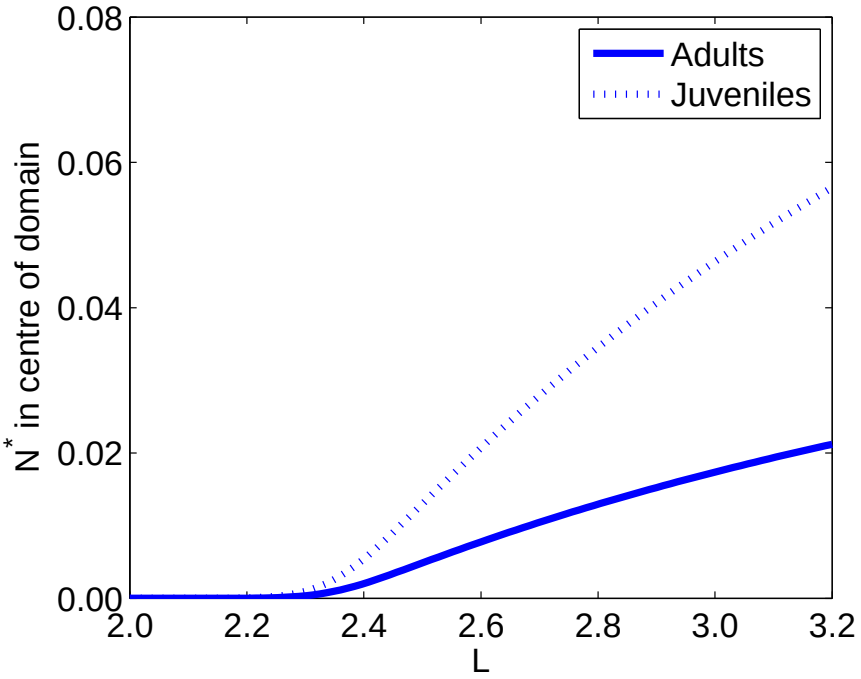

Figure 1.9: Stable steady states of the IMP model for our example (1.8.9). The solid line represents those in the larger adult class N_2 and the dotted line represents the new, smaller larvae N_1. Parameters are $\alpha = 0.8$, $\beta = 0.7$, and $r = 0.6$, and the length is scaled to the mean dispersal distance. Initial conditions were populations with density of both stages at 0.5 everywhere in the domain. Observe the match between the bifurcation value predicted in (1.8.37) of $L* = 2.35$ and that determined numerically.

avoid this computationally expensive situation and to better allow for comparison between kernels and growth functions.

Chapter 2

Approximating the critical domain size

As we have seen in the previous chapter, finding analytic solutions to an integrodifference equation is often a technical exercise in integration, and in most scenarios, the problem is not analytically tractable. Simulations which then require numerical integration are computationally costly and make it difficult to compare IDEs with different dispersal kernels [106]. For efficiency and overall insights, it is often desirable to determine a good approximation to this modelling framework in order to exploit its benefits without needing to find exact solutions.

2.1 Existing approximations; the fraction of natural larval settlement (FNLS)

We will first briefly mention an approximation technique which also, in some sense, redefines persistence. Here, we do not provide any novel work on this topic, but include it since the techniques used form the foundation for the new work in the following sections.

An intuitive, general definition of persistence for marine populations requires that the recruits-per-larva be greater than the inverse of the number of larvae produced in the lifetime of a recruit. For example, if the average recruit produces a million larvae over their lifetime, then on average at least one in a million larvae must survive to recruitment in order for the population to persist. Industrial fishing operates on the assumption that the recruits-per-larva figures for a population below maximum density are considerably greater than those required for mere persistence. It is important for fishery management to determine what fraction of the unfished recruits-per-larva is sufficient to sustain a population in order to avoid overfishing.

Based on these ideas, Botsford et al. (2001) defined the *fraction of natural larval settlement* (FNLS) as the fraction of larvae produced at a given location that settle within the marine reserve bounds. They defined persistence as having an FNLS value greater than the inverse of the larvae produced per recruit over the lifetime of the recruit [11, 56, 113], based on the conservative assumption that only the larvae that end up in reserves go on to reproduce. Fisheries management typically require an FNLS value which varies between 20 and 70%; we will follow Botsford et al. (2001) and use an FNLS value of 35% for illustrative purposes [11, 56, 64].

Lockwood et al. (2002) built on this notion and incorporated the *dispersal success function* developed earlier by Van Kirk and Lewis [113]. The dispersal success function $s(y)$ describes the probability that an individual starting at some point y settles within the domain Ω, as given by

$$s(y) = \int_{\Omega} k(x, y)dx. \tag{2.1.1}$$

The average dispersal success on the domain is then

$$S = \frac{1}{|\Omega|} \int_{\Omega} s(y) dy. \tag{2.1.2}$$

While it is difficult to compare results between IDEs with different kernels using the method of Section 1.5, here it is relatively straightforward to look at the difference that the shapes of the distributions make. In order to do so, we can normalize the dispersal kernels to the effective mean, as mentioned in Section 1.4.1, in order to isolate information about the shape.

Lockwood et al. (2002) have shown that there is a consistent trend amongst the kernels when it comes to dispersal success functions. They found that for all dispersal kernels which they considered, the population collapses if the reserve size is equal to the mean dispersal distance (recall the condition that dispersal success be at least 35%) providing a lower bound for the minimum domain size for all kernels [56]. Looking at Figure 2.1 (similar to that found in Lockwood et al. (2002)), we see that the average dispersal success also indicates a general consistency amongst the kernels, regardless of how the tail is distributed. Figure 2.1 indicates that increasing the size of the patch dramatically increases the fraction of larvae settling in reserves for patch sizes up to twice the mean dispersal distance, but after that, the gains in survival slow down significantly with respect to additional area.

In spite of the consistency across kernels of varying kurtosis, they also observed that the variation in reserve size at the 35% level is at least 50% of the mean dispersal distance and we can see this in Figure 2.1. Obviously, knowing the specific shape of a population's dispersal probability function would shed further light on the necessary sizing. However, without specific information on dispersal patterns, a reserve approx-

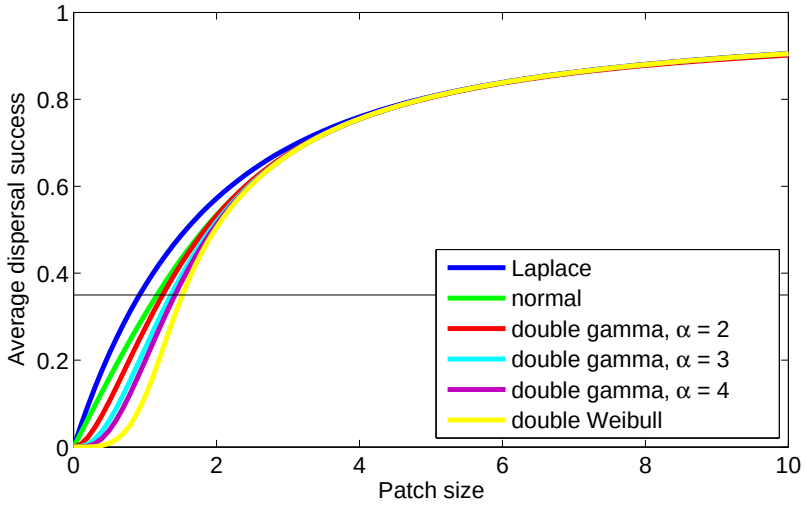

Figure 2.1: Average dispersal success as a function of patch size, scaled to the mean dispersal distance of the kernels (modified from Figure 3 in Lockwood (2002)). The horizontal line is the assumed 35% persistence condition.

imately two to four times the mean dispersal distance seems to be a safe guideline, given the uncertainty in selecting model specifications.

Up to this point, we have described two possible methods of determining the conditions necessary for a population to persist on a closed domain; we can explicitly determine the domain size at which an IDE switches stability from a trivial to a non-trivial steady state, or we can find the length at which the FNLS value is 0.35. It is important to know the limitations of each of these two methods, in order to be able to place the appropriate weight on their results. If determining persistence by looking at the bifurcation structure of an IDE, we should keep in mind that for many kernels and growth functions, analytic results such as those provided in the worked examples are not obtainable. The FNLS approximation is much easier to work with and less cumbersome, but unfortunately it does not fully capture the dynamics of a population.

Observe in the definition of dispersal success (2.1.1) that the demographic parameters

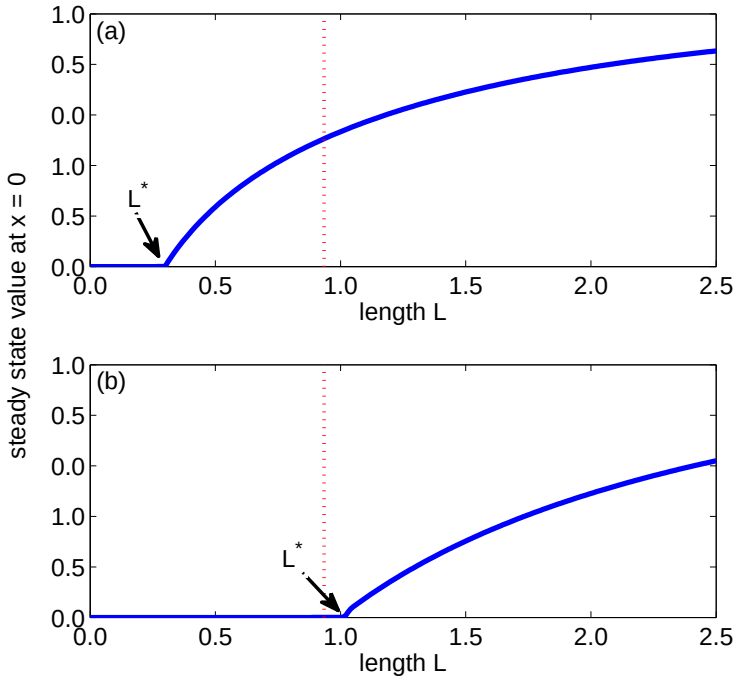

Figure 2.2: Stable steady state of an IDE with Ricker growth and the Laplace dispersal kernel. Parameters are $D = \alpha = 1$ and $K = 1$. In (a), $r = 2$ and in (b), $r = 1$. The dotted vertical line denotes the domain length at which the average dispersal success is 0.35 according to (2.1.4) and the two arrows denote the bifurcation value L^*, as determined by (1.5.20).

of the species are never taken into account. Thus it is feasible that if growth rates are very low, an FNLS value of 35% may not be sufficient to sustain a population. Similarly, if growth rates are high, less than 35% of dispersing larvae may need to end up in a reserve in order for a population to persist.

It is illustrative to compare the critical domain sizes given by the two methods visually. For example, we can compare the bifurcation structure from the zero steady state to a non-trivial steady state of an IDE with Ricker growth and a Laplace dispersal kernel. We can observe the bifurcation value as determined in (1.5.20) and compare this to the FNLS domain requirements. The dispersal success function $s(y)$

for the Laplace dispersal kernel, as defined in (2.1.1), is

$$s(y) = 1 - \frac{1}{2}\left(e^{-\sqrt{\frac{\alpha}{D}}y} + e^{\sqrt{\frac{\alpha}{D}}(y-L)}\right), \tag{2.1.3}$$

and the average dispersal success function as defined in (2.1.2) is

$$S = 1 + \frac{1}{L}\sqrt{\frac{D}{\alpha}}\left(e^{-\sqrt{\frac{\alpha}{D}}L} - 1\right). \tag{2.1.4}$$

Figure 2.2 depicts two possible parameter regimes, as well as qualitatively illustrating what happens for the other dispersal kernels and growth functions mentioned, which is that for low reproductive rates, the critical domain size predicted by the IDE is much higher than that found using the FNLS criteria, and for high reproductive rates, the first bifurcation point of the IDE steady state solution is lower than that of the FNLS criteria. As we can see in Figure 2.2, if using the dispersal success conditions to determine persistence, we may make the reserve too small or unnecessarily large. It is important that adequate attention be paid to the demographic parameters in order to avoid under-estimation of the domain length needed in order to sustain the population. This is especially true in the case with advection, as we will see in the next section.

2.1.1 Alongshore currents and the FNLS condition

We will now turn to briefly consider the FNLS persistence condition in the presence of an alongshore current using the methods recapitulated in Section 2.1, as we will use these results in the subsequent sections. Recall from the previous section on the case without advection that it is the mean dispersal distance rather than the thickness of the tails of the distribution which is the chief determinant of the critical domain size. Here we will see that increasing the strength of advection in the model causes the size of the tails of the dispersal kernels to have more influence. By way of example, we

turn again to the asymmetric Laplace kernel (1.7.4) whose dispersal success function is given by

$$s(y) = \left(\frac{1}{2} - \frac{1}{4\sqrt{\frac{1}{4} + \frac{\alpha D}{v^2}}}\right)\left(1 - \exp\left\{-\left(\frac{v}{2D} + \sqrt{\frac{v^2}{4D^2} + \frac{\alpha}{D}}\right)y\right\}\right)$$
$$- \left(\frac{1}{4\sqrt{\frac{1}{4} + \frac{\alpha D}{v^2}}} + \frac{1}{2}\right)\left(\exp\left\{\left(\frac{v}{2D} - \sqrt{\frac{v^2}{4D^2} + \frac{\alpha}{D}}\right)(L-y)\right\} - 1\right),$$

and average dispersal success by

$$S = 1 + \left(\frac{1}{L}\right)\left(\frac{vD - 2D\sqrt{\frac{v^2}{4} + \alpha D}}{-4\alpha D - v^2 - 2v\sqrt{\frac{v^2}{4} + \alpha D}}\right)\left(\exp\left\{-\left(\frac{v}{2D} + \sqrt{\frac{v^2}{4D^2} + \frac{\alpha}{D}}\right)L\right\} - 1\right)$$
$$- \left(\frac{1}{L}\right)\left(\frac{vD + 2D\sqrt{\frac{v^2}{4} + \alpha D}}{4\alpha D + v^2 - 2v\sqrt{\frac{v^2}{4} + \alpha D}}\right)\left(1 - \exp\left\{\left(\frac{v}{2D} - \sqrt{\frac{v^2}{4D^2} + \frac{\alpha}{D}}\right)L\right\}\right).$$

The shape of these functions can be seen in Figure 2.3. If we let $v = 0$ (i.e. there

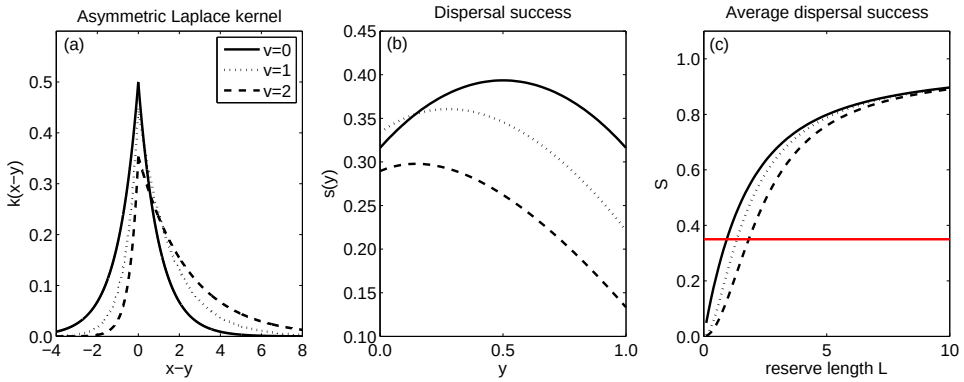

Figure 2.3: Dispersal success approximations for the asymmetric Laplace kernel with varying advective strengths. (a) The dispersal kernel for varying advective strengths, (b) the dispersal success approximation $s(y)$ for each y in the domain [0,1], and (c) the average dispersal success S for a reserve of length L between 0.1 and 10 times the effective mean dispersal distance in the absence of advection. The horizontal line is the assumed 35% persistence condition.

is no advection) in the average dispersal success function for the asymmetric Laplace kernel, we obtain the average dispersal success function for the symmetric Laplace

kernel, as we would expect. This can be seen in Figure 2.4, along the left edge of the right plot.

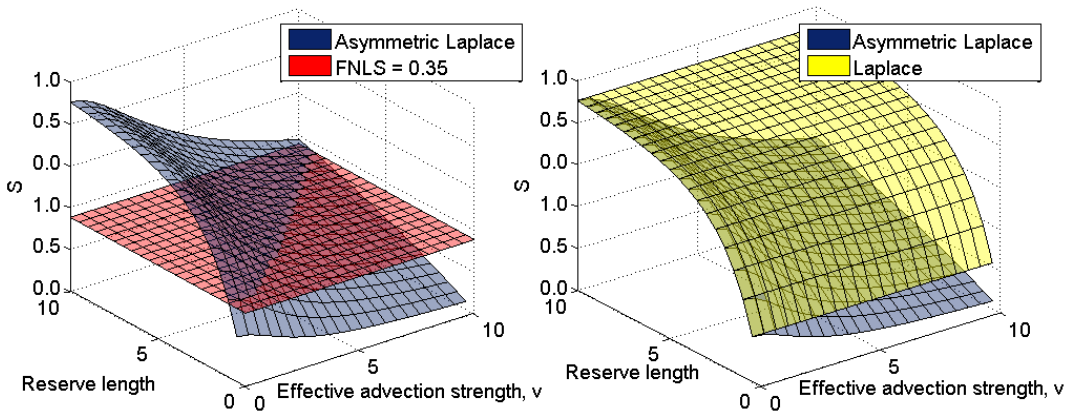

Figure 2.4: A plot of the average dispersal success S for the asymmetric Laplace kernel. On the left, a constant FNLS value of 0.35 is plotted for comparison, and on the right, the average dispersal success of the regular Laplace kernel is plotted. Observe how the Laplace and the asymmetric Laplace kernels produce the same curve along the left axis where $v = 0$, as expected.

We turn now to comparison between kernels with different mechanistic underpinnings. As we can see in Figure 2.5, the differences between the critical domain sizes as determined by the FNLS condition are exacerbated with increased advection. It also seems to be that those kernels which are mechanistically derived from the assumption of a fixed dispersal time respond less strongly to increased advection than those derived from the assumption that larvae settle out of the pelagic stage at a constant rate.

It is an interesting exercise to again compare the necessary reserve length for persistence between the two methods. As we can see in Figures 2.6 and 2.7, because the method using the dispersal success approximation does not take into account the growth rate of the population, low growth rates can result in an underestimation of the critical domain length. At low advective speeds, as in the case without advection, the critical domain size is most influenced by the mean dispersal distance rather

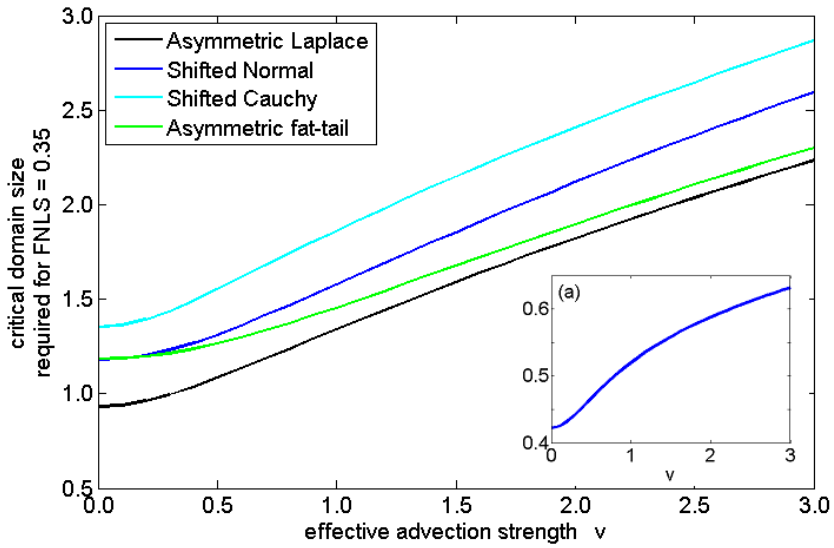

Figure 2.5: Domain lengths required to achieve FNLS = 0.35 for various kernels, taking into account alongshore advection. Parameters are $D = 0.5$, $\alpha = 0.5$, $t_0 = \pi/2$, $\rho = 2/\pi$ and $\mu = 1$ in order to give the kernels an effective mean of 1 (or, in cases without a mean (i.e. distributions with fat tails), for it to be the "standard" kernel as described in Table 1.2. In (a) we see the range of required domain lengths for the same advection values which, for the chosen kernels, amounts to the critical domain length for the asymmetric Laplace kernel subtracted from that of the shifted Cauchy kernel.

than rare long distance events (i.e. the thickness of the tails of the kernels). In the presence of increased advection, however, the critical domain size depends heavily on rare long distance events, as it is the few rare individuals who disperse "upstream" which are able to prevent the population from being washed out of the reserve area entirely. Ecologically, this makes sense, as without a strong current, the best strategy is to keep individuals inside the reserve, whereas in the presence of advection, it is more valuable to have a few individuals dispersing against the flow [62].

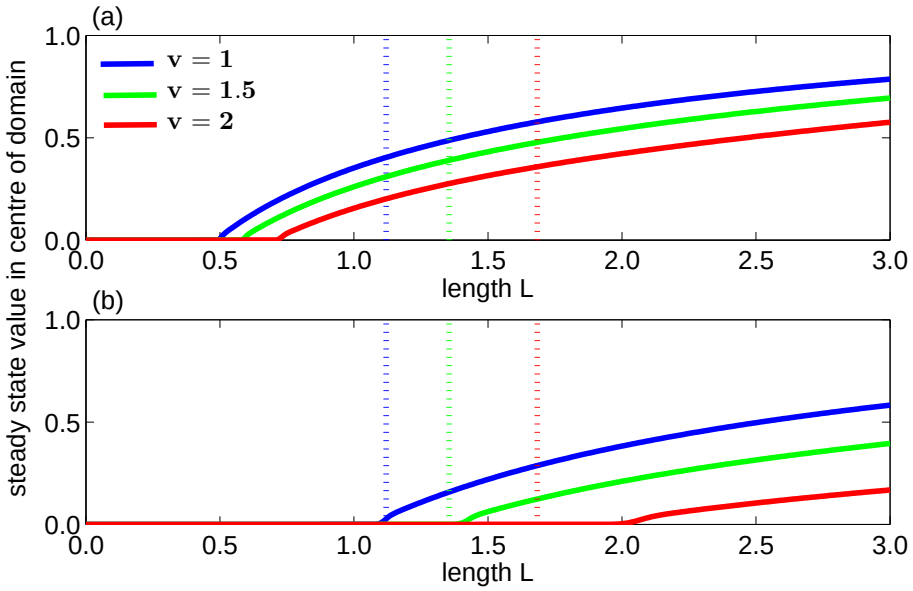

Figure 2.6: Stable steady states of an IDE with Ricker growth dynamics and the asymmetric Laplace kernel with varying levels of advection v. Length is scaled to the mean dispersal distance. In (a), $r = 1.7$ and in (b), $r = 1.1$. The vertical dotted lines are the corresponding critical domain sizes determined by the requirement that $FNLS = 0.35$.

2.2 Modified average dispersal success approximation

While considering the FNLS value of a population lends some insight into whether it is the tails or the mean of the dispersal kernel which impacts population dispersal success, this approximation method is based on some strong assumptions (e.g. the assumption that the critical FNLS value is 35%) and does not take into account the demographic rates associated with the population. In order to predict the reserve size for a population with more accuracy, we turn our attention towards a better approximation. Here we will use ideas from the previous methods by approximating the point of bifurcation from a zero stable steady state to a non-zero one using the FNLS approximation. We will deem this critical length value to be the minimum length which is sufficient for persistence, as in Section 1.5 (though this assumption

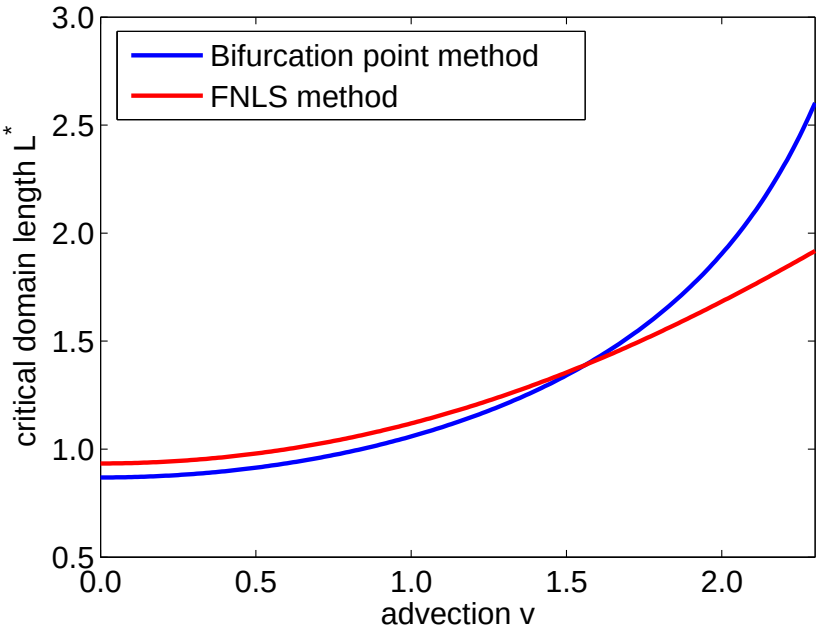

Figure 2.7: Comparison of the critical domain lengths required for persistence for the two methods for varying advection strengths. We consider the bifurcation structure of an IDE from Chapter 1 and compare this to L^* required to achieve an FNLS value of 0.35. $r = 1.1$ and L^* is scaled to the mean dispersal distance. The IDE here has Ricker growth and an asymmetric Laplace dispersal kernel. As we can see, large advection values exacerbate differences between the critical domain sizes determined by the two methods.

will be considered further in the next chapter on extinction rates for low population numbers). In this section, we will introduce a novel approximation to an IDE which can be used to approximate the critical domain size for a wide variety of dispersal kernels and growth functions.

As demonstrated for a single reserve in Figure 2.8, an IDE has the same growth rate dependent bifurcation structure as its growth function $f(N_t)$ but the bifurcation value r^* is greater because of individuals lost to the unfavourable habitat outside the reserve. As the size of a single reserve tends to infinity, the bifurcation value of the IDE tends to that of the non-spatial growth function. If we are unconcerned with the population's spatial distribution inside the reserve area, we can approximate the loss

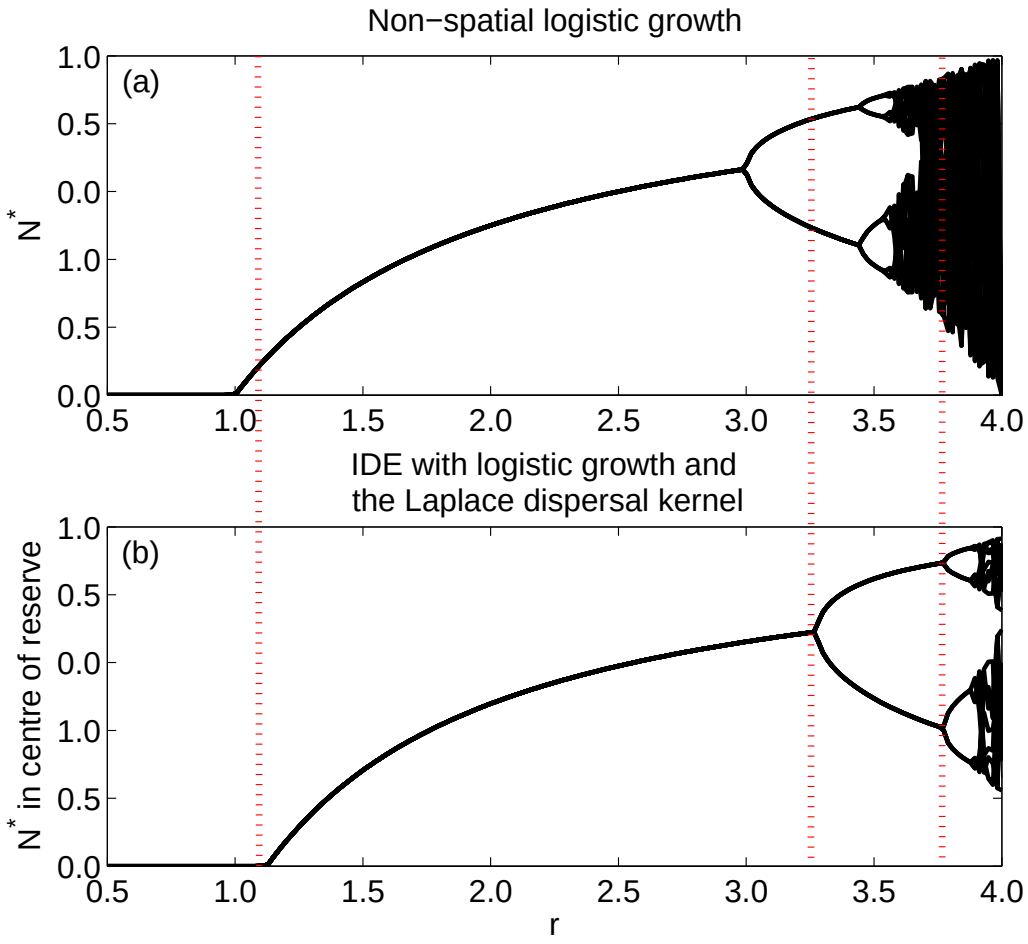

Figure 2.8: (a) Bifurcation structure of the logistic map (A.0.1). Initial condition is $N_0 = 0.5$. (b) Bifurcation structure of an IDE with the logistic map and the Laplace dispersal kernel with a domain 7 times the size of the mean dispersal distance. Initial condition is N = 0.5 in the centre of the domain. As we can see by observing the vertical dotted lines, the loss of individuals to the unfavourable habitat outside the domain in the spatial model causes the solutions to bifurcate for larger values of r.

of individuals due to dispersal to the fished areas by simply multiplying the growth function by some number, say $A \leq 1$, so that

$$\bar{N}_{t+1} = Af(\bar{N}_t), \tag{2.2.1}$$

where $\bar{N}_t$ denotes the total population inside the domain. Now, given that the growth functions considered in this work are of the form $f(N_t) = rN_t g(N_t)$, where r is the

intrinsic rate of growth, we can see that changing A results in the same behaviour as changing r in the non-spatial growth function. As we will see shortly, this A value need not change linearly as the length, width, or spacing of reserves change.

When looking for a suitable value for A, we will first consider the average dispersal success function of Van Kirk and Lewis (1997) which we have been using to approximate the FNLS up to this point. Recall from the previous section that for a single reserve of length L, the average dispersal success is

$$S = \frac{1}{L}\int_{-L/2}^{L/2} s(y)dy, \tag{2.2.2}$$

where $s(y)$ is the dispersal success function for a given point y,

$$s(y) = \int_{-L/2}^{L/2} k(x,y)dx. \tag{2.2.3}$$

An important observation by Van Kirk and Lewis (1997) is that the dispersal success function also provides a fairly reasonable approximation to the population's long time distribution over its patch, as can be seen in Figure 2.9. While the average dispersal success function provides a rough estimate of the fraction of individuals which stay within the domain from one time step to the next, it assumes a constant distribution of individuals throughout the patch. A better approximation to the true fraction of dispersing individuals which are retained would be obtained if we could weight the dispersal success values by the population at each point, such as

$$\widehat{S} = \frac{1}{|\Omega|}\int_{\Omega}\left(\frac{N_t(y)}{\frac{1}{|\Omega|}\int_{\Omega} N_t(z)dz}\right)s(y)dy. \tag{2.2.4}$$

Unfortunately, (2.2.4) is a useless approximation, as the need for an approximation is motivated by the very fact that we usually cannot obtain an explicit solution for

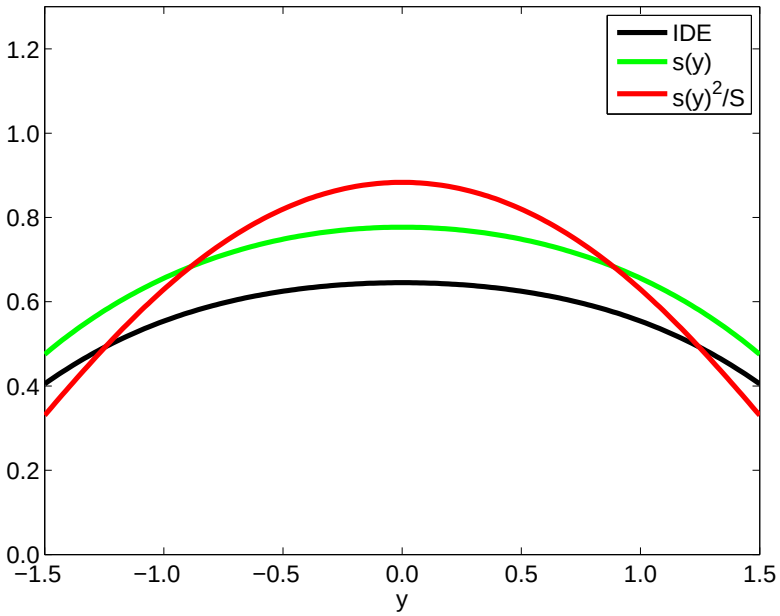

Figure 2.9: Comparison of the steady state solution to an IDE with a Laplace dispersal kernel and logistic growth, with the dispersal success function and the modified dispersal success function. The domain is three times the mean dispersal distance and $r = 3.5$. The modified dispersal success function accentuates differences from the average value by increasing the higher values in the domain centre and decreasing the lower values near the edges.

$N_t(y)$. If instead we approximate the shape of the population by the dispersal success function at each point, we obtain a novel approximation which we will now refer to as the *modified average dispersal success* function $\widehat{S}$. Substituting $s(y)$ and S into (2.2.4) for $N_t(y)$ and $|\Omega|^{-1}\int_\Omega N_t(z)dz$ respectively results in

$$\widehat{S} = \frac{1}{|\Omega|}\int_\Omega \left(\frac{s(y)}{\frac{1}{|\Omega|}\int_\Omega s(z)dz}\right) s(y)dy = \frac{1}{|\Omega|}\int_\Omega \left(\frac{s(y)}{S}\right) s(y)dy. \tag{2.2.5}$$

This can also be interpreted as having a modified dispersal success function at each point, $s(y)^2/S$, as seen in Figure 2.9. In Figure 2.10, we compare the long time behaviour of an IDE with that of the growth function multiplied by the two dispersal success functions. As we can observe in Figure 2.11, this modified approximation $\widehat{S}$ predicts greater average dispersal success than the approximation of Van Kirk

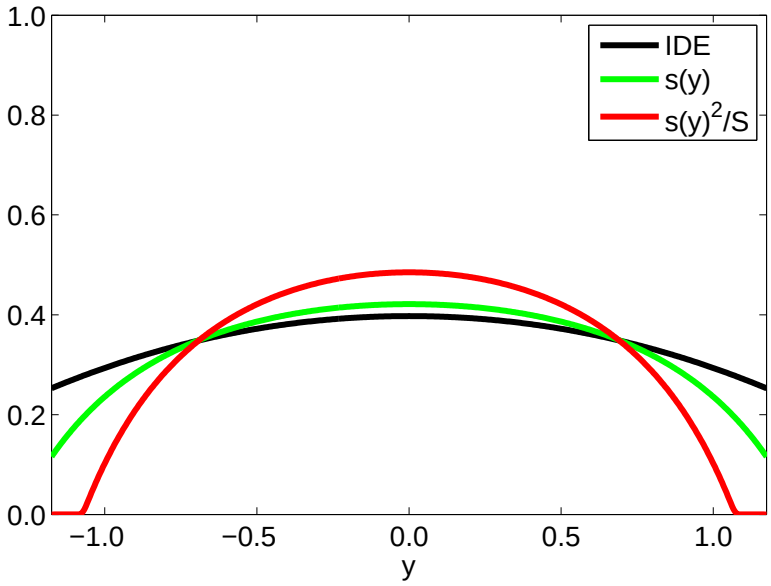

Figure 2.10: The asymptotic behaviour of an IDE, with logistic growth and a Laplace dispersal kernel, and the two approximations, i.e. $N_{t+1}(x) = s(x)rN_t(x)(1 - N_t(x))$ and $N_{t+1}(x) = (s(x)^2/S)rN_t(x)(1 - N_t(x))$. Parameters are $L = 2.35$ and $r = 2.5$. In the approximations,which do not allow for a spatially explicit description of dispersal, if not enough larvae are expected to remain in the domain at the edges of the reserve, the population near the edges of the domain will tend to zero.

and Lewis (1997) for all kernels considered. This is because it weights the (higher) dispersal success of individuals located in the centre of the domain more heavily than the (lower) dispersal success of those at the edges when calculating overall dispersal success for an existing population.

We now look at a simple example, again using the Laplace dispersal kernel,

$$k(x) = \frac{1}{2b} \exp\left(-|x|/b\right) \tag{2.2.6}$$

where $b = \sqrt{D/\alpha}$ is the mean dispersal distance. We have again chosen the Laplace kernel in order to enable direct comparison between the approximations and the analytic expression for the critical domain length, since the Laplace kernel provides one of the few examples in which we can find an analytic expression for both.

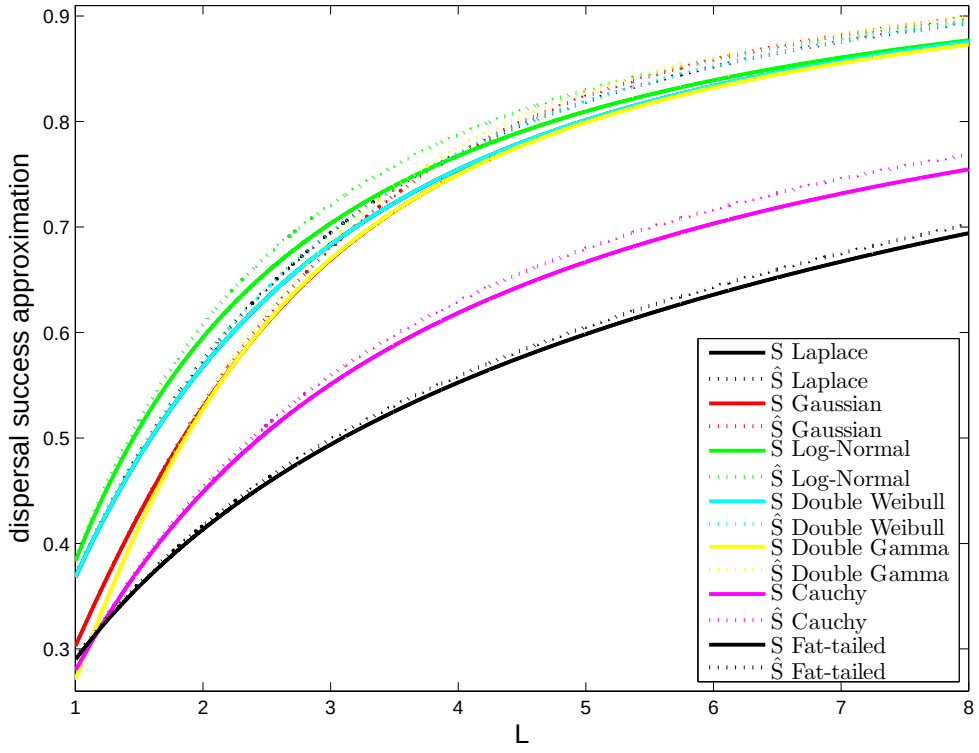

Figure 2.11: Comparison of two dispersal success approximations for a variety of kernels from Table 1.2. S is the approximation of Van Kirk and Lewis (1997) and $\widehat{\mathrm{S}}$ is our new approximation. Reserve length is scaled to the mean dispersal distance. The two approximations are very similar for domain lengths close to the mean dispersal distance, but as L increases, the modified approximation predicts higher dispersal success for all kernels. For the Gaussian distribution, $\sigma = \sqrt{\pi/2}$. For the log-normal distribution, $\sigma = 1$, $\mu = -0.5$. For the double Weibull distribution, $\alpha = 1$ and $\beta = 1$. For the double Gamma distribution, $\alpha = 2$, $\beta = 0.5$. For the Cauchy distribution, $b = 1$ and for the fat-tailed distribution, $\alpha = 1$, $\rho = 2$.

Following the method of the previous chapter, if we twice differentiate a linearized IDE with a Laplace kernel and logistic growth function and apply the boundary conditions, we obtain an explicit solution for the critical domain length. For an IDE of this form, the critical domain size L^* can be expressed explicitly as

$$L^* = \frac{2\,b}{\sqrt{r-1}} \tan^{-1}\left(\frac{1}{\sqrt{r-1}}\right). \tag{2.2.7}$$

Using the average dispersal success function S for a single reserve of length L according to equations (2.2.3) and (2.2.2), the dispersal success function at a given point y is

$$s(y) = 1 - 2\,\mathrm{e}^{-\left(\frac{L}{2}+y\right)/b} - 2\,\mathrm{e}^{\left(y-\frac{L}{2}\right)/b} \tag{2.2.8}$$

and the average dispersal success is

$$S = 1 + \frac{b\left(\mathrm{e}^{-L/b} - 1\right)}{L}. \tag{2.2.9}$$

For logistic growth (which experiences a bifurcation in the stable steady state at $r = 1$ in the non-spatial model), the approximation to the critical domain length L_S^* is the solution to

$$S = 1 + \frac{b\left(\mathrm{e}^{-L/b} - 1\right)}{L} = \frac{1}{r}. \tag{2.2.10}$$

The corresponding modified dispersal success approximation for the Laplace kernel according to (2.2.5) is

$$\widehat{S} = \frac{2\,L\,\mathrm{e}^{\frac{L}{b}} - b + 4\,L\,\mathrm{e}^{\frac{2\,L}{b}} + 8\,b\,\mathrm{e}^{\frac{L}{b}} - 7\,b\,\mathrm{e}^{\frac{2\,L}{b}}}{4\,\mathrm{e}^{\frac{L}{b}}\left(b + L\,\mathrm{e}^{\frac{L}{b}} - b\,\mathrm{e}^{\frac{L}{b}}\right)}, \tag{2.2.11}$$

and so the domain length $L_{\widehat{S}}^*$ at which the solution bifurcates using $\widehat{S}$ as the approximation to A in 2.2.1 can be found by setting

$$\widehat{S} = \frac{2\,L\,\mathrm{e}^{\frac{L}{b}} - b + 4\,L\,\mathrm{e}^{\frac{2\,L}{b}} + 8\,b\,\mathrm{e}^{\frac{L}{b}} - 7\,b\,\mathrm{e}^{\frac{2\,L}{b}}}{4\,\mathrm{e}^{\frac{L}{b}}\left(b + L\,\mathrm{e}^{\frac{L}{b}} - b\,\mathrm{e}^{\frac{L}{b}}\right)} = \frac{1}{r}. \tag{2.2.12}$$

In Figure 2.12, the $\widehat{S}$ approximation provides a closer value of L^*, the bifurcation value of L which we have also designated as the critical domain size, than the S approximation. In Figure 2.13, we see that it is a better approximation for a range of r values. Note that this is most significant for values of r slightly larger than 1,

which is also the parameter regime where the two approximations perform worst.

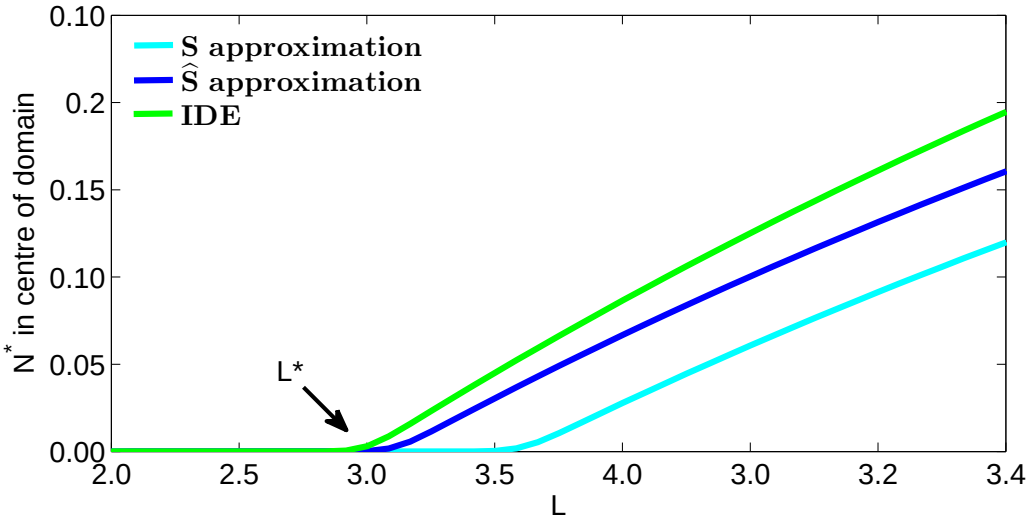

Figure 2.12: Comparison of the stable steady states of the two approximations and an integrodifference equation with a Laplace dispersal kernel and logistic growth. $r = 1.5$, and L is scaled to the mean dispersal distance. Initial condition is $N_0(x) = 0.5$, $\forall x \in [-L/2, L/2]$.

While the modified average dispersal success approximation does a good job of approximating the IDE bifurcation behaviour, the corresponding weighted dispersal success approximation at each point $s(y)^2/S$ does not appear to more closely resemble the population distribution inside the domain than $s(y)$ does, as was observed in Figure 2.9. In spite of this, $\widehat{S}$ still seems to capture the number of individuals being lost outside the reserve better than S does, and thus it does a better job of approximating the critical domain size. As we can see in Figure 2.14, this holds for a variety of kernels.

2.3 Approximations on reserve networks

Turning our attention to reserve networks, we will attempt to approximate the relationship between the width and spacing of patches at which the steady state solution

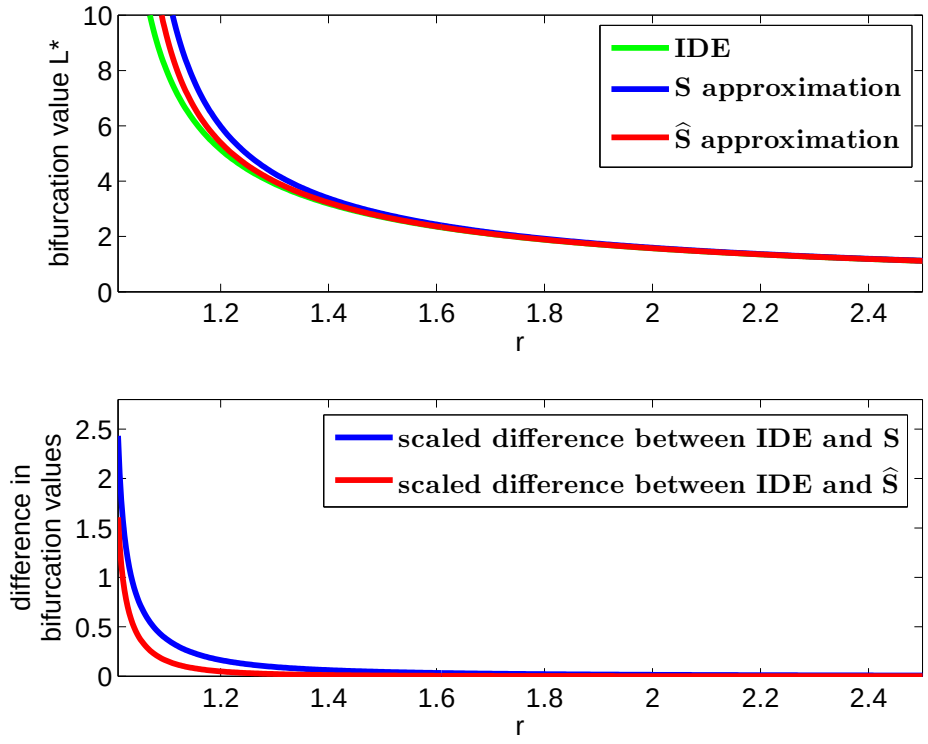

Figure 2.13: (a) Critical domain length for persistence (i.e. for the existence of a non-trivial stable steady state). L^* is scaled to the mean dispersal distance. (b) The difference between the critical domain lengths for the two approximations as predicted in (a), scaled to the IDE value of L^*. Here we can see that for r values close to 1, there is the greatest difference between the critical domain size predicted by the IDE and the two approximations. It is also for r values close to 1 that the novel $\widehat{S}$ approximation here most clearly outperforms the S approximation.

bifurcates from the zero steady state to a non-zero solution as was discussed in Section 1.6. Recall that for an infinite network of reserves (like that seen in Figure 1.5) of length w and periodicity L, the integrodifference equation for the population is of the form

$$N_{t+1}(x) = \sum_{n\in\mathbb{Z}} \int_{nL-w/2}^{nL+w/2} k(x,y) f(N_t(y); y) dy. \tag{2.3.1}$$

The first approximation to A in (2.2.1) that we will mention here for a reserve network is perhaps the most intuitive [20]. As proposed in Dewhirst and Lutscher (2009), we could take A simply to be the fraction of coastline in reserves, i.e. $A = w/L$, which

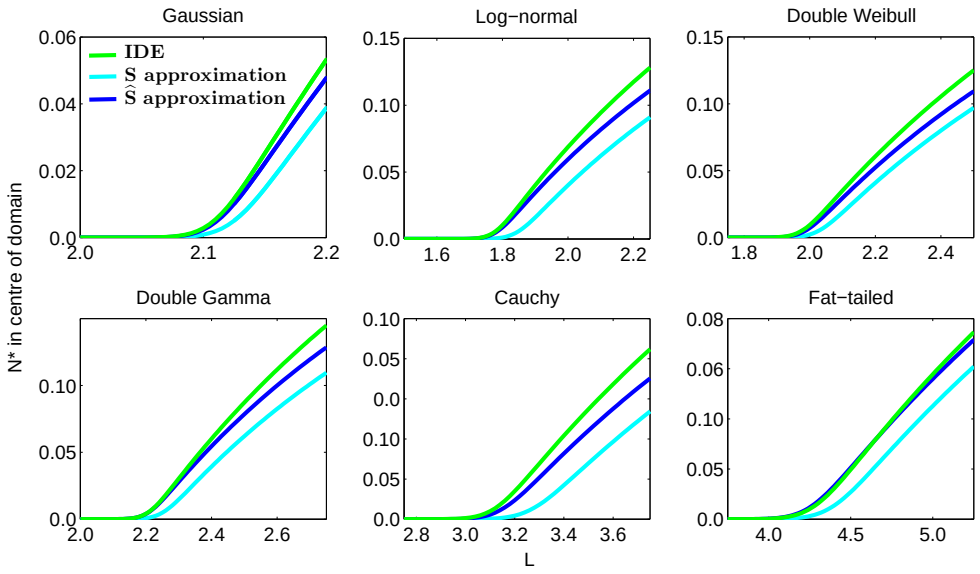

Figure 2.14: Stable steady states for a variety of dispersal kernels and domain lengths. Each IDE and approximation are subject to logistic growth with growth rate $r = 1.5$ and other parameters are as follows: for the Gaussian distribution, $\sigma = \sqrt{\pi/2}$, for the log-normal distribution, $\sigma = 1$, $\mu = -0.5$, for the double Weibull distribution, $\alpha = 1$ and $\beta = 1$. For the double gamma distribution, $\alpha = 2$, $\beta = 0.5$, for the Cauchy distribution, $b = 1$ and for the fat-tailed distribution, $\alpha = 1$, $\rho = 2$. We can see here that in every case, the new approximation bifurcates much nearer to the IDE than the average dispersal success approximation, and this holds for all r values above some critical value, below which the population cannot persist on a domain of any size. Note that as r grows, the difference between the two approximations decreases for all of the kernels.

results in

$$\bar{N}_{t+1} = \frac{w}{L} f(\bar{N}_t). \tag{2.3.2}$$

We could also use the average dispersal success function for A. For an infinite network of reserves, the average dispersal success for a patch (and thus, by symmetry, for every patch), is

$$S = \frac{1}{w} \int_{-w/2}^{w/2} s(y)dy, \tag{2.3.3}$$

where

$$s(y) = \sum_{n=-\infty}^{\infty} \int_{nL-w/2}^{nL+w/2} k(x, y)dx. \tag{2.3.4}$$

By the same reasoning as before, we will see if a modified average dispersal success function of the form

$$\widehat{S} = \frac{1}{w}\int_{-w/2}^{w/2} \frac{s^2(y)}{S} dy \tag{2.3.5}$$

provides a better estimate for the critical domain size. This is again based on the assumption that the population will be more dense in the centre of the domain and that $s(y)$, the dispersal success approximation at each point, adequately approximates the population density. As was found in the case of a single reserve, we can see in Figure 2.15 that again the modified dispersal success function predicts greater dispersal success than the previous approximation from Van Kirk and Lewis (1997). We can only find an explicit expression for the relationship between parameters at the bifurcation point in a few cases, such as those above with a Laplace kernel. We will now compare the approximations to the bifurcation point of the IDE as determined by equation (1.6.10), which is the persistence condition for the width and spacing of a network of reserves and an IDE with a Laplace dispersal kernel and logistic growth. In this case, the dispersal success function is

$$s(y) = \frac{\mathrm{e}^{\frac{y}{b}}\left(\mathrm{e}^{\frac{w}{b}}-1\right)}{2\,\mathrm{e}^{\frac{w}{2b}}\left(\mathrm{e}^{\frac{L}{b}}-1\right)} - \frac{1}{2\,\mathrm{e}^{\frac{w+2y}{2b}}} - \frac{1}{2\,\mathrm{e}^{\frac{w-2y}{2b}}} + \frac{\left(\mathrm{e}^{\frac{w}{b}}-1\right)}{2\,\mathrm{e}^{\frac{y}{b}}\,\mathrm{e}^{\frac{w}{2b}}\left(\mathrm{e}^{\frac{L}{b}}-1\right)} + 1, \tag{2.3.6}$$

and the average dispersal success S for a given patch (and by symmetry, for every patch), is

$$S = \frac{w + b\left(\mathrm{e}^{\frac{-w}{b}}-1\right) + \frac{b\left(\mathrm{e}^{\frac{w}{b}}-1\right)^2}{\mathrm{e}^{\frac{w}{b}}\left(\mathrm{e}^{\frac{L}{b}}-1\right)}}{w}. \tag{2.3.7}$$

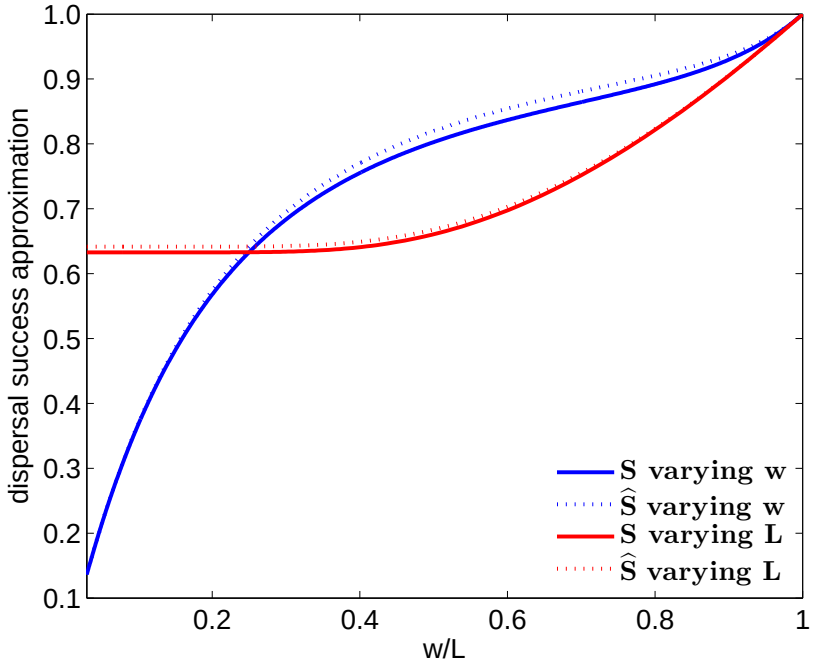

Figure 2.15: Comparison of the two dispersal success approximations on a network of reserves for the Laplace kernel. As in Figure 2.11, the approximation S is that of Van Kirk and Lewis (1997) and the second approximation $\hat{S}$ is the new modified average dispersal success approximation. Note that for both approximations the dispersal success values do not depend only on the fraction of coastline in reserves (i.e. w/L) but rather on the sizing and spacing relative to the mean dispersal distance. In the case where w varied, $L = 10$, and in the case where L varied, $w = 2.5$ (both scaled to the mean dispersal distance of the kernel). As in the case of a single reserve, we can see here that the modified approximation with $\widehat{S}$ predicts slightly greater dispersal success than that using S.

The modified average dispersal success $\widehat{S}$ for a patch is

$$\widehat{S} = \left[\frac{1}{\left((w-b)\mathrm{e}^{\frac{2L+2w}{b}} - b\mathrm{e}^{\frac{L+w}{b}} + (b+w)\mathrm{e}^{\frac{2w}{b}} - b\mathrm{e}^{\frac{3w}{b}} + b\mathrm{e}^{\frac{2L+w}{b}} + b\mathrm{e}^{\frac{L+3w}{b}} - 2w\mathrm{e}^{\frac{L+2w}{b}}\right)}\right] \mathrm{x}$$
$$\left[(4w-7b)\mathrm{e}^{\frac{2L+2w}{b}} - 6b\mathrm{e}^{\frac{L+w}{b}} - b\mathrm{e}^{\frac{2L}{b}} + (7b+4w)\mathrm{e}^{\frac{2w}{b}} + (2w-8b)\mathrm{e}^{\frac{3w}{b}} + b\mathrm{e}^{\frac{4w}{b}}\right.$$
$$\left.+(8b+2w)\mathrm{e}^{\frac{2L+w}{b}} + 6b\mathrm{e}^{\frac{L+3w}{b}} - 12w\mathrm{e}^{\frac{L+2w}{b}}\right]\left(\frac{1}{4}\right) \tag{2.3.8}$$

and if we take the limit of (2.3.8) as $L \to \infty$, the modified average dispersal success for a single reserve area results as a special case, as we would expect.

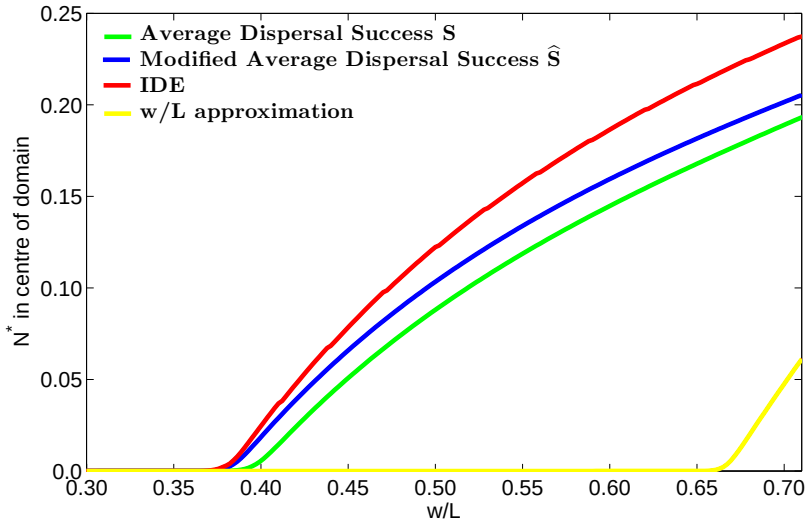

Figure 2.16: Stable steady states of an IDE and the three approximations of Section 2.3, for varying fractions of coastline in reserves. Here we vary w, keeping L constant at 7 times the mean dispersal distance. The IDE has a Laplace kernel and logistic growth, with $r = 1.5$, and an initial condition of 0.5 everywhere in the domain.

We can see in Figures 2.16 and 2.17 a similar bifurcation structure as in the single reserve case, regardless of whether we vary L or w in order to change the fraction of coastline in reserves (w/L). Looking at Figures 2.18 and 2.19 , we see that as the reserves become further apart (i.e. we increase L), the width of reserve necessary to sustain a population, w^*, gets larger, with the eventual limit of $w^* = L^*$, the critical domain size of a single isolated reserve with the same demographic parameters. In this case, we can also see that the new dispersal success approximation $\widehat{S}$ again outperforms S exactly where this matters most, i.e. where they both perform most poorly, which in this case is for large values of L, where w^* is close to L^*.

It is interesting to now consider the effects of varying r on the closeness of the approximations to the IDE value. In Figure 2.20, for values of r greater than approximately

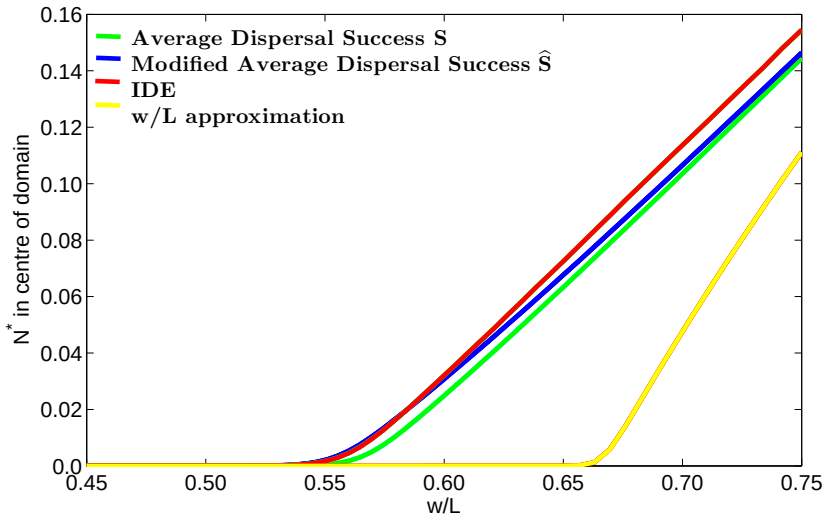

Figure 2.17: Stable steady states of an IDE and the three spatially implicit approximations, for varying fractions of coastline in reserves. Here we vary L, keeping w constant at 2.25 times the mean dispersal distance. The IDE has a Laplace kernel and logistic growth, with $r = 1.5$, and an initial condition of 0.5 everywhere in the domain.

1.5, both S and $\widehat{S}$ provide a very close approximation to the IDE. For r values close to 1, however, a boundary effect occurs. As we decrease r from 1.5, the approximations start to fail, but as we get very close to $r = 1$, the fact that the population cannot persist on a domain of any size if there is any loss due to dispersal dominates the other mechanisms at play. Thus all three of the approximations, as well as the IDE, have critical domain lengths tending to infinity. We can see the profile for varying r when L is 7 times the mean dispersal distance in Figure 2.21. $\widehat{S}$ still outperforms S, and this is again most evident where the two approximations perform most poorly.

If we now hold w constant and look at the maximum periodicity for persistence, we can see in Figure 2.22 that as the width of each reserve increases, the reserves can be further apart, and indeed as w tends towards the critical domain size for a single isolated reserve, L^* tends towards infinity. Looking at Figure 2.23, we see that yet again, the new approximation $\widehat{S}$ outperforms S where they both perform most poorly,

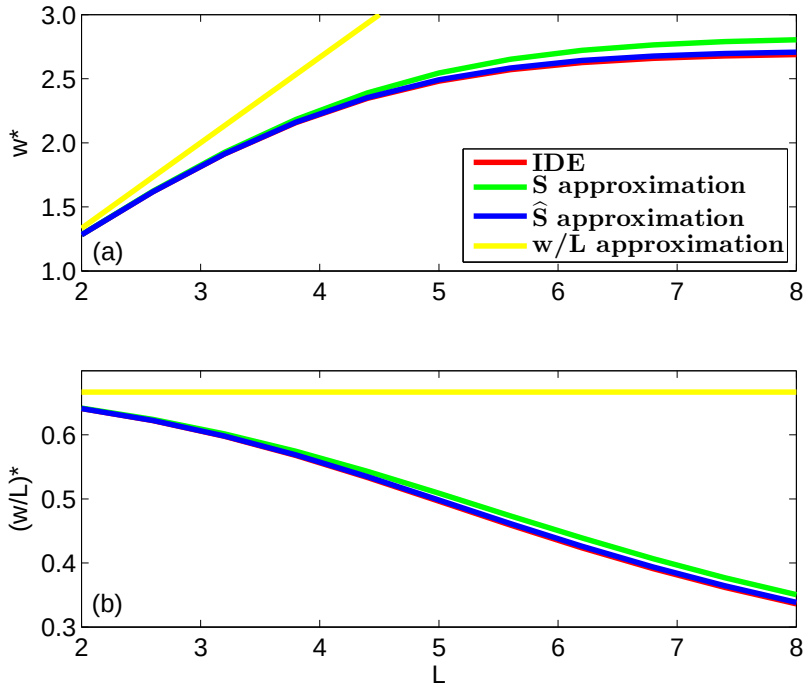

Figure 2.18: (a) The bifurcation value w^* for varying L values for an IDE with a Laplace kernel and logistic growth. (b) Plot of the corresponding fraction $(w/L)^*$ at which the system bifurcates for varying L values. The growth rate r in the good patches is 1.5 and both w and L are scaled to the mean dispersal distance of the Laplace kernel. Observe that the bifurcation relationship between width and spacing is not linear for the IDE, S, or $\widehat{S}$ approximations. Note also that as L continues to increase, the bifurcation value for w^* tends to what L^* would be on a single domain given the same growth rate (i.e. $L^* = 2.703$ for a single patch with $r = 1.5$ by (2.2.7)).

for values of w approaching the value of L^* for a single reserve. These observations are not only consistent for the parameter values seen in the figures above, they hold for a range of different r values.

If we look at Figure 2.24 we can see that, for a given width, $\widehat{S}$, S, and w/L provide the best approximations for smaller values of r and, as before, $\widehat{S}$ most strongly outperforms S and w/L where they are both the weakest, which here is for larger w values. A plot of this for a chosen value of w can be seen in Figure 2.25.

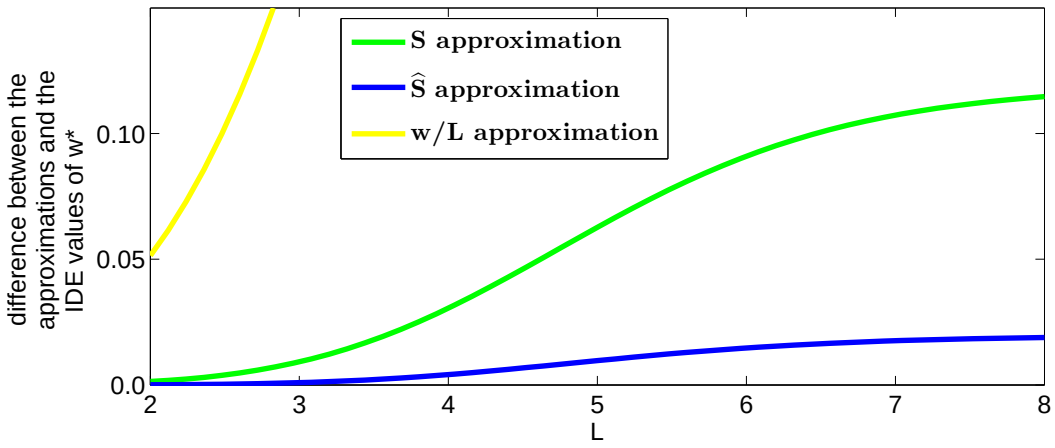

Figure 2.19: The difference between the bifurcation value of w^* predicted by the three approximations, compared with the bifurcation value of the IDE. Parameters are the same as in Figure 2.18.

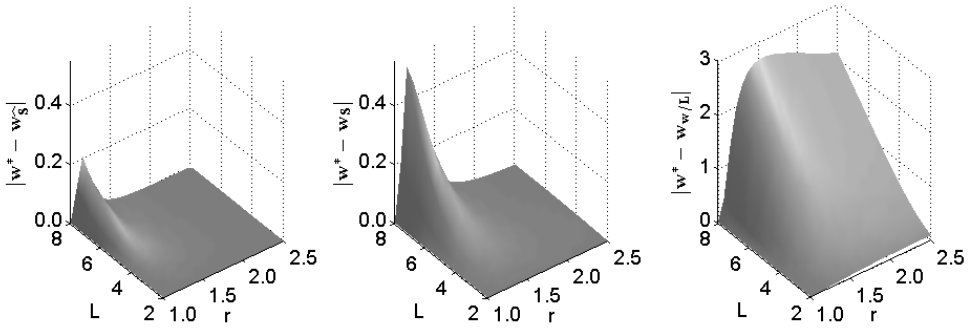

Figure 2.20: Difference between the IDE bifurcation value w^* and the critical domain size predicted by the three approximations $\widehat{S}$, S, and w/L. L and w are scaled to the mean dispersal distance. Note the change of scales on the z-axis in the third plot.

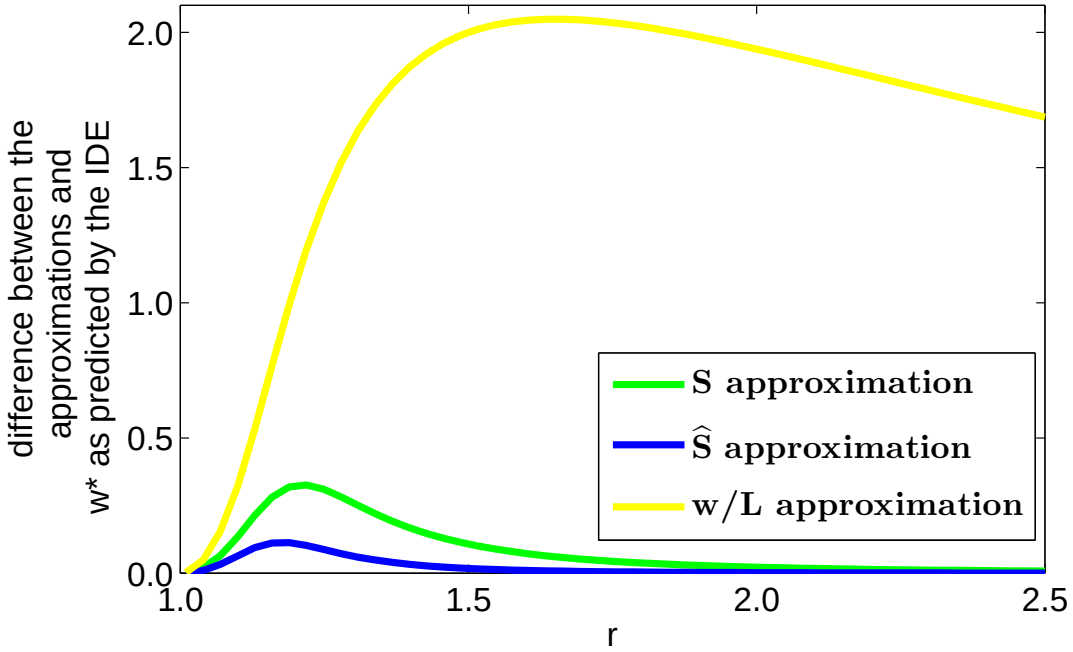

Figure 2.21: Cross-section from Figure 2.20 with $L = 7$. Observe that for values of r between 1 and 2, the approximations do not perform as well as for other values of r, but the modified approximation $\widehat{S}$ still is a better approximation to the IDE than either w/L or S.

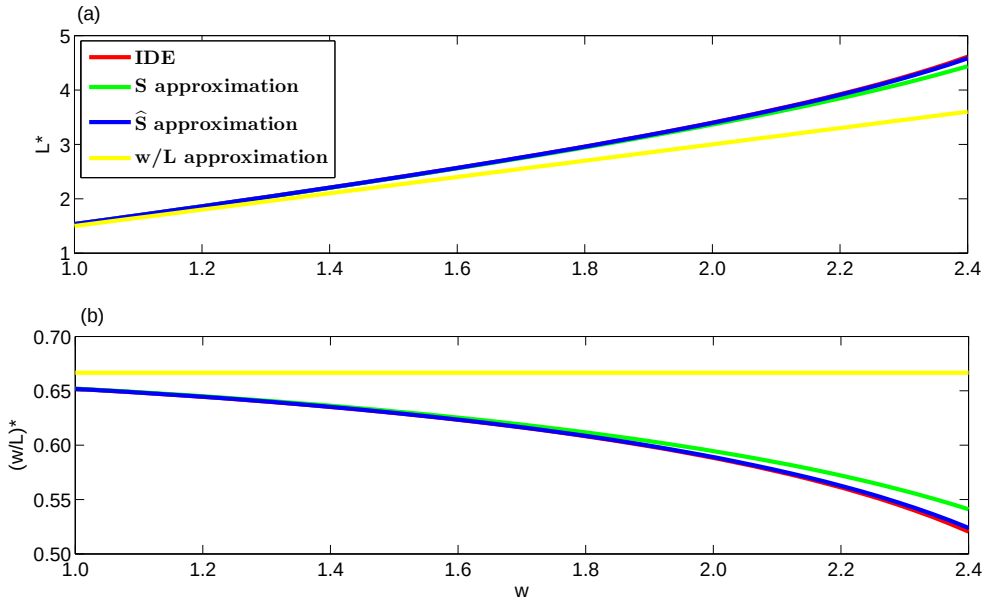

Figure 2.22: (a) The bifurcation value L^* for varying w values for an IDE with a Laplace kernel and logistic growth. The growth rate in the good patches is 1.5 and both w and L are scaled to the mean dispersal distance of the Laplace kernel. (b) The corresponding fraction $(w/L)^*$ at which the system bifurcates for varying w values. Observe again that the bifurcation relationship between width and spacing is not linear for the IDE, the S or $\widehat{S}$ approximation. Note, also, that as w tends to the critical domain size L^* for a single reserve, $(w/L)^*$ tends towards zero (i.e. L tends towards infinity) as we would expect.

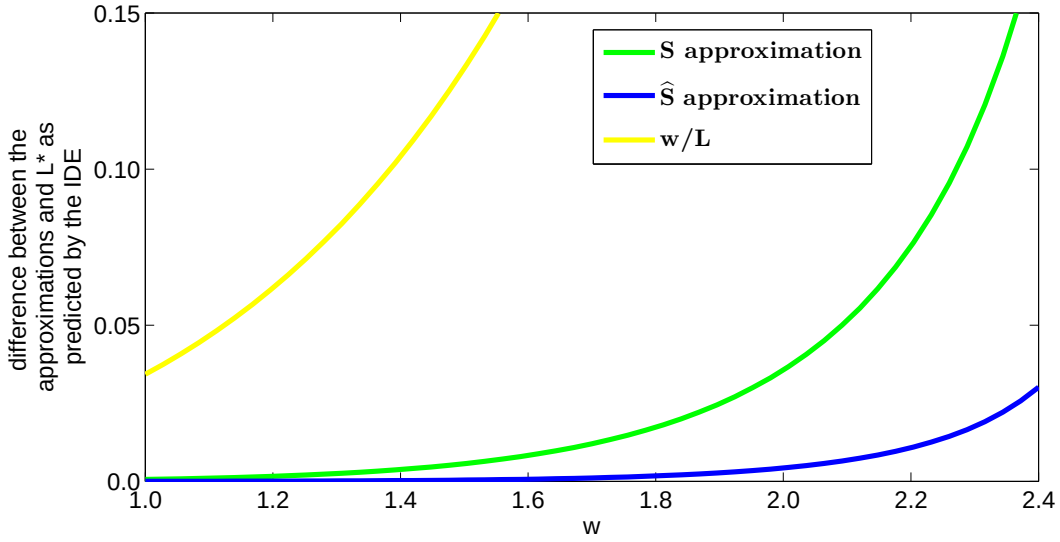

Figure 2.23: The difference between the bifurcation value of L^* predicted by the three approximations compared with the actual bifurcation value of the IDE. Parameters are the same as in Figure 2.22.

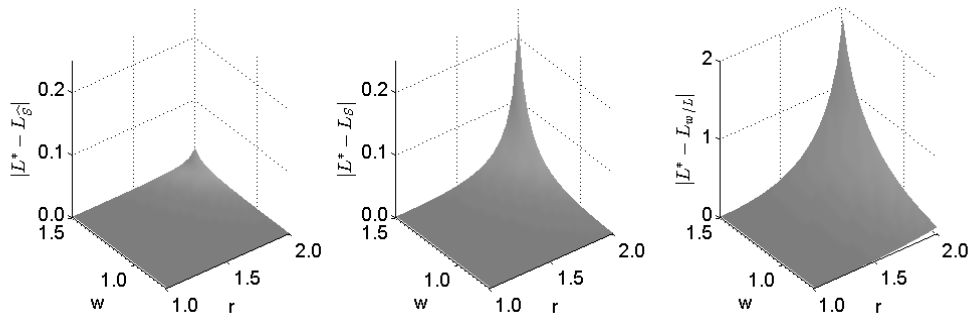

Figure 2.24: Difference between the IDE bifurcation value L^* and the critical domain size predicted by the three approximations $\widehat{S}$, S, and w/L. L and w are scaled to the mean dispersal distance. Note the change in scale on the z-axis in the third plot.

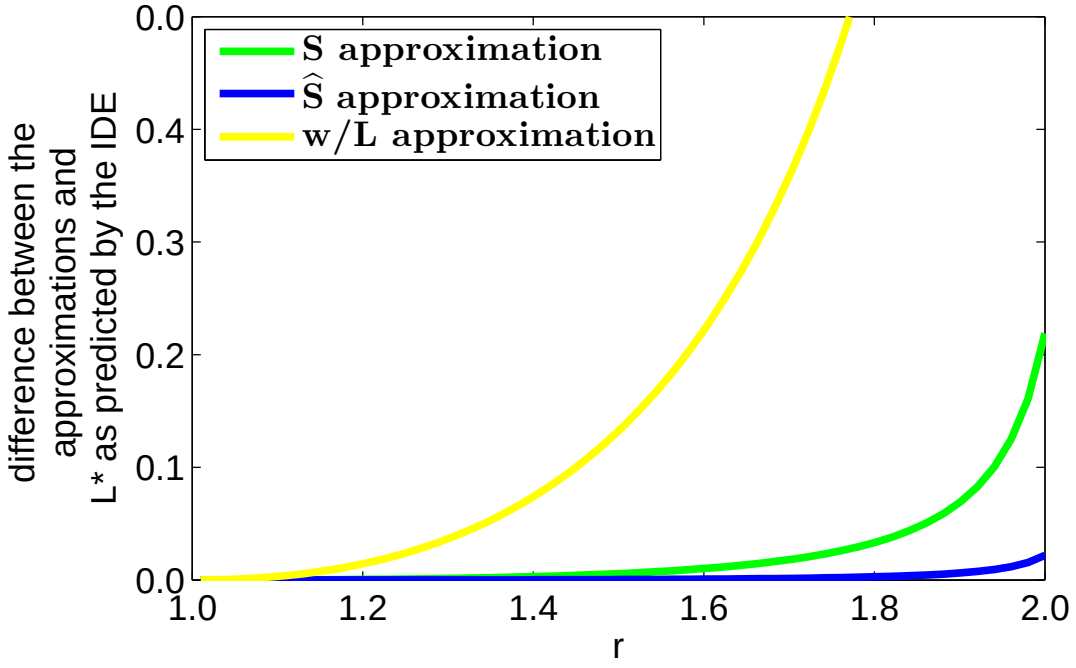

Figure 2.25: Cross-section from Figure 2.24, with $w = 1.5$. Observe that for increasing values of r, the approximations fail, but the modified approximation $\widehat{S}$ is much closer to the IDE here than either the w/L approximation or the S approximation.

2.4 Approximations and alongshore currents

We now allow for the possibility of advection and investigate whether these approximations are still useful. Recall from Section 2.1 that advection tends to exacerbate the differences between the FNLS approximation and the analytic solution. We again incorporate advection into the dispersal kernels of our IDE, and, following the previous sections, we will look to the Laplace kernel for an example, which becomes the asymmetric Laplace kernel in the presence of advection,

$$k(x) = \begin{cases} A\exp(a_1 x), & x \leq 0 \\ A\exp(a_2 x), & x \geq 0 \end{cases}, \tag{2.4.1}$$

where

$$a_{1,2} = \frac{v}{2D} \pm \sqrt{\frac{v^2}{4D^2} + \frac{\alpha}{D}}, \tag{2.4.2}$$

and

$$A = \frac{a_1 a_2}{a_2 - a_1} = \frac{\alpha}{\sqrt{v^2 - 4\alpha D}}. \tag{2.4.3}$$

As with the standard Laplace kernel, we can find the critical domain size L^* (i.e. the length at which the stable steady state solution bifurcates from the zero solution to a non-zero one) of the asymmetric Laplace kernel by differentiating the IDE twice with respect to x and applying the relevant boundary conditions. Recall from (1.7.5) that for an IDE with an asymmetric Laplace kernel and logistic growth,

$$L^* = \frac{4\arctan\left(\frac{1}{\sqrt{\frac{4ra_1|a_2|}{(a_1-a_2)^2}-1}}\right)}{(a_1-a_2)\sqrt{\frac{4ra_1|a_2|}{(a_1-a_2)^2}-1}}. \tag{2.4.4}$$

Turning now to the two approximations of interest, S and $\widehat{S}$, and scaling to the mean dispersal distance, we find that

$$s(y) = \frac{A\left(\mathrm{e}^{\frac{\mathrm{a}_2\,(L-2\,y)}{2}} - 1\right)}{\mathrm{a}_2} - \frac{A\left(\mathrm{e}^{\frac{-\mathrm{a}_1\,(L+2\,y)}{2}} - 1\right)}{\mathrm{a}_1}, \tag{2.4.5}$$

and

$$S = \frac{A\left(\mathrm{e}^{-a_1 L} + a_1 L - 1\right)}{L{a_1}^2} - \frac{A\left(a_2 L - \mathrm{e}^{a_2 L} + 1\right)}{L{a_2}^2}. \tag{2.4.6}$$

When we start to look at the modified average dispersal success, though, we encounter a problem in our assumptions. The motivation behind the modified average dispersal success function comes from the idea that we can estimate the long-term behaviour of a population by the dispersal success function, $s(y)$. Intuitively, we can imagine that if there is a unidirectional current, the dispersal success function is going to be greatest at the upstream edge of the domain, since propagules there have the best chance of settling in the domain when subject to a downstream current. For varying values of v, we can see this if we look at $s(y)$ in Figure 2.26. It does not, however, make sense

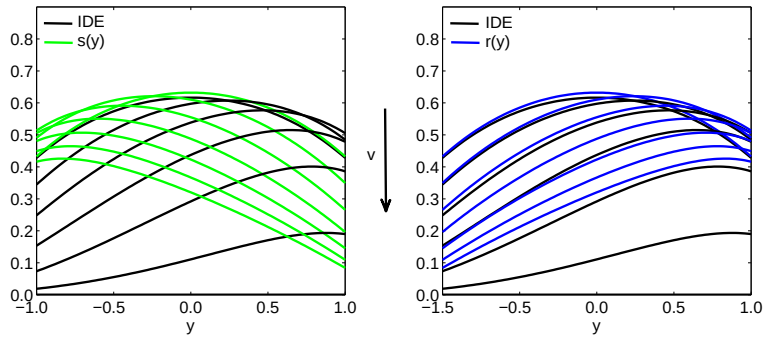

Figure 2.26: Comparison between the dispersal success function, redistribution function, and the long term behaviour of an IDE with an asymmetric Laplace kernel and logistic growth. Here $r = 4$ and the domain is twice the mean dispersal distance. Advection is weakest for the top curves and increases from $v = 0$ to $v = 3$ in increments of 0.5. As we can see here, the stronger the advection, the less $s(y)$ resembles the long term IDE solution and while $r(y)$ stays closer to the IDE solution, for large advection values it also does not respond as sensitively to the change in advection.

to assume this to be the shape of the population as we previously did, since now most

of the larvae which settle inside the domain will settle near the downstream edge. To reconcile this with our approximation, we employ the redistribution function $r(x)$ introduced in Lutscher and Lewis (2004) and defined as

$$r(x) = \int_{\Omega} k(y, x)dx. \tag{2.4.7}$$

For the asymmetric Laplace kernel, this is

$$r(x) = \frac{A\left(\mathrm{e}^{\mathrm{a}_2\left(\frac{L}{2}+y\right)} - 1\right)}{\mathrm{a}_2} - \frac{A\left(\mathrm{e}^{\mathrm{a}_1\left(y-\frac{L}{2}\right)} - 1\right)}{\mathrm{a}_1}, \tag{2.4.8}$$

and this can also be seen in Figure 2.26. The difference between $r(x)$ and $s(x)$ lies in the switch between $k(x, y)$ and $k(y, x)$. For symmetric kernels on an isotropic domain, $k(x, y) = k(y, x)$ and there is no need for a different measure of a population's successful redistribution. However, in the event that dispersal depends explicitly on the starting location or when the kernel is not symmetric, as in the present case, $r(x)$ provides a better estimate for the shape of the population distribution than $s(x)$.

Biologically, we can think of $s(x)$ as the probability that a dispersing individual which begins at x settles anywhere inside the domain by the end of a time step. In contrast, $r(x)$ is the probability that a propagule which begins anywhere in the domain ends up specifically at x by the end of a time step. This captures the downstream tendencies of populations subject to advection far better than $s(x)$.

Observe in Figure 2.26 that the two curves are simply mirror images of each other, reflected across the centre of the domain, and this will be true so long as the kernel does not depend explicitly on space, i.e. $k(x_1, y_1) = k(x_2, y_2)$ when $(x_1 - y_1) = (x_2 - y_2)$ for any x_1, x_2, y_1, y_2 in the domain. The average dispersal success can thus be defined

as

$$S = \frac{1}{|\Omega|}\int_{\Omega} s(y)dy = \frac{1}{|\Omega|}\int_{\Omega} r(y)dy. \tag{2.4.9}$$

When attempting to approximate the population via the newly introduced modified average dispersal success function, we will now multiply the average dispersal success function's integrand through by $r(y)/S$ rather than $s(y)/S$, as we previously did, in order to capture both the population distribution shifting downstream and the dispersal success of the individuals in that distribution, so that the modified dispersal success function subject to advection is

$$\widehat{S} = \int_{\Omega} \frac{r(y)}{S} s(y)dy. \tag{2.4.10}$$

For the asymmetric Laplace kernel this is

$$\begin{aligned}\widehat{S} = &\left[\frac{1}{\mathrm{a_1 a_2}\left(\mathrm{a_1}-\mathrm{a_2}\right)\left(\mathrm{e}^{L\mathrm{a_1}}\left(\mathrm{a_1}^2\mathrm{e}^{L\mathrm{a_2}}-\mathrm{a_1}^2-\mathrm{a_2}^2+L\mathrm{a_1 a_2}^2-L\mathrm{a_1}^2\mathrm{a_2}\right)+\mathrm{a_2}^2\right)}\right]\mathrm{x}\\ &\Big[-A\left(\left(2\mathrm{a_1}^4+2\mathrm{a_1}^2\mathrm{a_2}^2-4\mathrm{a_1}^3\mathrm{a_2}+L\mathrm{a_1}^3\mathrm{a_2}^2-L\mathrm{a_1}^4\mathrm{a_2}\right)\mathrm{e}^{L(\mathrm{a_1}+\mathrm{a_2})}\right.\\ &+\left(-4\mathrm{a_1 a_2}+2\mathrm{a_2}^2+2\mathrm{a_1}^2-L\mathrm{a_1}^2\mathrm{a_2}-2\mathrm{a_1}^2\mathrm{e}^{L\mathrm{a_2}}+L\mathrm{a_1 a_2}^2\right)\mathrm{a_2}^2\\ &+\left(-2\mathrm{a_1}^4-2\mathrm{a_2}^4-2\mathrm{a_1}^2\mathrm{a_2}^2+4\mathrm{a_1 a_2}^3+4\mathrm{a_1}^3\mathrm{a_2}+L\mathrm{a_1 a_2}^4-L\mathrm{a_1}^4\mathrm{a_2}\right.\\ &\left.\left.-3L\mathrm{a_1}^2\mathrm{a_2}^3+3L\mathrm{a_1}^3\mathrm{a_2}^2\right)\mathrm{e}^{L\mathrm{a_1}}\right)\Big].\end{aligned} \tag{2.4.11}$$

However, in spite of the changes to $\widehat{S}$, the IDE is still far more sensitive to advection than either the S or $\widehat{S}$ approximations. In Figure 2.26, as advection strength increases, the dispersal success and redistribution functions are no longer a close approximation to the shape of the equilibrium solution, and this is only worsened with increasing advection. In Figures 2.27 and 2.28, for small values of advection, the approximations predict critical domain sizes close to that of the IDE, but as advection increases, the approximations grow increasingly further away from the IDE value until the advection value reaches V_p, where the population cannot persist on a domain of any size as all

individuals are swept downstream. This is because of the inability of the spatially implicit approximation to capture the effects of wash-out. In the spatially implicit approximation, the population gets swept downstream, but so long as the domain is large enough, it can remain within the reserve area (this is why there is no critical advection value for the approximations). The IDE, however, captures the fact that the population will tend to zero upstream, as the population is washed downstream, even though the total population size may remain constant or even increase. See Figure 2.29 for an illustration of this wash-out effect.

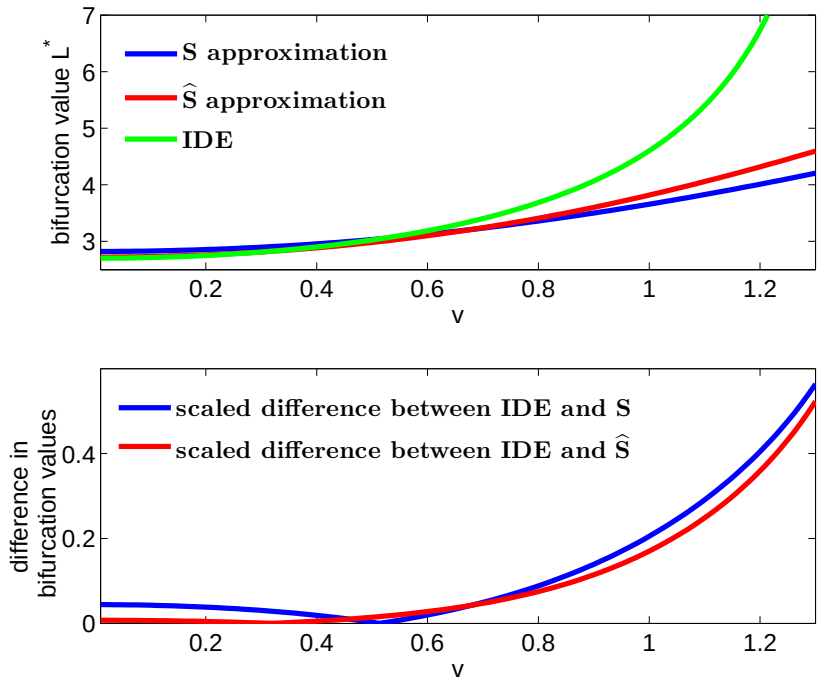

Figure 2.27: (a) Critical domain size of an IDE with an asymmetric Laplace dispersal kernel and logistic growth with $r = 1.5$, as compared with the two approximations. As v increases towards its critical value, where the population cannot persist on a domain of any size, the approximations diverge from the IDE. (b) Differences between the critical domain sizes of the IDE and the two approximations as in (a), scaled to the critical domain size of the IDE.

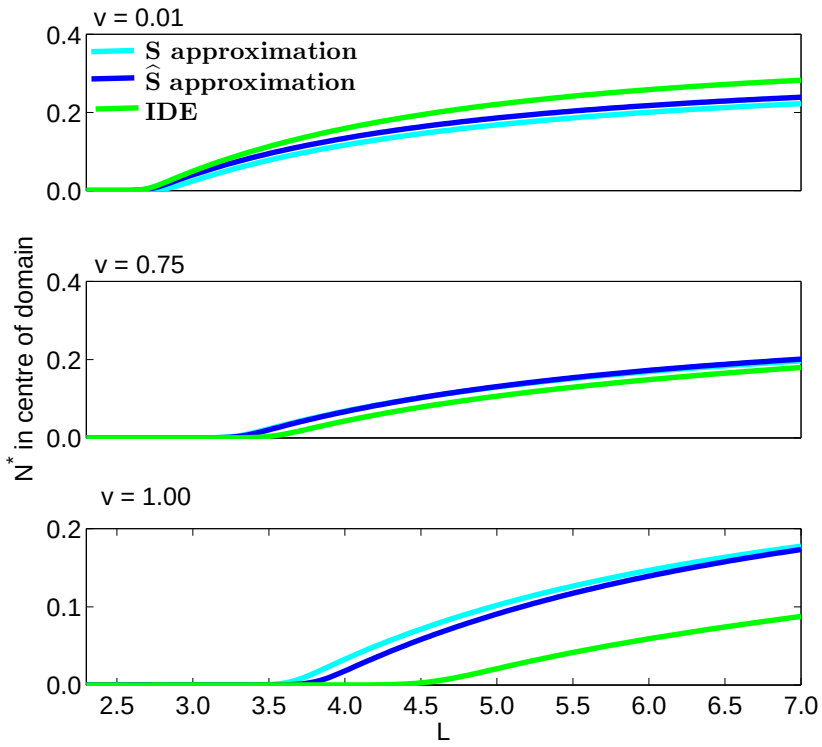

Figure 2.28: Stable steady states for varying L values and three different advection strengths. The IDE has logistic growth and an asymmetric Laplace dispersal kernel, and in all of the figures, $r = 1.5$. The initial condition for the population is 0.5 everywhere in the domain. As we can see, as we increase advection v, the bifurcation behaviour of the IDE is much more strongly affected than either of the two approximations.

2.5 Approximations and size-structured populations

We now explore the efficacy of these approximations for integrodifference matrix population (IMP) models. A size-structured modification to the dispersal success function was made by Lutscher and Lewis (2004) and here we will find that our novel modified average dispersal success function also outperforms the standard approximation for stage- or size-structured populations. We employ their definition of the dispersal success function for a matrix, which will now need to be determined for each entry in the dispersal matrix $\mathbf{K}(x, y)$. For each $k_{ij}(x, y)$ in $\mathbf{K}(x, y)$ we can determine $s_{ij}(y)$ which is the probability that an individual who was produced by an individual in

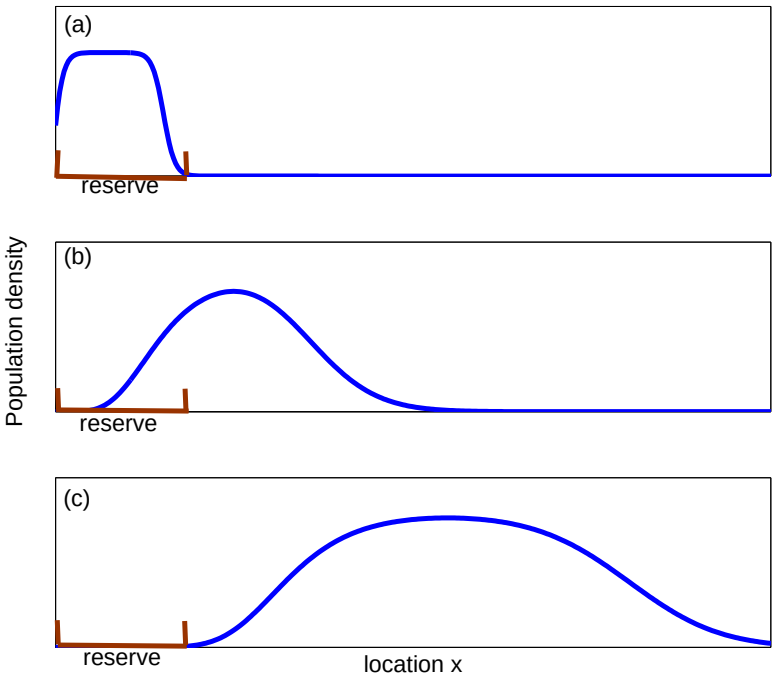

Figure 2.29: Schematic of the wash-out effect which is captured by an IDE but not by the spatially implicit model. Observe that the total population persists, but the population within the reserve does not. (a) shows the initial population distribution within the reserve, (b) shows it after 10 generations subject to advection, and (c) is after 25 generations.

stage j at location y settles in the domain of interest Ω. The matrix of dispersal success functions for a given point y is then

$$\mathbf{s}(y) = \underbrace{\int_\Omega \mathbf{K}(x,y)dx}_{(a)} = \underbrace{\left(\int_\Omega k_{ij}(x,y)dx\right)}_{(b)} = \underbrace{(s_{ij}(y))}_{(c)} \tag{2.5.1}$$

where (a) is integration over a matrix and so each entry is integrated irrespective of the others, and the brackets around (b) and (c) denote matrices. Unless no individuals are lost to fished areas outside the domain, then $0 \leq s_{ij}(y) \leq 1$. As before, we can take an average of $\mathbf{s}(y)$ for all of the y values in Ω in order to obtain the matrix form

of the average dispersal success function $\mathbf{S}$,

$$\mathbf{S} = \frac{1}{|\Omega|}\int_{\Omega}\mathbf{s}(y)dy = \frac{1}{|\Omega|}\int_{\Omega}\int_{\Omega}\mathbf{K}(x,y)dxdy, \tag{2.5.2}$$

where again the integration is over each entry in the matrix. If we wish to include an alongshore current in the IMP model, we would have to again consider the redistribution function introduced in Lutscher and Lewis (2004). They define the redistribution matrix as

$$\mathbf{r}(x) = \int_{\Omega}\mathbf{K}(x,y)dy = \left(\int_{\Omega}k_{ij}(x,y)dy\right) = (r_{ij}(x)). \tag{2.5.3}$$

As in the scalar case, if the kernel is symmetric and does not depend explicitly on the starting location, then $\mathbf{r}$ and $\mathbf{s}$ are the same (i.e. $\mathbf{K}(x,y) = \mathbf{K}(y,x)$ implies $\mathbf{r} = \mathbf{s}$), which would hold in any of the symmetric kernels at which we have previously looked.

Lutscher and Lewis (2004) describe $\mathbf{N}^*(x)$ as the non-zero equilibrium solution to an IMP, and $\mathbf{N}_*$ as its spatial average, and then look at $|\mathbf{N}^*(x) - \mathbf{N}_*|$. If this is small (and we can assume it is for patch sizes which are large compared to the mean dispersal distance) then the dispersal success approximation

$$\mathbf{N}^*(x) = [\mathbf{s}(x) \circ \mathbf{R}(\mathbf{N}_*)]\mathbf{N}_*, \tag{2.5.4}$$

is of first order in $|\mathbf{N}^*(x) - \mathbf{N}_*|$ [60] and in the case of non-symmetric kernels, we have a similar result for

$$\mathbf{N}^*(x) = [\mathbf{r}(x) \circ \mathbf{R}(\mathbf{N}_*)]\mathbf{N}_*. \tag{2.5.5}$$

Integrating both sides, they obtain the spatial average $\mathbf{N}_*$ as the approximate solution of the corresponding algebraic equations

$$\mathbf{N}_*(x) = [\mathbf{S} \circ \mathbf{R}(\mathbf{N}_*)]\mathbf{N}_*. \tag{2.5.6}$$

For non-symmetric kernels,

$$\mathbf{N}_*(x) = [\mathbf{D} \circ \mathbf{R}(\mathbf{N}_*)]\mathbf{N}_*. \tag{2.5.7}$$

where

$$\mathbf{D} = \frac{1}{|\Omega|}\int_\Omega \mathbf{r}(y)dy = \frac{1}{|\Omega|}\int_\Omega\int_\Omega \mathbf{K}(y,x)dxdy. \tag{2.5.8}$$

Note that for any sedentary stages whose entry in $\mathbf{K}(x,y)$ is the Dirac delta function, the corresponding entry in either $\mathbf{S}$ or $\mathbf{D}$ will be 1, as all individuals who start in the domain, stay in the domain, since they do not disperse at all. We can see an example of how well these approximations perform when approximating example (1.8.9) in Figures 2.30 and 2.31.

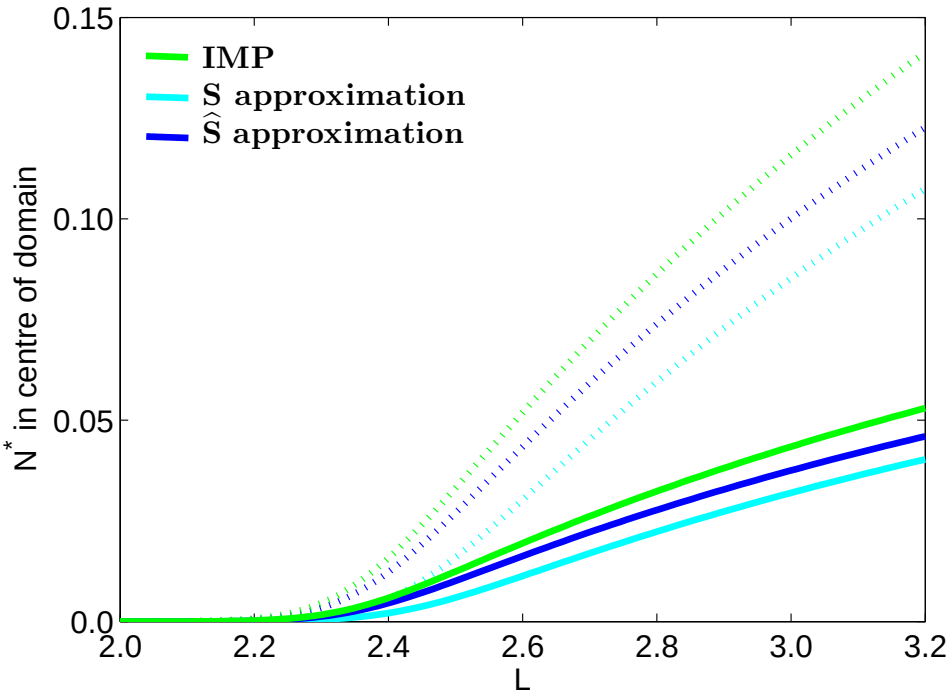

Figure 2.30: Comparison of the stable steady states of the IMP model of example (1.8.9) and the two approximations, S and $\widehat{S}$. The solid line represents those in the larger adult class, the dotted line represents those in the larval stage. Parameters are $r = 0.6$, $\alpha = 0.8$, $\beta = 0.7$, and L is scaled to the mean dispersal distance. Initial conditions are population density of 0.5 of both stages everywhere in the domain.

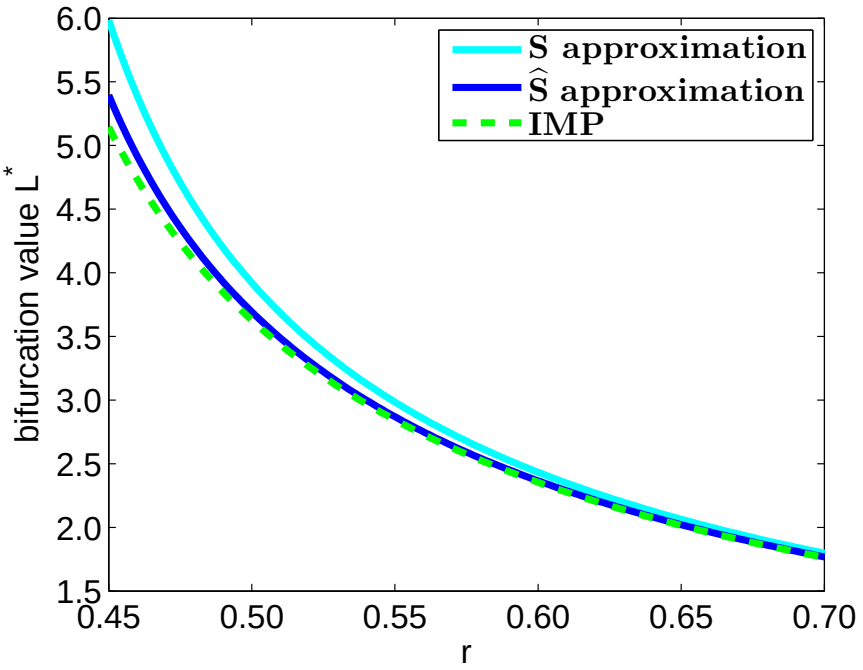

Figure 2.31: Comparison of the critical domain length as determined by the IMP and two approximations to (1.8.9) where $\alpha = 0.8$ and $\beta = 0.7$. As we can see, once again the modified dispersal success approximation remains closer to the IBM solution than the standard dispersal success function, especially for values of r close to the critical value, past which the population cannot persist on a domain of any size.

2.6 Discussion and conclusions about approximating IDEs

While IDEs provide us with a way to model a variety of dispersal patterns and growth functions, they are seldom analytically tractable and the critical domain size can often only be obtained via methods involving numerical integration which is computationally costly. More importantly, it is difficult to gain understanding of the effects of various parameters, or the properties of the growth function or dispersal kernels. Approximations to an IDE framework are thus useful for ecologists and those wishing to compare the effects of different dispersal patterns, and reproductive or mortality rates. The standard approximation introduced by Van Kirk and Lewis (1997) has been used in two different ways; first, to determine the FNLS and corresponding re-

quired domain size to achieve some desired level of larval retention, and second, to approximate an IDE by a spatially implicit model.

In this chapter, we have introduced a novel approximation to the proportion of individuals which successfully settle within the reserve area, based on assumptions about population distribution within the reserve area, using the dispersal success function. This modified average dispersal success function consistently provides a better approximation to the critical domain size required for persistence than the Van Kirk and Lewis (1997) approximation. This is most apparent in parameter regimes close to critical demographic values. Whether a population of interest has parameters in these regions is another issue and will be species and environment specific, but since the novel approximation seems to always be a closer approximation, it should be used in place of the average dispersal success function.

The novel modified dispersal success approximation introduced in this chapter allows for a spatially implicit model with a domain of a single large reserve, an idealized network of infinitely many evenly sized and spaced reserves, populations in areas subject to alongshore currents, and stage- or size-structured populations.

Looking at where both the Van Kirk and Lewis (1997) approximation, as well as our novel approximation fail also sheds some light on the dynamics of populations subject to advection. The explicit spatial dependence of an IDE allows it to capture the effects of "wash-out", while the spatially implicit approximation techniques do not. In this case, the new approximation still outperforms that of Van Kirk and Lewis (1997), but caution should be used if considering populations subject to strong advection.

Some insight about IDEs can also be gained by considering these approximations. Since being able to approximate the proportion of individuals which successfully settle within the reserve area results in a critical domain size close to that of the original IDE, this seems to be the main aspect of dispersal which drives the bifurcation behaviour of an IDE. Thus even if a suitable mechanistic kernel is not available, if the proportion of individuals locally retained can be determined empirically, the resulting necessary domain size as determined by the simple map approximation to the IDE can be examined.

We now consider some of the uncertainty inherent in finite populations. We will find in the next chapter that the approximation introduced in Chapter 2 is also useful in stochastic models and allows for similar insights.

Chapter 3

Uncertainty at low population densities

In this work, we are interested in marine populations which have been heavily exploited by fishing practices or other anthropogenic involvement. Our focus is thus on populations often well below the environmental carrying capacity. Depending on the extent of overfishing in the area, population numbers may be very low, especially initially when a marine reserve is first created. It is at these low population densities that the previous chapter's deterministic approaches may no longer be accurate. We turn our attention now to consider an analogous stochastic model and some approximations to it in order to be able to say something about the required reserve size for a small initial population.

When looking to create a stochastic analogue to the IDE framework employed in the previous sections, we will maintain our assumption of a population with dispersing larvae and sedentary adults. As in the deterministic case, we will start by considering a non-structured population (i.e. *all* of the individuals reproduce and then undergo a dispersal process), in order to be able to determine the effects of stochasticity on

the extinction dynamics without conflating any results with those caused by more complicated population structures. Unlike in the deterministic models of Chapters 1 and 2, it is no longer certain in the stochastic model whether a population will tend towards extinction or survive into the future. Stochastic models, like those developed in this chapter, are often used in *population viability analyses*, where models use demographic and environmental information to predict future population dynamics. Incorporating stochasticity into an IDE framework will allow us to consider questions of importance to conservation biologists, fishery managers, and policy-makers.

It is important to consider what it means to conservationists and fishery managers for a population to be "viable". Obviously, in the biological world, every population has a certain risk of extinction, no matter how secure it may seem. Natural disasters and anthropogenic catastrophes can quickly wipe out large portions of populations, making them susceptible to smaller chance events or other disasters. Conservation biologists have come up with a variety of measures of acceptable extinction risk deemed to be low enough to meet conservation goals.

One common way to determine whether or not a management strategy will achieve conservation objectives is to determine the *minimum viable population,* MVP (recall that several useful terms and abbreviations can be found in Table 1.1). This is the population size necessary to ensure a specified probability of persistence for a given period of time [27]. This idea first emerged in Shaffer (1981), where an MVP was described as the minimum population having a 99% chance of persisting for 1000 years despite the effects of natural catastrophes and demographic, environmental, and genetic stochasticity [27].

Traill et al. (2010) put forth an interesting idea, which was to see if perhaps there

exists a "magic number" which satisfies the MVP requirements for a large range of species. They proposed that, across taxa, anything greater than 5000 individuals should suffice as an MVP estimate [112]. While this idea was appealing in its simplicity, several reasons why this is not a possibility were pointed out by Flather et al. (2011), where they revisited the uncertainty assumed by Traill et al. and found that the corrected MVP for each of the populations considered ranged from 425 individuals to 54,712, rather than all of the values being near 5000 [27]. Others have advised against using MVP estimates as precise conservation targets, but rather suggest using them to explore possible mechanisms behind population decline or to compare management strategies [14].

Another means of quantifying extinction risk is to consider the *time to extinction* of a population, though we will only briefly touch on that in this chapter, as it deals with populations assumed to be in decline and, in general, pertains to a part of the possible parameter space which we would like to avoid. Another way to consider population persistence is through the *probability of extinction* of a population. What is deemed to be an acceptable probability of extinction may vary, from an extinction risk of 5% over the next 50-100 years [27], a 99% probability of persistence for 40 generations or a 90% probability of persistence for 100 years [14]. Something we will look at extensively in this work is the *probability of ultimate extinction*, which is the limit of the probability of extinction as we let time tend to infinity.

Ginzburg (1982) used quasiextinction probabilities to assess population viability, and this may more accurately capture extinction risk than requiring the population to reach zero. This is because models often contain insufficient information to deal with populations at extremely low densities [1]. We do not consider this further, but mention it as an alternative way to measure extinction risks.

The methods we will consider here have been motived by and applied widely to studies of genetics (see e.g. [24, 46]). In this chapter, we will first look at demographic stochasticity by developing a spatially explicit individual-based model (IBM) in Section 3.3.1, which most closely mimics the IDE framework previously considered. Assuming the IBM to be the most realistic way to incorporate uncertainty into an IDE, we will compare subsequent spatially implicit approximations to it. The first way we approximate the results of the IBM simulations is by scaling up to the population level in Section 3.3.2 where we make a similar approximation to that made in Section 2.2 based on the idea that we can avoid computationally costly explicit spatial dependence by assuming that during each time step a fixed proportion A of the population is lost via dispersal to areas subject to heavy fishing pressure.

In Section 3.3.3 we modify a simple Galton-Watson branching process to include this loss via dispersal into fished areas, in order to obtain some useful analytic results. Here we can use classical results on simple branching processes to say something about the reserve size required to achieve specific conservation goals. We compare these results with both the corresponding deterministic models as well as the simulations from the stochastic IBM.

In the second part of the chapter, starting with Section 3.4, we address the same questions using many of the same methods, but this time accounting for environmental stochasticity as well. In Section 3.4.1 we reformulate our IBM to include dependence on a random environmental variable, and then we again consider the dynamics at the population level in Section 3.4.2. The branching process framework used to investigate the effects of demographic stochasticity is modified in Section 3.4.3 to include environmental variation, using the theory of branching processes in

random environments.

3.1 Accounting for various types of stochasticity

When looking to incorporate uncertainty into a model, there are many different sources of stochasticity to consider. First, there is demographic stochasticity, which affects the fitness of each individual independently from the others. We will here treat this as a random variable with a given distribution obtained through statistical study [22, 52, 101]. Demographic stochasticity is most important for populations with very low numbers, as individual level fluctuations in growth and death rates most significantly effect subsequent generations for smaller populations.

The other type of stochasticity we will mention here is important in populations of any size, not only very small populations [52]. Environmental stochasticity is due to series of small or moderate fluctuations in the environment that affect the demographic rates of all individuals in a population in the same way [52]. These events affect all individuals simultaneously and in a similar fashion, and could be things such as a period of different temperatures or changes in the availability of a certain food source [54]. In natural populations, environmental stochasticity was previously thought to be more important than demographic stochasticity in determining the probability and causes of extinction [53] but this has recently been challenged by Melbourne and Hastings (2008). The comparative risk of extinction caused by various types of stochasticity is an interesting area, and one which we hope the present work may help to shed some light on for similar models.

In the remainder of this chapter, we will look at these two types of stochasticity and compare how the reserve size required to meet conservation goals in our stochas-

tic models compares to that determined by the deterministic models of the previous chapters.

3.2 Existing results

To the best of our knowledge, stochastic analogues to integrodifference equations have only been studied by those interested in calculating the invasion speed of travelling waves subject to some form of variability. Kot et al. (2004) used density independent branching random walks to stochastically simulate an IDE with density independent growth and we will draw from their work here in Sections 3.3.3 and 3.4.3. They considered an IDE with linear growth,

$$N_{t+1}(x) = R \int_{-\infty}^{\infty} k(x-y) N_t(y) dy$$

and ultimately determined that, in this particular case, stochastic variation in dispersal and reproduction does not lower the asymptotic invasion speed [50]. They chose to use a linear IDE in order to examine the simplest model which could then be compared to a density dependent process in order to separate the effects caused by any nonlinearities as opposed to those due to stochasticity. We will also assume linear growth, with the added justification that many of the populations we are interested in will be well below the environmental carrying capacity, having been under heavy fishing pressure, and for many growth functions, a linear growth rate is a close approximation to the nonlinear growth function at very low densities in the absence of an Allee effect.

Much of the work we will look at here builds on previous results on *non-spatial* stochastic population models (e.g. [22, 52, 54]). Leigh (1981) has derived an approximate formula relating the average time to extinction of a spatially homogeneous pop-

ulation subject to environmental fluctuations to various other factors. These factors include the population's initial size, its carrying capacity (assuming the population has some maximum value determined by the environment), its intrinsic growth rate, and the impact of the environmental variation [54].

Lande et al. (1993) used a model with simple exponential growth up to some carrying capacity C at which point the growth rate is zero. They then compared the risks of extinction from different stochastic factors using their calculations on the scaling of the times to extinction. It is a well known result of models formulated like this that for populations subject to demographic stochasticity, the time to extinction increases exponentially with the carrying capacity if the growth rate is positive, and it scales to a logarithmic increase in C if the growth rate is negative [52]. In the case of environmental stochasticity, the time to extinction scales asymptotically as a power of the carrying capacity if the growth rate is positive, and if the growth rate is negative, then the time to extinction again scales logarithmically to C [52]. They also found that for populations with sufficiently large growth rates and initial conditions over a certain size, the time to extinction does not change as the initial population size varies. This occurs as these populations will tend towards their carrying capacity where they will fluctuate for several generations before finally going extinct due to stochastic fluctuations. They posited that their results provide a general qualitative scaling relationship for many single-population models and that the relative risks of extinction that they found are general properties of these dynamics [52].

A different approach was taken by Hiebeler (1997), who looked at a variety of ways to incorporate space into stochastic single species models. He first performed spatial simulations using cellular automata and then explored several analytic approximations, using two versions of mean field theory which differed in the assumed spatial

correlations [40]. The approach we will take will vary from those above in its formulation but should serve to add to this wider body of literature on single species spatial stochastic models.

3.3 Demographic stochasticity

In this section, we will explore the effects of incorporating demographic stochasticity into our model. As in much of the literature, we will focus on models of linear growth, which will enable us to avoid the complex behaviour caused by nonlinear growth functions. This is a reasonable approximation given our biological assumptions, since we are assuming that population density in reserve areas is initially well below carrying capacity and, given a wide range of common growth models, linear growth can be assumed near the zero steady state.

3.3.1 Individual based models with demographic stochasticity

Ideally, we would be able to simulate every individual fish in a population via an IBM and track the movement of each of their offspring. This is the simplest and perhaps most intuitive way to examine possible outcomes, but unfortunately this is computationally expensive and the results are difficult to compare. In addition, using this method, the tools have not yet been developed to be able to say anything analytically regarding the probability of extinction and so it is difficult to determine sensitivity to various factors. Here we include a brief description of an IBM analogous to an IDE in order to be able to compare our later approximations to these results.

The IBM formulation we will consider consists of a domain of length L (describing the reserve area), an initial population of size z evenly distributed throughout

the domain at generation $n = 0$, and a dispersal kernel $k(x, y)$ which, as before, is a probability density function describing the probability of movement of an individual during one time step from location y to x. As in the deterministic models, we will only model females in all of our work on stochastic populations, assuming that there are always an adequate number of males to fertilize the eggs at the population levels of interest. As we are considering only females, each individual reproduces according to a mass probability function $\{p_i\}$ for $i = 0, 1, 2, \ldots$ where p_i is the probability of an individual having i offspring in one reproductive period. Note that this process will not explicitly incorporate individual deaths, but rather p_1 is the probability that either the female produced one offspring and then died, or that she produced no offspring but survived to the next generation. Thus parental survival is included in the term "offspring" in this chapter. Note that $\sum p_i = 1$. At the start of each generation, we first determine, for each individual, the random variable which determines the number of offspring produced, as drawn from $\{p_i\}$. Each of these offspring then disperses according to the dispersal kernel and if they remain within the domain, they survive to the start of the next time step and the process is repeated.

In order to investigate the probability of extinction (unless otherwise stated, we will take this to mean the probability of the total population size being zero) by a given generation n or the ultimate probability of extinction, it is necessary to run many simulations of the model. We plot some examples of these values in Figure 3.1 and 3.2. This representation will be a common way for us to compare subsequent approximations to the IBM in the following sections. As we can observe in Figure 3.1, the higher the expected reproductive rate ($\xi = \sum ip_i$ with summation over i), the lower the probability of extinction by a given generation n. When ultimate extinction is uncertain, however, the variance will affect the ultimate extinction probability, as we can see in Figure 3.2. If ultimate extinction is not certain, then the probability of

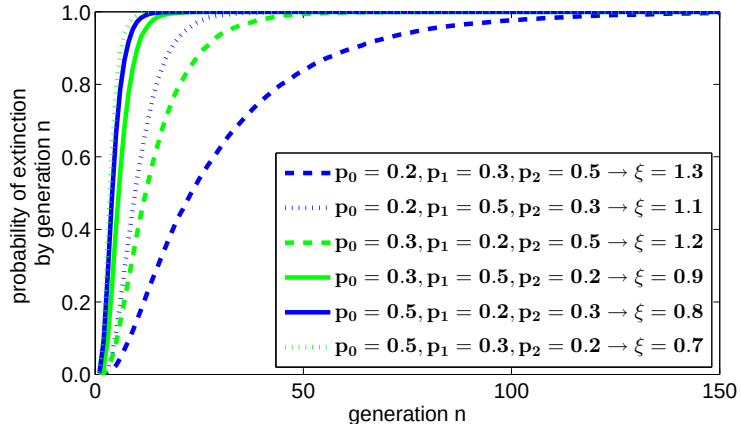

Figure 3.1: Probability of extinction by generation n as found by the IBM simulation. Initial population is 10 individuals on a domain of length 3.5 times the mean dispersal distance, with growth probabilities as listed in the legend. Dispersal follows a Laplace dispersal kernel. Using Matlab, we performed 10000 simulations in order to obtain these results.

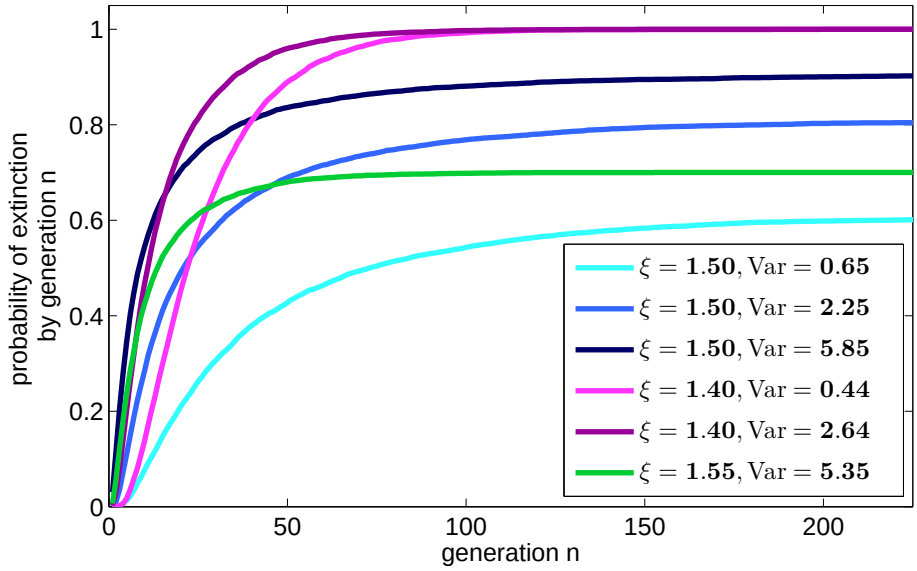

Figure 3.2: Probability of extinction by generation n as found by the IBM simulation for various expected reproductive rates ξ and variances of the probability mass function $\{p_i\}$. As we can see here, it is the expected reproductive rate which determines whether extinction is certain, but if it is not certain, then it is a combination of the expected reproductive rate and the variance which determine the ultimate extinction probability. Curves were obtained over 10000 simulations for a population initially of size 10, on a domain of 2.8 times the mean dispersal distance, with dispersal according to a Laplace dispersal kernel.

extinction by a given generation depends on the interplay between the variance and the expected reproductive rate, ξ.

3.3.2 Population level models with demographic stochasticity

As in the deterministic model, we will create an approximation which is based on the idea that we can disregard the location of individuals inside a reserve area and only consider changes to the *total* population size. We do this by approximating the individual dispersal behaviour of the IBM with a scalar describing the proportion of individuals which successfully remain within the reserve after a dispersal period. Recall from the deterministic model that this was A in (2.2.1). There we assumed that the total population $\bar{N}_n$ at time n could be approximated by the recursion relation

$$\bar{N}_n = \int_{-L/2}^{L/2} \int_{-L/2}^{L/2} k(x,y) r \, N_{n-1}(y) dy dx \approx \bar{A} \bar{r} \bar{N}_{n-1} \tag{3.3.1}$$

for some $0 \leq \bar{A} \leq 1$ which approximated the proportion of individuals which survived the dispersal process from time $n-1$ to n. Here $\bar{r}$ is the expected individual growth rate of the assumed linear growth function. We now apply this same concept in an attempt to approximate the findings of our stochastic IBM.

In Section 3.3.1, we assumed that the number of offspring of an individual is a random variable r with a probability mass function $\{p_i\}$ with expected value $\mathbb{E}(r) = \xi$ and variance σ_r^2. If we look at the average of these random variables for each individual in a population of size $\bar{N}_n$, by the Central Limit Theorem we have that the average number of offspring $\bar{r}$ converges to a normally distributed random variable with mean $\mathbb{E}(\bar{r}) = \xi$ and variance $\mathrm{Var}(\bar{r}) = \sigma_r^2 / \bar{N}_n$. Because we are dealing with a population, we cannot allow $\bar{r}$ to be negative in any given iteration of the model, and so to avoid

this problem, we will from here on assume the distribution of $\bar{r}$ to be normally distributed as described above, but with all of the probabilities of a negative distribution relocated to zero.

Let us consider the scalar which allows us to make our model spatially implicit, which we will again call A at the level of the individual. We first assume that individuals are evenly distributed throughout the domain at any given time (we will revisit this assumption later). Then we select position y at random from within $[-L/2,\, L/2]$ and we will assume that the individual settles within the domain according to the dispersal success function $s(y)$ at each point in the domain as described in Chapter 2. Given these assumptions and again employing the Central Limit Theorem, the average value $\bar{A}$ for a population of size $\bar{N}_n$ is a normally distributed random variable with mean $\mathbb{E}(\bar{A}) = S$, where S is the average dispersal success as described in Chapter 2. The variance of the distribution of $\bar{A}$ will be $\mathrm{Var}(\bar{A}) = \sigma_S^2/\bar{N}_n$, where σ_S^2 is the variance of $s(y)$,

$$\sigma_S^2 = \mathrm{Var}(s(y)) = \int_{-L/2}^{L/2} (s(y) - S)^2 dy, \tag{3.3.2}$$

over the domain. Now in each generation we start with a population of size $\bar{N}_n$, determine $\bar{r}$ and $\bar{A}$ as described above, and then $\bar{N}_{n+1} = \bar{A}\bar{r}\bar{N}_n$. It is important to note here that we now change our definition of extinction from requiring the death of all individuals to requiring the population size to get below a certain value. This is to account for the fact that even if $\bar{A}$ is less than 1 for many generations in a row, the population level approximation will only tend asymptotically towards zero but not achieve it. Throughout this section, this threshold, which we will call the quasiextinction threshold, will commonly be $\bar{N} < 1$. As we can see in Figure 3.3, this approximation performs fairly well when compared to the IBM and is less computationally costly than the IBM. We will refer to this spatially implicit approximation as the S population level approximation.

However, as discussed in the previous chapter, the population will likely not be evenly distributed throughout the domain and, as we did in the deterministic approximations, we can weight our dispersal success functions by $s(y)/S$ under the assumption that more individuals are in the centre of the domain than near the edges and that $s(y)$ provides a good approximation to the population distribution inside the reserve. We again select y at random from within $[-L/2, L/2]$ but now the distribution of our random variable A is the modified dispersal success function $s(y)^2/S$ of Chapter 2. Scaling up to the population level, the average value $\bar{A}$ will be drawn from a normal distribution where the expected dispersal success rate is the modified average dispersal success introduced in Chapter 2, $\mathbb{E}(\bar{A}) = \widehat{S}$. The variance of $\bar{A}$ will be $\mathrm{Var}(\bar{A}) = \sigma^2_{\widehat{S}}/\bar{N}_n$, where $\sigma^2_{\widehat{S}}$ is the variance of $s(y)^2/S$ over the domain,

$$\sigma^2_{\widehat{S}} = \mathrm{Var}(s(y)^2/S) = \int_{-L/2}^{L/2} \left(\frac{s(y)^2}{S} - S \right)^2 dy. \tag{3.3.3}$$

We will call this case the $\widehat{S}$ population level approximation.

By way of example, let us assume offspring are produced according to the probability mass function $\{p_0 = 0.1, p_1 = 0.3, p_2 = 0.6\}$, so that $\mathbb{E}(\bar{r}) = 1.5$ and $\mathrm{Var}(\bar{r}) = 0.45/\bar{N}_n$. Now suppose dispersal is according to a Laplace distribution, scaled to the mean dispersal distance. If we assume that the average dispersal success approximation S describes the loss of individuals outside the domain due to strong fishing pressure, then $\bar{A}$ is a random variable chosen from a normal distribution with mean

$$\mathbb{E}(\bar{A}) = S = (L + (1/\exp(L) - 1))/L \tag{3.3.4}$$

and variance

$$\mathrm{Var}(\bar{A}) = \frac{\sigma_S^2}{\bar{N}_n} = \left(L - \frac{7}{4} + 2\,S + L\,S^2 + \frac{L}{2\,\mathrm{e}^L} + \frac{2}{\mathrm{e}^L} - \frac{1}{4\,\mathrm{e}^{2\,L}} - 2\,L\,S - \frac{2\,S}{\mathrm{e}^L} \right) \Big/ \bar{N}_n,$$

assuming that L is scaled to the mean dispersal distance. If we compare this to the assumption that the modified average dispersal success approximation $\widehat{S}$ describes the loss of individuals outside the domain, then the distribution of $\bar{A}$ has mean

$$\mathbb{E}(\bar{A}) = \widehat{S} = \frac{4\,L - 7 + \frac{2\,L}{\mathrm{e}^L} + \frac{8}{\mathrm{e}^L} - \frac{1}{\mathrm{e}^{2\,L}}}{4\,L\,S} \tag{3.3.5}$$

and variance

$$\mathrm{Var}(\bar{A}) = \frac{\sigma_{\widehat{S}}^2}{\bar{N}_n} = \left(\frac{7}{2} + \left(S^2 - 2 + S^{-2} - \mathrm{e}^{-L}\right) L - \frac{269}{96\,S^2} - \frac{4}{\mathrm{e}^L} + \frac{1}{2\,\mathrm{e}^{2\,L}} + \frac{3\,L}{S^2\,\mathrm{e}^L} + \frac{3\,L}{8\,S^2\,\mathrm{e}^{2\,L}} + \frac{5}{4\,S^2\,\mathrm{e}^L} + \frac{3}{2\,S^2\,\mathrm{e}^{2\,L}} + \frac{1}{12\,S^2\,\mathrm{e}^{3\,L}} - \frac{1}{32\,S^2\,\mathrm{e}^{4\,L}} \right) \Big/ \bar{N}_n.$$

We can see how these two population level approximations compare to the corresponding IBM in Figures 3.3, 3.4, 3.5, and 3.6 for the Laplace, Cauchy, Gaussian, and double Weibull distributions. It is here that we first see that the modified average dispersal success approximation of Chapter 2 outperforms the traditional average dispersal success function not only in the deterministic IDE but also in a stochastic framework, for a variety of kernels with varying kurtosis. Again, this is because even in the stochastic model, the population will tend to be more dense in the centre of the reserve area, and so again the $\widehat{S}$ approximation better captures this uneven population distribution than does the standard S approximation. We tend to lose fewer individuals to the fished areas outside the reserve than the S approximation assumes,

since there are more individuals in the centre of the reserve, and those individuals are more likely to be retained.

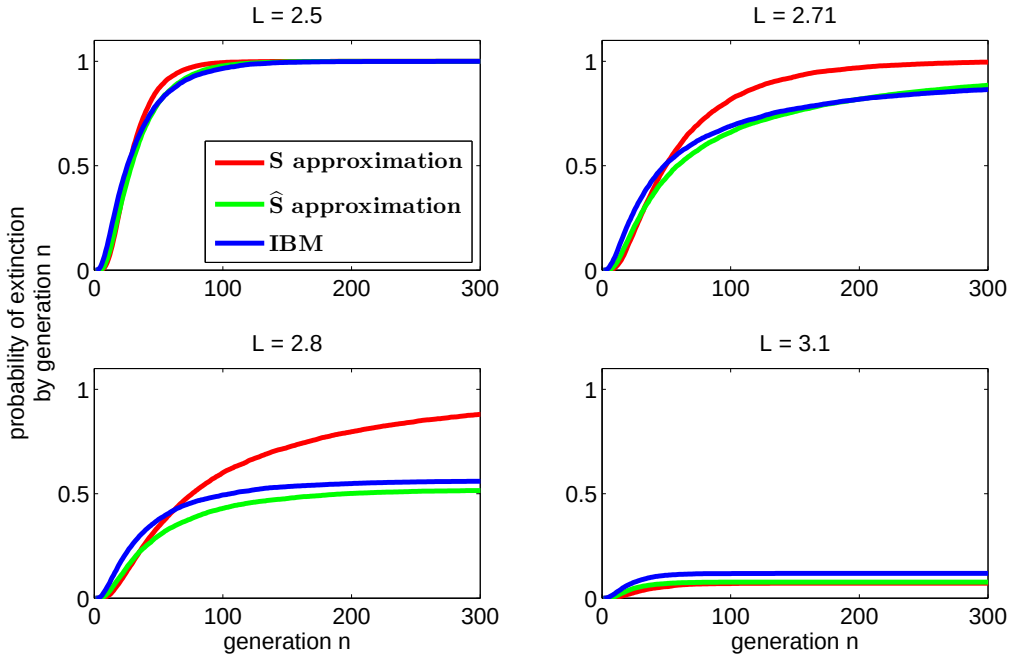

Figure 3.3: Stochastic population level approximations to the IBM, with r subject to probability mass function $p_0 = 0.1$, $p_1 = 0.3$ and $p_2 = 0.6$, so that $\mathbb{E}(\bar{r}) = 1.5$ and $\mathrm{Var}(\bar{r}) = 0.45$. Dispersal is according to a Laplace distribution and the domain length L is scaled to the mean dispersal distance. Simulations were run 10000 times from an initial population $N_0 = 10$ and the quasiextinction threshold is $\bar{N}_n < 1$ for the population level approximations. We chose the domain values to be around the critical domain size $L^* = 2.703$ as determined in the corresponding deterministic IDE model with $r = 1.5$, logistic growth, and a Laplace dispersal kernel.

The number of surviving offspring of an individual at the next time step is determined by the product of the above two positive random variables, r and A. We could also consider $B = Ar$ as a single independent random variable. Since A and r are independent, their means are multiplicative, and so

$$\mathbb{E}(B) = \mathbb{E}(A)\,\mathbb{E}(r) \tag{3.3.6}$$

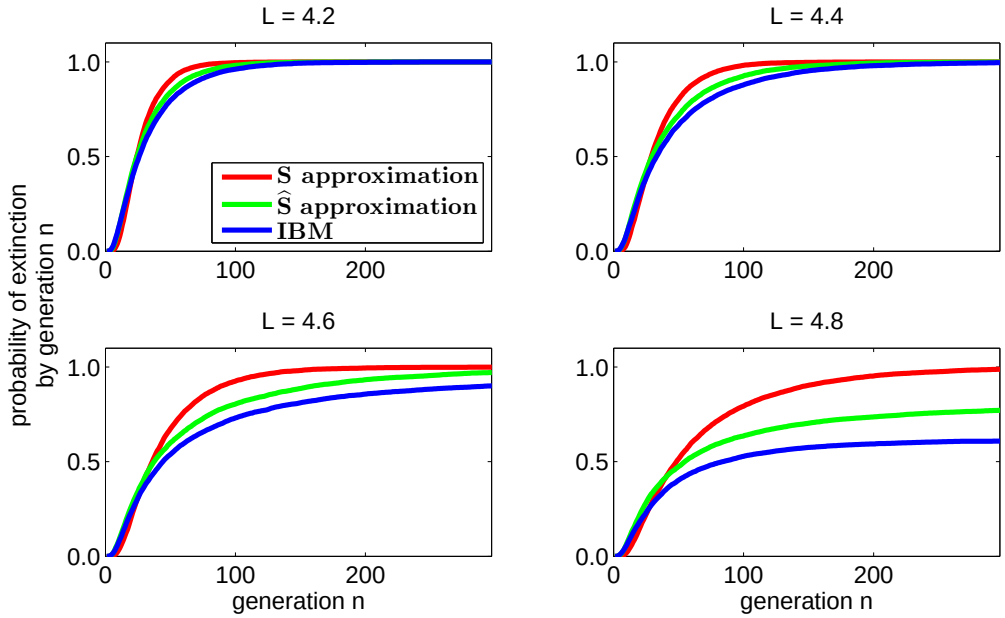

Figure 3.4: Stochastic population level approximations to the IBM as in Figure 3.3, but here dispersal is according to a Cauchy distribution.

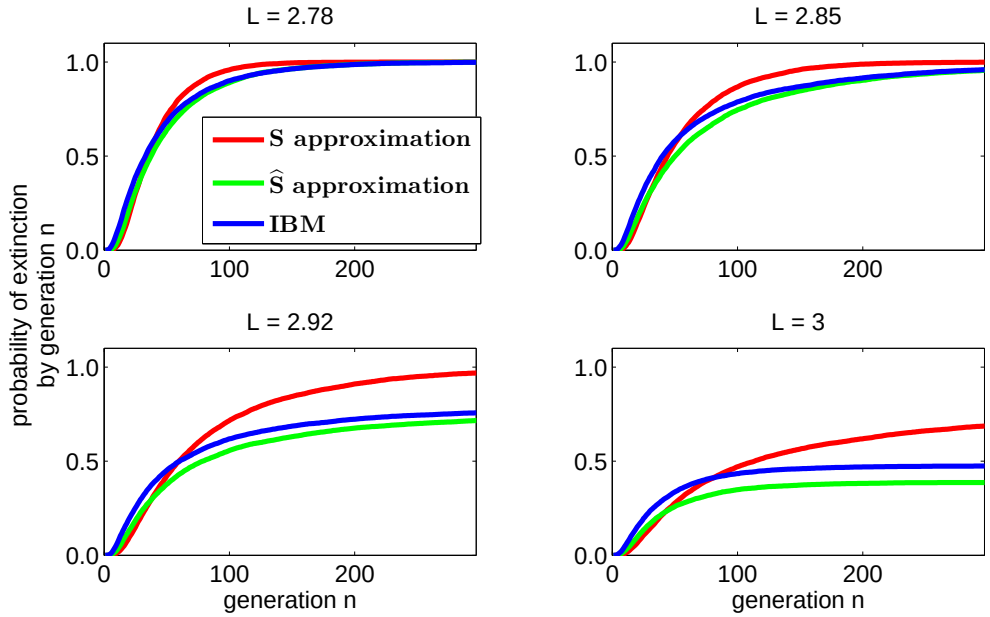

Figure 3.5: Stochastic population level approximations to the IBM as in Figure 3.3 and 3.4, but here dispersal is according to a Gaussian distribution.

and the variance is

$$\mathrm{Var}(B) = \sigma_B^2 = \mathbb{E}(A)^2\,\sigma_r^2 + \mathbb{E}(r)^2\,\sigma_A^2 + \sigma_A^2\,\sigma_r^2. \tag{3.3.7}$$

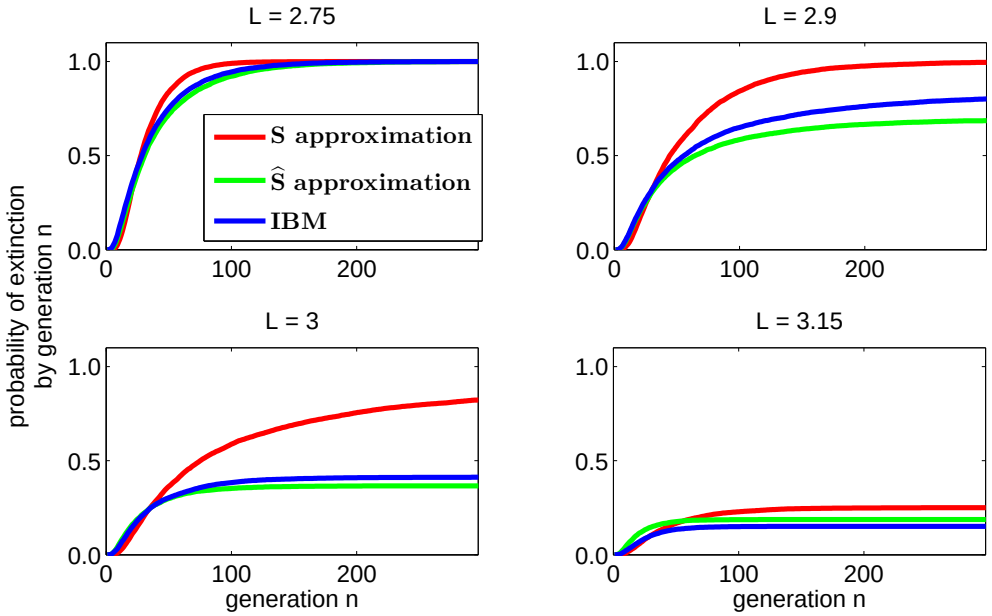

Figure 3.6: Stochastic population level approximations to the IBM as in Figure 3.3, 3.4, and 3.5 but here dispersal is according to a double Weibull distribution with $\alpha = 2$ and $\beta = 2/\sqrt{\pi}$.

Since we are here interested in the population level model rather than the individual, we can ignore the shape of the distribution of B and again look simply to the average values of the random variable B. Again applying the Central Limit Theorem we find that at the population level, $\bar{B}$ is normally distributed with an expected value of $\mathbb{E}(B)$ as above and variance $\sigma_B^2/\bar{N}_n$. Note that unlike in an IBM, the population here will never truly go extinct (here we define extinction as the steady state $\bar{N}_n = 0$) unless $\bar{B}$ may take the value zero. Rather we need to set some "quasiextinction threshold" (e.g. [32, 52]), for example where a population is considered extinct if $\bar{N}_n \leq 1$.

For a deterministic model of the form $\bar{N}_{n+1} = \bar{B}\,\bar{N}_t$, if $\bar{B} > 1$, the population tends to infinity and for $\bar{B} < 1$, the population tends towards extinction. For the deterministic model with $\bar{B} < 1$, we can calculate the time to extinction by setting $\bar{B}^n \bar{N}_0 = 1$

(recall that the quasiextinction threshold is 1) and solving for n as

$$n = \frac{-\ln(\bar{N}_0)}{\ln(\bar{B})}. \tag{3.3.8}$$

In the population level stochastic model considered here, the expected value of $\bar{N}_{n+1}$ is $\bar{B}^{n+1}\bar{N}_0$, but now even with $\bar{B} > 1$, extinction may still occur. The above dependence on $\ln(\bar{N}_0)$ was also found by Lande (1993) when considering the time to extinction of a continuous time stochastic model [52]. He found that the deterministic dependence of extinction time on the logarithm of the initial population in a continuous model carried over to his stochastic models and as we can see in Figure 3.7, this seems to hold here when we include space implicitly into our discrete time stochastic model.

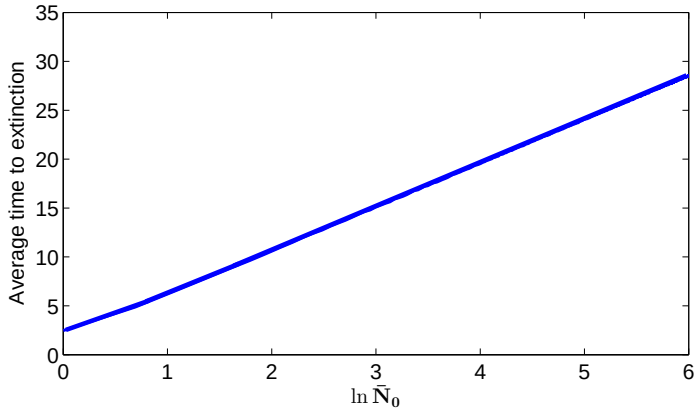

Figure 3.7: Average time to extinction for varying initial conditions, for a population with certain ultimate extinction. Here $\mathbb{E}(\bar{B}) = 0.8$ and $\mathrm{Var}(B) = 0.3$. As predicted by both deterministic models, as well as the continuous time stochastic model of Lande (1993), the average time to extinction scales with $\ln \bar{N}_0$. Plot was made from 10000 simulations for each value of $\bar{N}_0$ with a quasiextinction threshold set at $\bar{N}_n <= 1$.

3.3.3 Approximation to an IBM; a modified branching process

While the population level approximation of the previous section is computationally less expensive than the IBM, it does not provide any new understanding of the driving processes or variables. We turn now to a different approximation in order to be able to explore extinction probabilities for reserves of various sizes analytically. By using the approximation presented in this section, we will be better able to understand and explore the mechanisms leading to extinction. We again will make use of the spatially implicit approximations developed in Chapter 2 where we explored a novel approximation to the proportion of individuals lost to fishing pressures outside a reserve area. In this section, we will consider a modified Galton-Watson process, which we now adapt to suit our population of interest by including an extra "death step" following the reproduction process. Using branching processes will allow us to deal with a population of discrete individuals experiencing stochastic variation in both their dispersal and reproduction [50].

3.3.3.1 The standard Galton-Watson branching process

We here include a brief review of the standard formulation and results of a Galton-Watson branching process in order to motivate the proposed spatially implicit modification. We will also find that as the domain length L tends to infinity, our results on the probability of extinction tend asymptotically towards those of the standard non-spatial Galton-Watson branching process as outlined in this section.

The Galton-Watson branching process was originally motivated by the desire of French aristocracy to predict the extinction of family names [46, 114]. It has since been applied to studies of nuclear chain reactions, the survival of mutant genes, and population biology [24]. It is based on the simple assumption that individuals in each

generation have r offspring, independently of each other, where r is an independent and identically distributed (iid) random variable with probability mass function $\{p_i\}$, $i = 0, 1, 2, \ldots$ and each p_i is the probability that an individual produces i offspring in one generation. This corresponds to the probability generating function $f(s) = \sum p_i s^i$ for s on the unit interval and, by definition,

$$\sum_{i=0}^{\infty} p_i = 1. \tag{3.3.9}$$

The population size is a sequence of random variables $\{Z_n\}$, which describe the population size in the n^{th} generation, given an initial population $Z_0 = z$.

It then follows that the mean reproductive rate is

$$\xi = \mathbb{E}(r) = \sum_{i=0}^{\infty} i\, p_i = f'(1), \tag{3.3.10}$$

and the expected size of the n^{th} generation is

$$\mathbb{E}(Z_n) = z\, \xi^n. \tag{3.3.11}$$

However, unlike in parallel deterministic models, there is still a chance of extinction, even for mean reproductive rates greater than 1. The realized population size Z_{n+1} is found via a recursion relation which sums the descendants of each of the individuals in generation n, so that

$$Z_{n+1} = \sum_{j=0}^{Z_n} r_{j,n} \tag{3.3.12}$$

where $r_{j,n}$ is an integer valued random variable describing the number of offspring of the jth individual in generation n [114].

Continuing to disregard the effects of space, we will briefly outline the classical results on extinction probabilities for the standard Galton-Watson branching process. We first consider the case where $Z_0 = 1$, since the results for $Z_0 = z \neq 1$ follow easily. The probability of extinction d by time m of the lineage of one individual in the first generation can be found via the recursion relation

$$d_m = \underbrace{p_0}_{\text{(a)}} + \underbrace{p_1 d_{m-1}}_{\text{(b)}} + \underbrace{p_2 (d_{m-1})^2}_{\text{(c)}} + \dots \tag{3.3.13}$$

This is quite intuitive, as (a) is the probability that the original individual had no offspring, (b) is the probability that it produced one offspring and that this individual's lineage went extinct in the next $m-1$ generations, and similarly, (c) is the probability that it produced two offspring and that both of their lineages died out in the subsequent $m-1$ generations. This pattern continues for all possible numbers of offspring [6].

The probability that extinction occurs at some point in the future, or the ultimate extinction probability, is the limit

$$d = \lim_{m \to \infty} \Pr\left(Z_m = 0\right). \tag{3.3.14}$$

Clearly d_m must reach a limit as m increases, since it is an increasing function in m and is bounded above by 1. As it reaches this limit, d_m tends to d_{m+1} and so in order to find the probability of extinction far in the future, we consider extinction as a steady state since once a population has died out, there is no possibility of it growing again, given the absence of immigration. Then, as in any recursion equation, we can find the asymptotic extinction probability by setting $d_m = d_{m-1}$ and solving

$$d = p_0 + p_1 d + p_2 d^2 + p_3 d^3 + \dots \tag{3.3.15}$$

which is equivalent to

$$d = \sum_{i=0}^{\infty} p_i \, d^i = f(d), \tag{3.3.16}$$

where $f(d)$ is the probability generating function in d. This has a trivial solution of $d = 1$, but may also possess further solutions less than 1. The trivial case exists when each individual produces exactly one individual in the subsequent generation, in which case the probability of extinction is $d = 0$ and the population size remains constant over time. Disregarding the trivial case, Galton and Watson's classic result shows that if the mean number of offspring produced by an individual ξ (recall that $\xi = f'(1)$) is less than or equal to one (known as the *subcritical* and *critical* cases), then the population will die out almost surely. If ξ is larger than one (the *supercritical* case), then the extinction probability is strictly less than 1 and the population will tend to grow exponentially [6, 46].

By way of example of the above, we consider a population similar to those we have previously used, with either zero, one, or two offspring with reproductive probabilities $\{p_0, p_1, p_2\}$. Then the extinction probability at time m can be found through (3.3.13), and the ultimate extinction probability will be the smallest solution to

$$d = p_0 + p_1 d + p_2 d^2. \tag{3.3.17}$$

If $f'(1) = p_1 + 2p_2 > 1$, then the smallest solution will be less than 1, and if $f'(1) < 1$, then the smallest solution will be $d = 1$. We have illustrated the possible cases in Figure 3.8. We will now use the above well-established framework and results to consider a novel *spatially implicit* branching process.

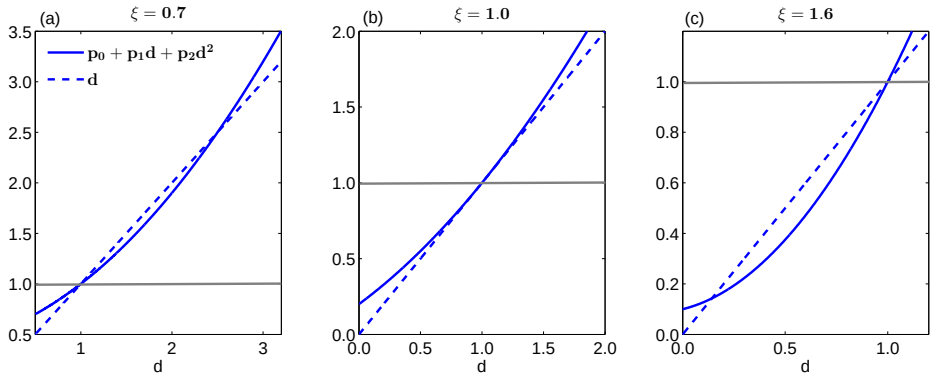

Figure 3.8: Three possible extinction behaviours for a Galton-Watson branching process with different expected values for r. As we can see here, for $\xi = \mathbb{E}(r) < 1$, the non-trivial root is greater than one, and for $\xi > 1$, the nontrivial root is less than one. The horizontal lines serve simply to illustrate more clearly how the second root compares to $d = 1$. In (a), $p_0 = 0.5$, $p_1 = 0.3$, and $p_2 = 0.2$. In (b), $p_0 = 0.2$, $p_1 = 0.6$, and $p_2 = 0.2$, and in (c), $p_0 = 0.1$, $p_1 = 0.2$, and $p_2 = 0.7$.

3.3.3.2 A spatially implicit modified branching process

Let us consider the possibility that, in addition to birth-and-death processes like those outlined above, a certain fraction of each new generation is lost because they disperse outside the reserve area where they are harvested before they can reproduce. Let F be the fraction of the population lost in this way, so that $1 - F$ is the probability that an individual successfully settles within a reserve area.

Now the probability of extinction by generation m is dependent upon both the usual birth-death process, as well as the dispersal behaviour of the individuals. We will maintain consistency with the IBM regarding the order of these two processes within one time step, so that individuals first reproduce according to the probability generating function $f(s)$, and then these individuals disperse, being lost to fishing pressure outside the reserve with probability F. Given these assumptions, we obtain a modified

version of (3.3.13),

$$\begin{aligned} d_m = \underbrace{p_0}_{(\mathrm{a})} + \underbrace{p_1\, d_{m-1}(1-F)}_{(\mathrm{b}_1)} + \underbrace{p_1\, F}_{(\mathrm{b}_2)} + \underbrace{p_2\, (d_{m-1}(1-F))^2}_{(\mathrm{c}_1)} \\ + \underbrace{p_2\, F^2}_{(\mathrm{c}_2)} + \underbrace{2\, p_2\, F(1-F)\, d_{m-1}}_{(\mathrm{c}_3)} \ldots \end{aligned} \tag{3.3.18}$$

Here (a) remains the probability that the original individual had no offspring, and (b_1) describes the probability that the first individual produced one surviving offspring and that this individual's lineage went extinct in the subsequent $m-1$ generations. (b_2) is the probability that the single offspring of the first individual dispersed to unfavorable habitat before it could reproduce in the next generation. Following intuitively, (c_1) is the probability that the original individual produced two offspring and that both of their lineages died out in $m-1$ generations. (c_2) describes the probability that the two offspring dispersed to unfavourable habitat and were lost and (c_3) describes the probability that only one of them settled outside the reserve, while the other remained but had their lineage die out in $m-1$ generations. This pattern continues on in this way, following the visualization of an illustrative modified branching tree in Figure 3.9

Clearly, if there is no good habitat, the probability of extinction by any time step will be 1, since $d_m = p_0 + p_1 + p_2 + \ldots$ when $F = 1$. We can re-write (3.3.18) as

$$d_m = \sum_{v=1}^{\infty} \sum_{q=1}^{v} \binom{v}{q} p_{v-1} \left[(1-F) d_{m-1}\right]^{q-1} F^{(v-q)}, \tag{3.3.19}$$

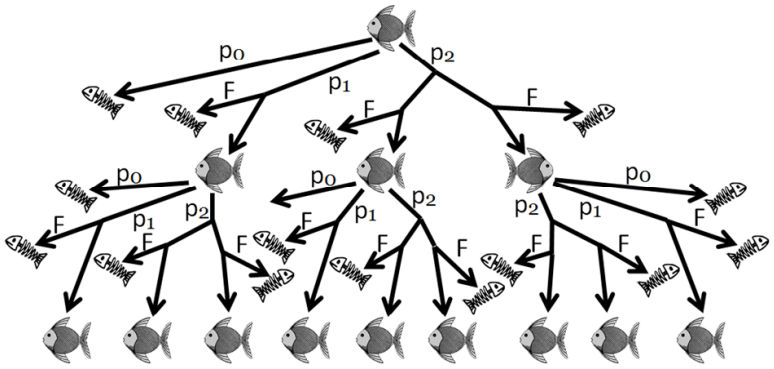

Figure 3.9: A sample branching tree modified to include a fraction of individuals lost via dispersal to unfavourable habitat. The first individual is at the top, and we assume this species can have a maximum of 2 offspring per generation, with reproduction according to probabilities p_0, p_1, and p_2. Following reproduction, individuals are lost with probability F via dispersal to non-reserve areas and those which survive to the next generation then start the process again.

and the probability of extinction as $m \to \infty$ (far in the future) can thus be found by solving for d in

$$d = \sum_{v=1}^{\infty} \sum_{q=1}^{v} \binom{v}{q} p_{v-1} \left[(1-F)d\right]^{q-1} F^{(v-q)} = f[(1-F)d + F] \tag{3.3.20}$$

where $f[(1-F)d+F]$ is the probability generating function in $(1-F)d+F$. This can be seen by rearranging (3.3.20) to be

$$d = p_0 + p_1((1-F)d+F) + p_2((1-F)d+F)^2 + p_3((1-F)d+F)^3 + \ldots \tag{3.3.21}$$

Clearly $d = 1$ is again always a solution to the above equation. As before, whether there is a second, smaller solution is determined by the reproductive probabilities but now also by the value of F.

In order to use the results of Watson and Galton (1875), we need determine the expected value of offspring of this modified branching process in order to determine whether the process is supercritical, critical, or subcritical, and thus determine

whether extinction is certain. Let us define $\bar{p}_i$ as the probability of an individual producing i offspring which successfully settle from their dispersal phase (i.e. $\bar{p}_i$ is the reproductive probability including loss via dispersal outside the reserve). Then

$$\begin{aligned}
\bar{p}_0 &= p_0 + p_1 F + p_2 F^2 + \dots \\
\bar{p}_1 &= p_1(1-F) + 2p_2(1-F)F + 3p_3(1-F)F^2 + \dots \\
\bar{p}_2 &= p_2(1-F)^2 + 3p_3(1-F)^2 F + 6p_4(1-F)^2 F^2 + \dots \\
&\vdots \\
\bar{p}_q &= \sum_{v=q}^{\infty} \binom{v}{q, v-q} p_v (1-F)^q F^{v-q}
\end{aligned} \tag{3.3.22}$$

where

$$\binom{v}{q, v-q} = \frac{v!}{q!(v-q)!} \tag{3.3.23}$$

are multinomial coefficients. This results in the corresponding probability generating function

$$f(s) = \bar{p}_0 + \bar{p}_1 s + \bar{p}_2 s^2 + \bar{p}_3 s^3 + \dots \tag{3.3.24}$$

and so the expected reproductive value is

$$\xi = f'(1) = \bar{p}_1 + 2\bar{p}_2 + 3\bar{p}_3 + \dots \tag{3.3.25}$$

$$= \sum_{q=1}^{\infty} q\bar{p}_j = \sum_{q=1}^{\infty} \sum_{v=q}^{\infty} q \binom{v}{q, v-q} p_v (1-F)^q F^{v-q}. \tag{3.3.26}$$

Note that if we make the biologically reasonable assumption that these sums do not run to infinity but rather to some maximum reproductive rate, the summations both become finite. The above equation simplifies to the very intuitive result

$$\xi = \mathbb{E}[r]\,(1-F), \tag{3.3.27}$$

which can be shown using a simple proof by induction for both the infinite or finite sum case. Thus the expected reproductive rate of the modified Galton-Watson branching process is the product of the expected reproductive rate without the loss of individuals outside the reserve area and the proportion of individuals which successfully settle within the reserve bounds. Applying the results of Watson and Galton (1875), the criticality condition for the spatially implicit branching process is

$$\mathbb{E}(\xi) = \mathbb{E}[r]\,(1 - F) = 1, \tag{3.3.28}$$

and from this we can determine the proportion of individuals which must be retained within the reserve area in order to avoid certain extinction. For any F less than this critical value F^*, the population will be supercritical and for any $F \geq F^*$, eventual extinction is certain.

We come now to the question of how we can calculate or approximate F. Recall the approximations S and $\widehat{S}$ from Chapter 2, which are the dispersal success function of Van Kirk and Lewis (1997) and the newly introduced modified dispersal success function, respectively. We suppose, here, that $F = 1 - S$ and $\widehat{F} = 1 - \widehat{S}$ and we can then compare the resulting extinction risks with those from a spatially explicit IBM simulation.

To illustrate the use of the above theory, we work through a simple example. Suppose an individual in a population of initial size z reproduces according to the following probabilities: $p_0 = 0.1$, $p_1 = 0.3$, and $p_2 = 0.6$, for a mean reproductive rate $\xi = 1.5$. Let us assume dispersal occurs according to a Laplace distribution. Recall that we can determine the critical domain size required by a deterministic IDE model with logistic growth, an intrinsic growth rate of $r = 1.5$, and a Laplace dispersal kernel,

to be $L^* = 2.703$ times the mean dispersal distance by (1.5.20). For a domain of this size, $S = 0.6548$ and $\widehat{S} = 0.6647$ (see (2.2.9) and (2.2.11)), and so $(S\,\xi) = 0.9822 < 1$ and $(\widehat{S}\,\xi) = 0.9970 < 1$. So our branching process predicts that the critical domain size of the deterministic model is too small to sustain a population subject to demographic stochasticity. This simple stochastic model demonstrates what is intuitively clear; that if marine management is undertaken using only a deterministic model, the population will not survive. See Figure 3.10 to compare the probability of extinction for values of L around L^* for both the IBM and the branching process approximation using both S and $\widehat{S}$. In Figure 3.10, using $\widehat{S}$ to approximate $(1 - F)$ once again provides a better approximation to the spatially explicit model (in this case the IBM) than S.

We now consider a range of lengths around L^* and compare the probability of eventual extinction predicted by the two approximations to F. We can see in Figure 3.11 that both approximations result in the prediction of certain extinction up until some critical length value, at which point the ultimate extinction probability becomes less than one. The greater the initial population, the sharper the decline in the ultimate extinction probability for lengths larger than the critical value. The critical domain length at which the population's ultimate extinction probability changes from one to less than one can be found by solving for $S = 1/\xi$ and $\widehat{S} = 1/\xi$. This results in the critical domain sizes for our branching process approximation, $L^*_S = 2.821$ and $L^*_{\widehat{S}} = 2.722$, which are the critical values we see in Figure 3.11.

For conservation purposes, we are interested in the probability of extinction of groups of individuals, rather than of single individuals. The probability of an initial popula-

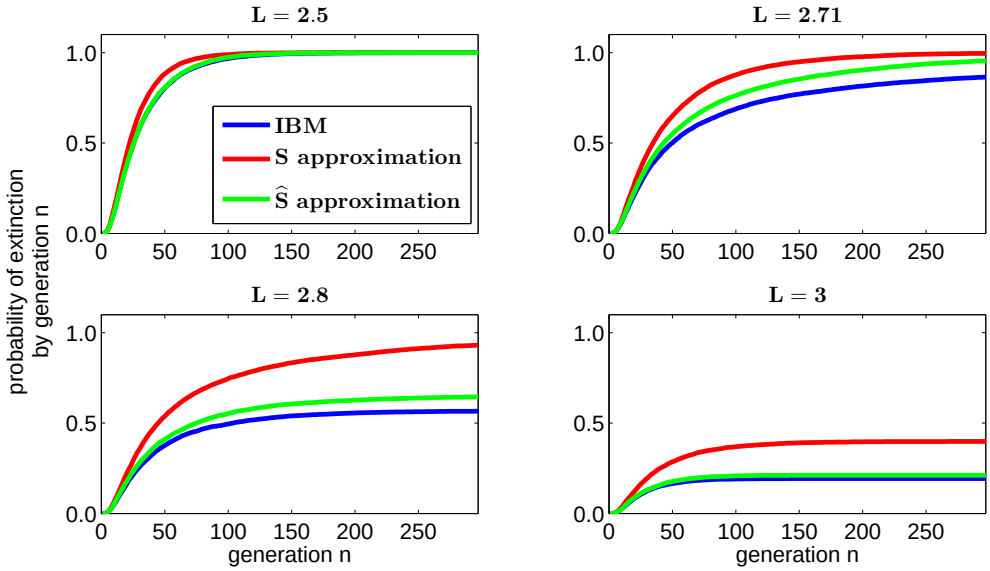

Figure 3.10: Comparison of the two modified branching process approximations to the IBM simulation on domains of various sizes close to the critical values predicted by the three models for the critical domain size. For the deterministic model $L^* = 2.703$, for the S approximation model, $L^*_S = 2.821$ and for the $\widehat{S}$ approximation, $L^*_{\widehat{S}} = 2.722$. The reproductive probabilities are $p_0 = 0.1$, $p_1 = 0.3$, and $p_2 = 0.6$ for an expected reproductive value $\xi = 1.5$. For each plot, 10000 simulations were performed on an initial population $Z_0 = 10$. Observe that $\widehat{S}$ provides a close approximation to the extinction behaviour of the IBM, outperforming that of S most notably for those values between L^*_S and $L^*_{\widehat{S}}$.

tion of size z going extinct by time m, i.e. $d_m(z)$ can be found by looking at

$$d_m(z) = (d_m)^z, \tag{3.3.29}$$

since each individual's probability of extinction is independent of the others'. So long as the probability of extinction of a single individual is less than one, as z increases, the probability of extinction for the entire population tends asymptotically toward 0. The probability of ultimate extinction for an initial population of size z can, similarly, be determined by

$$d(z) = d^z. \tag{3.3.30}$$

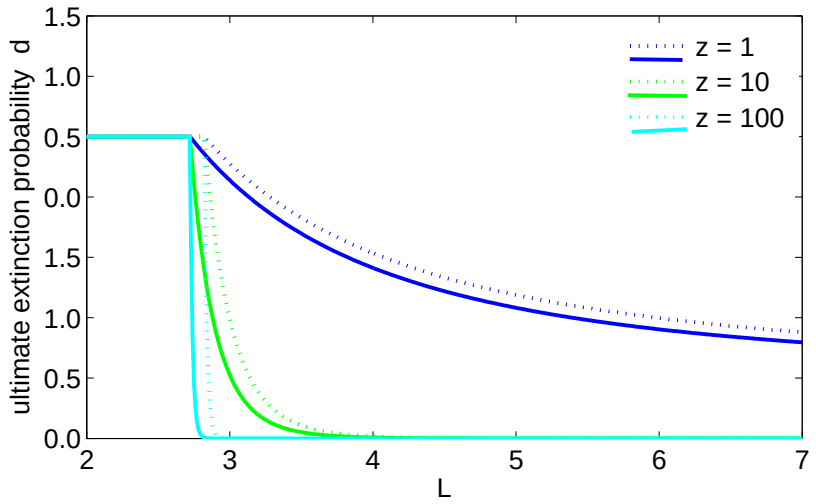

Figure 3.11: Probability of ultimate extinction for various reserve lengths and initial conditions. Here $p_0 = 0.1$, $p_1 = 0.3$, and $p_2 = 0.6$ and length is scaled to the mean dispersal distance. The dotted lines show the ultimate probability of extinction if the fraction of individuals surviving is represented as the average dispersal success S of Van Kirk and Lewis (1997) and the solid lines show the novel modified average dispersal success $\widehat{S}$ introduced in Chapter 2. Observe that the ultimate probability of extinction found using the $\widehat{S}$ approximation consistently predicts a smaller probability of extinction, following from our previous observation that, in general, $S < \widehat{S}$, and if more individuals are retained in the reserve, this will have a positive effect on survival probabilities.

For the example shown in Figure 3.11, the non-spatial probability of extinction is 0.17 when $z = 1$, as determined by equation (3.3.15). If Figure 3.11 included larger L values, the curve for $z = 1$ would asymptotically tend towards 0.17. As we can see in Figure 3.11, for any $L > L^*$, and an initial population greater than one, extinction is very unlikely, regardless of how much larger than L^* the length of the reserve is. Thus, under the assumptions of our model, for an initial population of a few hundred or thousand individuals, the reserve need only be slightly larger than L^* to ensure a very low chance of extinction. In this situation, increasing the reserve length far beyond L^* does little to further decrease the probability of extinction.

Let us now look at the problem from a different angle, where rather than assum-

ing the domain size to be that determined by a deterministic model, we assume a given conservation goal for d. By way of a quick example, let us require an ultimate extinction probability of no more than 10%. We know that with an initial population of z individuals we need $d^z = 0.10$. Let us suppose $z = 1000$, and so d need equal no more than $d = 0.998$. Solving (3.3.20) for F, we get $F = 0.333$, so the domain needs to be large enough to retain a proportion of individuals, $1 - F = 0.667$. We thus assume $S = \widehat{S} = 0.667$, and solving for the corresponding critical lengths yields $L_S^* = 2.823$ and $L_{\widehat{S}}^* = 2.726$.

Note here that if we assume an initial population of only one individual in the above example, this results in complex values of F. This is because, for the given values of p_0, p_1, and p_2, a simple branching process without loss of individuals due to dispersal already has a long-time extinction probability of $d = 0.167$. Thus there is more than a 10% chance of extinction for a population consisting of one individual even without any loss due to dispersal.

We have not gone into very much detail up to this point about the effect of the variance of the probability mass function $\{p_i\}$ on the population's extinction probability. As was shown by Watson and Galton (1875), certain extinction is determined only by the expected value of r. However, if extinction is not certain, as we have seen for the IBM, the variance will affect the ultimate extinction probability. The probability of extinction by a given generation thus relies on both the expected reproductive rate and the variance in the probability mass function $\{p_i\}$. The higher the expected reproductive rate, the lower the probability of extinction, and the greater the variance, the higher the probability of extinction. We can see the effect of changing the variance for a population with certain eventual extinction in Figure 3.12.

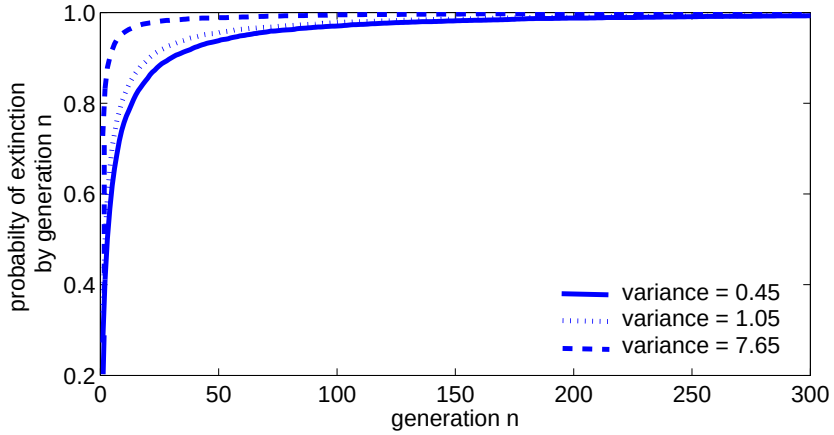

Figure 3.12: Probability of extinction of the lineage of a single individual calculated based on a modified Galton-Watson process. We here used $\widehat{S}$ on a domain of length $L = 2.7$ and assumed a Laplace dispersal kernel to approximate the proportion of individuals lost outside a reserve area. All three mass probability functions have the same mean of 1.5 but different variances. These plots were obtained over 10000 simulations.

3.3.4 Discussion and conclusions about demographic stochasticity

In this chapter thus far, we have considered a population subject to variability only in its demographic rates. This is the variability inherent in populations of discrete individuals who reproduce and die at different times and different rates. As we expected, the critical domain size for a population subject to stochasticity is larger than that of the deterministic model and increases with both decreasing growth rates and increasing variance.

Considering only demographic stochasticity, we first created an IBM in order to explicitly simulate each individual's variable reproductive rate and also its random dispersal distance. While the IBM most closely mimics the assumptions of the deterministic IDE framework, it is slow to simulate due to the computational costs associated with having each individual disperse independently. It also does not easily lend itself to comparison between different kernels, parameter sets, or growth functions. We thus

developed two approximations to the IBM which both perform well for a variety of domain lengths and initial population sizes. Using the Central Limit Theorem, we have found that scaling the IBM up to the population level provides a very close approximation to the probability of extinction, and it is much faster to obtain results via simulation. In order to obtain analytic results, we modified a Galton-Watson type branching process to implicitly include space, and this was able to also closely approximate the IBM while allowing for closer examination of the mechanisms behind population decline. As in the deterministic case, it seems that for the simplest case of a non-structured population on a single reserve, the many details of the dispersal kernel are not important, but rather the proportion retained is what drives the bifurcation behaviour.

Again we have seen that using the novel approximation $\widehat{S}$ to approximate the proportion of individuals which successfully settle within a reserve area proves to be a good approximation in many cases, outperforming the previously standard approximation S in the stochastic as well as deterministic models. This is because the population will again tend to be more dense in the centre of the reserve area, and so approximating the shape of the population density distribution within the reserve area and using this to weight the dispersal success function provides a close approximation to the proportion of individuals which successfully contribute to the next generation.

What is interesting to note, is that for large initial populations, it would appear that *how much* larger the domain is than the critical length value does not matter very much, given the rapid asymptotic decrease of the probability of extinction with an increase in the population size as found by the branching process approximations. That being said, given the difficulty in obtaining accurate parameter values, it would be prudent for conservationists to design a reserve area well away from this critical

length value in order to avoid population collapse.

3.4 Environmental stochasticity

We now turn our attention to the effects of a variable environment on population dynamics. Unlike in the case of demographic stochasticity, where the variability is due to random fluctuations in *individual* growth and survival rates, variation in environmental conditions affects *all* individuals similarly and simultaneously. In order to examine the effect this type of variability has on extinction probabilities, we will allow the population growth rates to fluctuate as a stationary time series (for examples, see [4, 52, 108]). We will now incorporate environmental variability into our stochastic analogue of the deterministic IDE [46, 52, 54]. Much of the work in this area has again been motivated by the study of genetics, and we will apply many of these results here, but now incorporating space in order to say something about the probability of extinction on a finite domain.

In this section, we will follow roughly the same structure as when we considered demographic stochasticity alone, first creating an individual based model which yields computationally intensive results via simulation. We then look at several approximations to this, first by considering a population level model using the Central Limit Theorem to scale up to a population level. We then consider a branching process, but now modified to include both a spatial component as well as random environments.

3.4.1 Individual based models with environmental stochasticity

There are many different ways in which we could reflect the variable nature of the environment in our model. Many have chosen to add a noise term into an otherwise

deterministic framework [70]. This can be either additive or multiplicative, depending on the model formulation, and in effect, it serves to alter the average birth rate. We will here choose to incorporate environmental variability directly into the growth rate of each individual, both because this can quite easily be incorporated into the branching processes of the previous section, and also because of the implied understanding of environmental stochasticity. We here take environmental variability to affect a population by changing the growth rate of every individual in the same way, by either shifting the mean and/or variance of the probability mass functions determining individual growth.

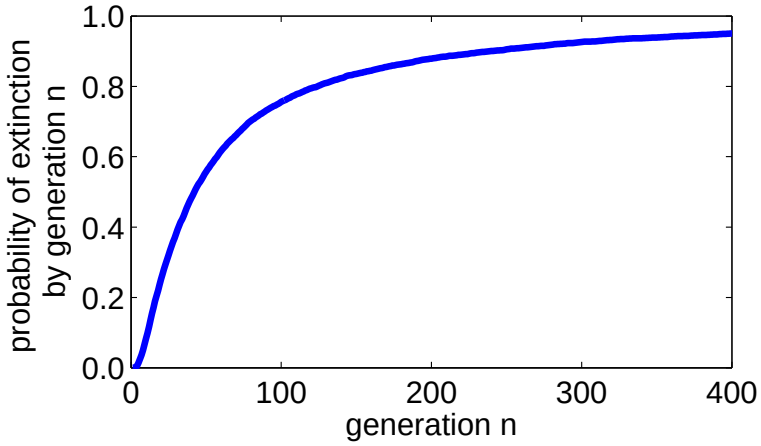

Figure 3.13: IBM as described in Section 3.4.1. We assume three possible environmental states which occur according to the probability mass function $\{h_1 = 0.4, h_2 = 0.4, h_3 = 0.3\}$. The corresponding probability mass functions for reproduction are $\{p_0^1 = 0.1, p_1^1 = 0.2, p_2^1 = 0.7\}$, $\{p_0^2 = 0.1, p_1^2 = 0.3, p_2^2 = 0.6\}$, and $\{p_0^3 = 0.2, p_1^3 = 0.3, p_2^3 = 0.5\}$. This plot was generated from 10000 simulations with $z = 10$.

We do this by introducing a sequence of iid environmental variables $\{\varsigma_n\}$, for $n = 0, 1, 2, \ldots$ where ς_n describes the environmental conditions in generation n selected from a countable number of environmental states ς^j, $j = 0, 1, 2, \ldots$. For the purposes of this section, we will denote the probability of a certain environment ς^j occurring for a given generation as h_j. These environmental variables could incorporate environ-

mental conditions such as the prevalence of predators, average temperatures, or the abundance of a food source. Each ς^j uniquely determines the probability generating function of the reproductive rates of each individual, so that it is now determined by the probability mass function, $\{p_i^j\}$, comprised of the probabilities of an individual having i surviving offspring, given environment ς^j. We thus have a sequence of corresponding iid probability generating functions $\{f_{\varsigma_n}\}$.

We now wish to incorporate this random environmental variable into our IBM. We begin with an initial population of size z evenly distributed throughout the reserve at generation $n = 0$. At the start of each generation, we generate a random number which determines the environment over that generation. This corresponds to a set of reproductive probabilities, as described by the probability generating function f_{ς_n}, which determine the number of offspring produced by each individual. After the number of each individual's offspring has been determined, we select the position of the offspring after the dispersal period according to a chosen dispersal kernel. Those individuals who settle within the reserve area survive and repeat this process over the next generation, while those who settle outside the reserve area are considered lost to fishing pressure. See Figure 3.13 for an example of an IBM with environmental stochasticity. As in the previous IBM presented in Section 3.3.1, this is computationally costly and results for different reproductive and environmental probabilities are difficult to standardize or compare, but we again will use the results as a benchmark against which we can measure and compare our approximations.

3.4.2 Population level models with environmental stochasticity

We again will rescale the IBM up to the population level using the Central Limit Theorem. This rescaling best mimics the IBM when the population size is not too

small, due to the constraints of the Central Limit Theorem, but even for an initial population of a single individual, we find that it closely predicts the cumulative extinction probabilities.

The method employed will be very similar to that in Section 3.3.2, where we disregarded the exact location of individuals inside the reserve and instead considered only the total population size $\bar{N}_n$. We again do not consider the movement of individuals, and will approximate the probability that an individual successfully disperses to a location inside the reserve bounds by some function of the domain size, taking account of the dispersal kernel. This leads to an approximation of the dynamics at the population level described by

$$\bar{N}_{n+1} = \bar{A}\,\bar{r}_n\,\bar{N}_n. \tag{3.4.1}$$

We again consider only linear population growth, as we are interested in the behaviour near the zero steady state of the deterministic model (i.e. for very small populations). We will draw both $\bar{r_n}$ and $\bar{A}$ from the same type of distributions as in Section 3.3.2, with the lone difference being that we will now incorporate environmental variation. This will be done in a similar manner to that employed in the IBM, where the reproductive probabilities in each generation are influenced by a random variable describing the environmental conditions over that generation ς_n. This may affect both the mean and variance of the population's growth rates uniformly across the population, and thus affects the mean and variance of the random variable $\bar{r_n}$. Recall from Section 3.3.2 that, depending on our assumptions about the distribution of the population on the domain, we can approximate $\bar{A}$ by a normal distribution with either mean S or $\widehat{S}$. We also again will need to employ some form of threshold value signifying extinction, as the population will never achieve zero unless we allow

either $\bar{A}$ or $\bar{r}$ to be zero, which would signify a catastrophe wiping out the entire population in one generation.

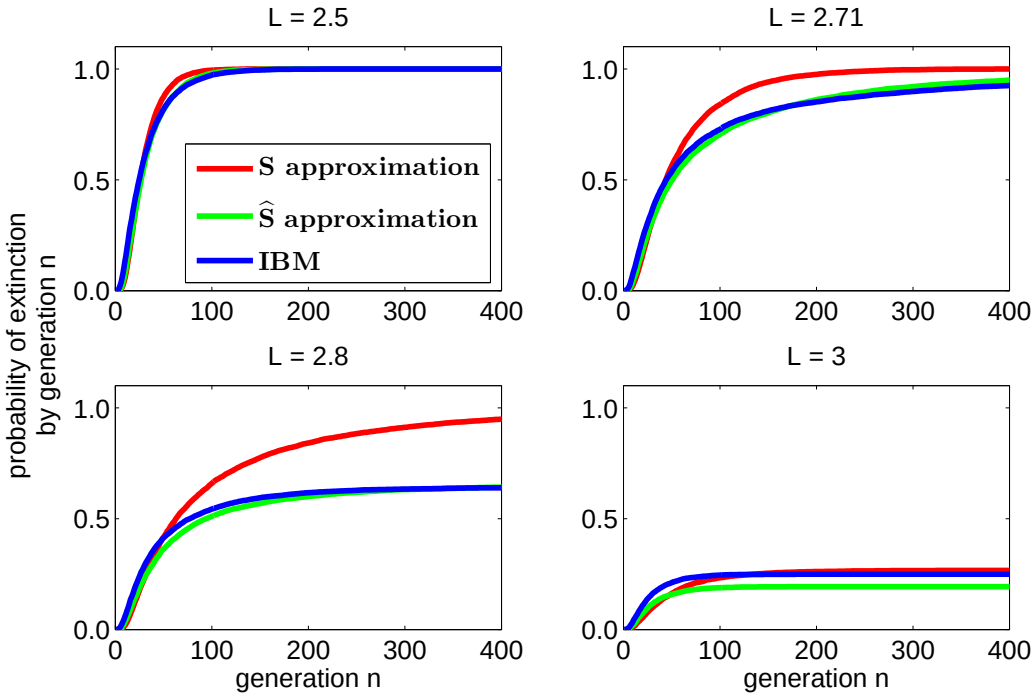

Figure 3.14: Stochasticity at the population level incorporating both environmental and demographic stochasticity as described in Section 3.4.2. We assume a Laplace dispersal kernel for consistency with previous illustrating examples. The IBM plotted here has a mean reproductive value of $\xi = 1.5$, which is the same as that of the population level models. Comparing the IBM to the population level models shows again that using $\widehat{S}$ to approximate $\bar{A}$ provides a close approximation. The IBM has probability mass functions of $\{p_0^1 = 0.1, p_1^1 = 0.2, p_2^1 = 0.7\}$ for environment ς^1, $\{p_0^2 = 0.1, p_1^2 = 0.3, p_2^2 = 0.6\}$ for environment ς^2, and $\{p_0^3 = 0.2, p_1^3 = 0.3, p_2^3 = 0.5\}$ for ς^3. The three environments occur according to $h_1 = 0.4$, $h_2 = 0.4$, and $h_3 = 0.2$. The initial population is 10 individuals and the quasiextinction threshold is $\bar{N}_n < 1$ for the population level models. This plot was generated over 10000 simulations.

We present a very simple example in order to illustrate this method. We will assume three different environmental states ς^1, ς^2, and ς^3, which occur with corresponding probabilities $h_1 = 0.4$, $h_2 = 0.4$ and $h_3 = 0.2$. Each of these environments has a corresponding expected growth rate of $\xi^1 = 1.6$, $\xi^2 = 1.5$, and $\xi^3 = 1.3$ and variance $\text{Var}^1 = 0.44$, $\text{Var}^2 = 0.45$, and $\text{Var}^3 = 0.61$. The expected value of $\bar{r}$ over all possible

environments is

$$\mathbb{E}(\bar{r}) = \xi_1 h_1 + \xi_2 h_2 + \xi_3 h_3 = 1.5. \tag{3.4.2}$$

Recall from the deterministic case that for a mean reproductive value of 1.5 in an IDE with logistic growth and dispersal according to a Laplace distribution, we have a critical domain size of $L^* = 2.703$. As we can see in Figure 3.14, approximating $\bar{A}$ in (3.4.1) by $\widehat{S}$ yields a close prediction of the probability of extinction, even for values of L close to this critical value, where the S approximation performs poorly.

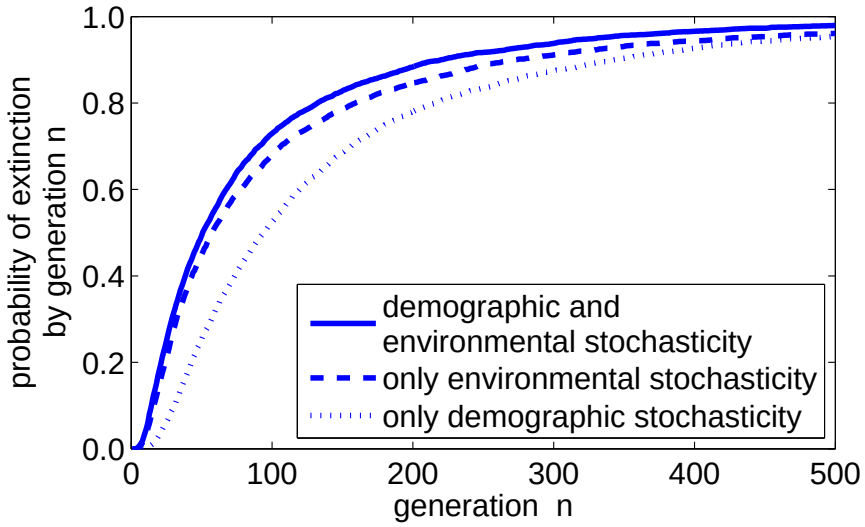

Figure 3.15: Probability of extinction as predicted by the $\widehat{S}$ population level approximation of Section 3.4.2 for a population subject to three different kinds of stochasticity. For a population subject to both environmental and demographic stochasticity, there are three possible environments which occur with probability $h_1 = 0.4$, $h_2 = 0.4$, and $h_3 = 0.2$. The corresponding expected growth rates and variances are $\xi^1 = 1.6$, $\text{Var}^1 = 0.44$, $\xi^2 = 1.5$, $\text{Var}^2 = 0.45$ and $\xi^3 = 1.3$, $\text{Var}^3 = 0.61$. For a population subject to only demographic stochasticity, it is as though $h_2 = 1$ and $h_0 = h_3 = 0$. When the population is subject only to environmental stochasticity, $\text{Var}^i = 0$ for all i values. We here set the quasiextinction threshold as $\bar{N}_n < 1$. This figure was generated over 10000 simulations with an initial condition $z = 10$.

We can use this $\widehat{S}$ population level approximation to examine the difference between the probability of extinction of a population subject to both environmental and demographic stochasticity, or to only one or the other. As illustrated in Figure 3.15,

our model results agree with the general theory that a population subject to multiple types of stochasticity has a higher probability of extinction.

As in the case where only demographic stochasticity was considered, we find that the $\widehat{S}$ population level approximation consistently outperforms the S population level approximation. The population level models are orders of magnitude faster to simulate than the corresponding IBM, but again we turn to a second approximation in order to obtain analytic results and gain further insights.

3.4.3 Approximation to an IBM; a modified BPRE

As before, we wish to approximate the spatially explicit IBM by a spatially implicit branching process in order to obtain some analytic results on the probability of extinction. To this end, we will again use a modified branching process to approximate the results of the IBM. Since we are looking to include the effects of environmental stochasticity on our population, we will incorporate random environments into a branching process of the Galton-Watson type as was first considered by Smith and Wilkinson (1969) and later generalized by Athreya and Karlin (1971). This was first done for iid random environments [108], though many of the subsequent results have been generalized to include any stationary ergodic sequence [4], and have come to be known as *branching processes in random environments* (BPRE).

Unfortunately, as was quickly observed by Smith and Wilkinson (1969) in their initial study, "the elegant functional equations that play such a vital role in the theory of the classical Galton-Watson process, and many published generalizations thereof, do not arise in the present study" [108]. Thus many of the results which we will mention here related to the probability of extinction by a given generation are approximations rather than explicit expressions of expected results. The only thing we will be able

to determine explicitly is a criticality condition for the probability of ultimate extinction, where the long time behaviour changes from certain extinction to extinction with probability strictly less than one.

3.4.3.1 Standard BPREs

We will here briefly reiterate the general BPRE framework of Smith and Wilkinson (1969) in order to be able to modify it to include implicit spatial dependence. We again consider a sequence of iid random variables $\{\varsigma_n\}$, each selected from the possible environments $\{\varsigma^i\}$ according to the probability mass function $\{h_i\}$. We take the reproductive probabilities of our population to be dependent on the environment in a given generation, so that p_i, which described the probability of an individual producing i offspring in one generation in the case of a constant environment, is now $p_i(\varsigma_n) = p_{i_n}$. This results in a family of probability generating functions for each environment ς^j,

$$f^j(s) = \sum_{\lambda=0}^{\infty} p_\lambda^j \, s^\lambda, \qquad s \in [0,1]. \tag{3.4.3}$$

The expected number of offspring in a fixed environment ς^j is then

$$\mathbb{E}(r^j) = \xi^j = f^{j\,\prime}(1) \tag{3.4.4}$$

and $\{\xi_n\}$ is a sequence of iid random variables [108]. Convention here dictates that we assume $P\{\xi^j < \infty\} = 1$ for all environments. We also follow convention and assume $P\{p_0^j + p_1^j < 1\} > 0$ for at least one value of j (that is, the generating function is strictly convex on the unit interval for at least one environment) [118].

As before, we have a sequence of iid random variables $\{Z_n\}$, whose state space is the non-negative integers, describing the population size in the n^{th} generation given an initial population size of $Z_0 = z$. We assume $Z_0 = 1$ from the remainder of this

section unless otherwise stated [108].

Turning our attention to the probability of extinction, we will not go over the derivation of these well-known results here, but rather use them in a novel way to look at the question of critical domain size. Smith and Wilkinson's most important result was to determine the probability of almost certain extinction for a given environmental state space [108]. They found that almost certain extinction (which they termed "mortality") occurs if

$$\mathbb{E}[\ln \xi] \leq 0, \tag{3.4.5}$$

where the expectation is taken over all possible environments. Traditionally, the case where $\mathbb{E}[\ln \xi] = 0$ has been called "critical" and those where it is strictly less than 1, "subcritical". The term "supercritical" or "immortal" is used to describe the case when the probability of ultimate extinction is strictly less than one, and the following two conditions are both necessary and sufficient for supercriticality [108]:

$$\mathbb{E}[\ln \xi] > 0, \quad \text{and} \tag{3.4.6}$$

$$\mathbb{E}[\,|\ln (1 - p_0)|\,] < \infty, \tag{3.4.7}$$

where again the expectation is over all possible environments. The first condition intuitively corresponds to the deterministic requirement that the reproductive rate be greater than one to avoid stability of the zero steady state in a simple map. The second condition serves to ensure that "catastrophes" do not occur, wiping out the entire population in one time step [108].

3.4.3.2 A spatially implicit modified BPRE

For a branching process like the one outlined above, let us again incorporate the possible loss of each offspring due to dispersal to fished areas with probability F. This

results in a structure like that of Figure 3.9, but this time with random environments, so that each $p_i = p_i(\varsigma^j) = p_i^j$ as outlined above. We will now formulate the probability generating functions by grouping our growth rates, not according to their reproductive rates *before* the dispersal period, but rather according to how many offspring successfully settle inside the reserve area *after* the dispersal period. We will denote these post-dispersal rates as $\bar{p}_i^j$. For a given generation and environmental variable ς^j, this results in

$$\bar{p}_0^j = p_0^j + p_1^j F + p_2^j F^2 + \dots \tag{3.4.8}$$

$$\bar{p}_1^j = p_1^j(1-F) + 2p_2^j(1-F)F + 3p_3^j(1-F)F^2 + \dots \tag{3.4.9}$$

$$\bar{p}_2^j = p_2^j(1-F)^2 + 3p_3^j(1-F)^2F + 6p_4^j(1-F)^2F^2 + \dots \tag{3.4.10}$$

$$\vdots \tag{3.4.11}$$

$$\bar{p}_q^j = \sum_{v=q}^{\infty} \binom{v}{q, v-q} p_v^j (1-F)^q F^{v-q} \tag{3.4.12}$$

where

$$\binom{v}{q, v-q} = \frac{v!}{q!(v-q)!} \tag{3.4.13}$$

are multinomial coefficients. We have reorganized our offspring probabilities so that $\bar{p}_i^j$ is the sum of all of the possible ways in which, over one generation, an individual can produce i offspring which survive the dispersal phase in environment ς^j. We now have the probability generating function

$$f^j(s) = \bar{p}_0^j + \bar{p}_1^j s + \bar{p}_2^j s^2 + \bar{p}_3^j s^3 + \dots \tag{3.4.14}$$

The expected reproductive value for a given environment ς^j is

$$\xi^j = f^{j\,\prime}(1) = \bar{p}_1^j + 2\bar{p}_2^j + 3\bar{p}_3^j + \ldots \tag{3.4.15}$$

$$= \sum_{q=1}^{\infty} q\bar{p}_q^j = \sum_{q=1}^{\infty}\sum_{v=q}^{\infty} q \binom{v}{q, v-q} p_v^j (1-F)^q F^{v-q}. \tag{3.4.16}$$

and, as in a constant environment, the above simplifies to

$$\xi^j = \mathbb{E}[r^j]\,(1-F), \tag{3.4.17}$$

which can again be shown using induction. As we would expect, the expected reproductive rate in a given environment is simply the product of the expected reproductive rate of the non-spatial model and the proportion of individuals that settle within the reserve area. If we apply the results on extinction outlined in Section 3.4.3.1 for the non-spatial branching process, the criticality condition in the spatially implicit case will be

$$\mathbb{E}(\ln \xi) = \mathbb{E}(\ln \mathbb{E}(r)) + \ln(1-F) = 0, \tag{3.4.18}$$

where the expectation is again taken over all possible environments. Thus for a given set of environmental conditions and corresponding reproductive rates, we can determine the critical proportion F^* which can be lost from a reserve area before extinction is certain. For any $F < F^*$, the population will be supercritical and for any $F \geq F^*$, eventual extinction occurs with probability one.

We will build on our previous examples to illustrate how this modified BPRE may be used. We will use a similar set of parameters to those used in Section 3.4.2 where we assumed an environmental state space of three possible environments, ς^1, ς^2, and ς^3 which occur with probability $h_1 = 0.4$, $h_2 = 0.4$ and $h_3 = 0.2$. Each of these environments has a corresponding probability mass function for the ran-

dom variable r which describes the number of offspring of an individual. For the first environment, reproductive probabilities are $\{p_0^1 = 0.1, p_1^1 = 0.2, p_2^1 = 0.7\}$. For the second environment they are $\{p_0^2 = 0.1, p_1^2 = 0.3, p_2^2 = 0.6\}$, and for the third, $\{p_0^3 = 0.2, p_1^3 = 0.3, p_2^3 = 0.5\}$. This results in the mean reproductive values $\xi^1 = 1.6$, $\xi^2 = 1.5$, and $\xi^3 = 1.3$ and corresponding variances $\text{Var}^1 = 0.44$, $\text{Var}^2 = 0.45$, and $\text{Var}^3 = 0.61$. For all of the above, the expected number of offspring ξ, is

$$\xi = \mathbb{E}(r) = \xi^1 h_1 + \xi^2 h_2 + \xi^3 h_3 = \mathbb{E}(f'(1)) = 1.5. \tag{3.4.19}$$

Recall from the deterministic case that for an intrinsic reproductive value of 1.5, logistic growth and a Laplace dispersal kernel, the critical domain size of an IDE is $L^* = 2.703$. Looking now to determine the probability of ultimate extinction, we have in the absence of loss via dispersal that

$$\mathbb{E}(\ln f'(1)) = 0.402 > 0 \tag{3.4.20}$$

and so the non-spatial process is supercritical. We now want to determine for what proportion of individuals lost outside the reserve is this expected value of the logarithm reduced to zero, i.e. what is the criticality condition in the presence of implicitly included space. As outlined above, we incorporate loss of individuals outside the reserve area with probability F into our probabilities p_i^j, so that the probability generating function $f^j(s)$ now has the spatially implicit coefficients

$$\bar{p}_0^j = p_0^j + p_1^j F + p_2^j F^2 \tag{3.4.21}$$

$$\bar{p}_1^j = p_1^j(1 - F) + 2p_2^j F(1 - F) \tag{3.4.22}$$

$$\bar{p}_2^j = p_2^j(1 - F)^2. \tag{3.4.23}$$

For our three environments, the above probabilities, and the knowledge that $\xi^j = (p_1^j + 2p_2^j)(1-F)$, we have that

$$\xi^1 = 1.6\,(1-F) \tag{3.4.24}$$

$$\xi^2 = 1.5\,(1-F) \tag{3.4.25}$$

$$\xi^3 = 1.3\,(1-F), \tag{3.4.26}$$

and so for the probability mass function with values h_1, h_2, h_3 as above, we have

$$\mathbb{E}(\ln \xi) = h_1 \ln(1.6(1-F)) + h_2 \ln(1.5(1-F)) + h_3 \ln(1.3(1-F)) \tag{3.4.27}$$

$$= 0.402 + \ln(1-F). \tag{3.4.28}$$

As expected, this is the sum of the non-spatial expected reproductive rate and $\ln(1-F)$. We can now find the critical proportion F^* of individuals lost by solving

$$\mathbb{E}(\ln \xi) = 0.402 + \ln(1-F) = 0, \tag{3.4.29}$$

which results in $F^* = 0.331$. We now use S and $\widehat{S}$ to approximate the proportion of settlers successfully settling, so that $S = \widehat{S} = 1 - F$, and then solve for the corresponding domain lengths. We then obtain the branching process approximation to the critical domain size for an ultimate extinction probability strictly less than one. For example, if we assume dispersal according to a Laplace kernel, we get the critical domain lengths $L_S^* = 2.846$ and $L_{\widehat{S}}^* = 2.744$ for the average dispersal success S and modified average dispersal success $\widehat{S}$ approximations, respectively. As we would intuitively expect, the critical domain sizes for the stochastic model are larger than those required for the deterministic model. We have plotted results around these critical values in Figure 3.16.

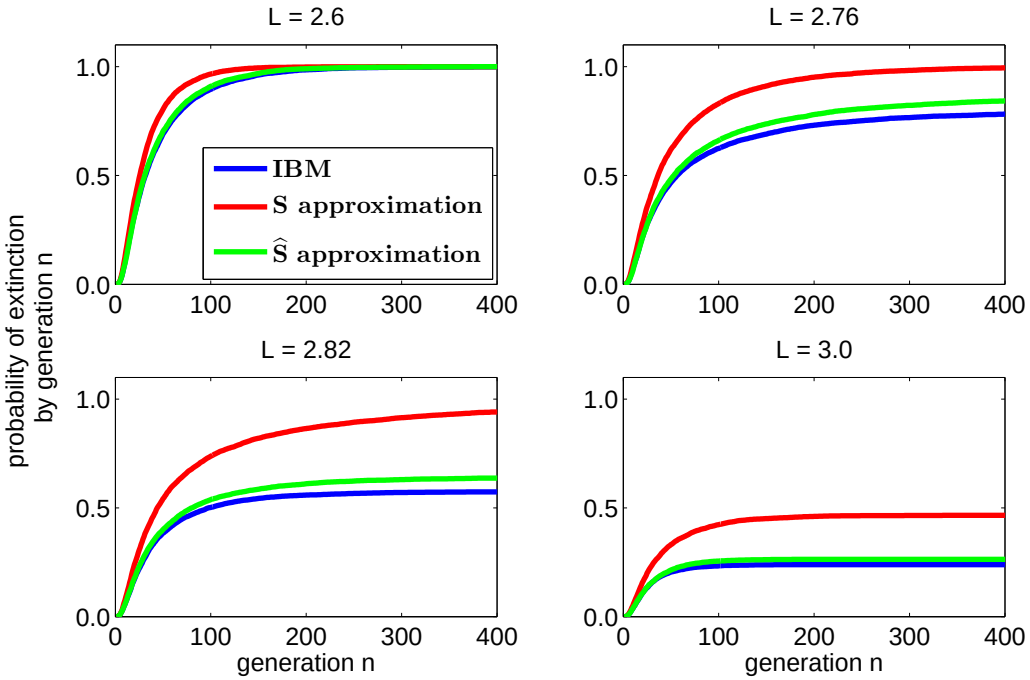

Figure 3.16: Comparison of an IBM with two branching process approximations using the S and $\widehat{S}$ approximations to the proportion of successful settlers, given dispersal according to a Laplace kernel. The initial population size is $Z_0 = 10$, and 10000 simulations were used to obtain these results. We assume three environments, ς^1, ς^2, and ς^3 which have the corresponding probability mass function $\{h_1 = 0.4, h_2 = 0.4, h_3 = 0.2\}$. The corresponding probability mass functions for reproduction are $\{p_0^1 = 0.1, p_1^1 = 0.2, p_2^1 = 0.7\}$, $\{p_0^2 = 0.1, p_1^2 = 0.3, p_2^2 = 0.6\}$, and $\{p_0^3 = 0.2, p_1^3 = 0.3, p_2^3 = 0.5\}$. Again we can see that the $\widehat{S}$ approximation provides a very close approximation to the IBM, even around the critical domain values of $L^* = 2.703$, $L_S^* = 2.846$, and $L_{\widehat{S}}^* = 2.744$.

Recall from Chapter 2 that the modified dispersal success approximation best outperformed the standard S approximation for small reproductive rates. This does not, interestingly, seem to be the case in the stochastic model. As we can see in figure 3.17, the $\widehat{S}$ approximation does not consistently perform better or worse for increasing or decreasing reproductive rates. There are too many other confounding factors here, such as whether the $\widehat{S}$ approximation to the critical domain size is larger or smaller than that considered, as well as the variance.

We have here determined the critical domain size which ensures a probability of ex-

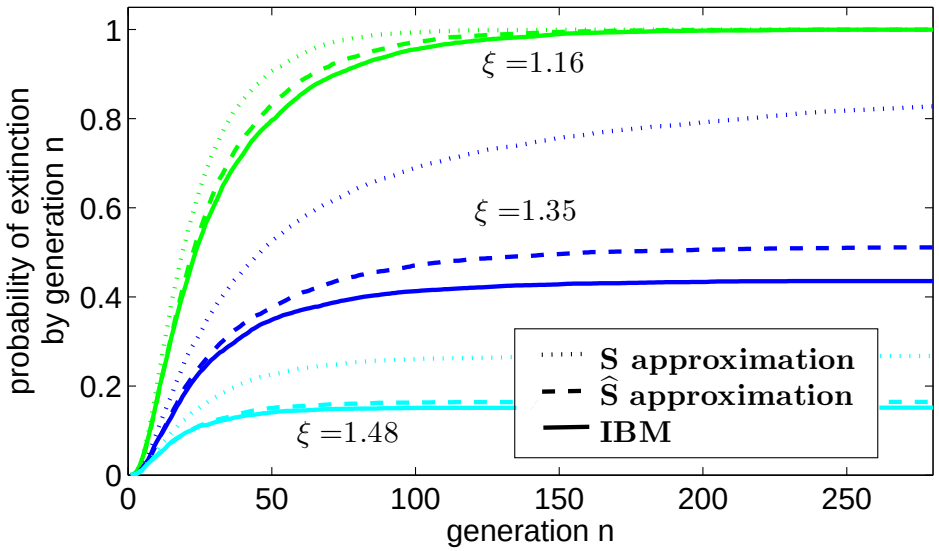

Figure 3.17: Plot of three different parameter regimes for the modified branching process and the initial IBM. Curves were generated from 8000 simulations from an initial condition of 10 individuals. We assumed five possible environments which result in reproductive probability mass functions $\{p_0^1 = 0.2, p_1^1 = 0.3, p_2^1 = 0.5\}$, $\{p_0^2 = 0.1, p_1^2 = 0.3, p_2^2 = 0.6\}$, $\{p_0^3 = 0.3, p_1^3 = 0.2, p_2^3 = 0.5\}$, $\{p_0^4 = 0.3, p_1^4 = 0.5, p_2^4 = 0.2\}$, and $\{p_0^5 = 0.1, p_1^5 = 0.2, p_2^5 = 0.7\}$. $L = 3.8$ times the mean dispersal distance. The green curve results when the probability mass function for environmental occurence is $\{h_1 = 0.5, h_2 = 0.3, h_4 = 0.2\}$, which results in an overall expected reproductive value of $\xi = 1.16$. The blue curve results from the probability mass function $\{h_1 = 0.4, h_3 = 0.3, h_5 = 0.3\}$ and the cyan curve from $\{h_2 = 0.1, h_4 = 0.2, h_5 = 0.7\}$ which result in expected reproductive values of $\xi = 1.35$ and $\xi = 1.48$ respectively.

tinction strictly less than one, based on a stochastic branching process with both environmental and demographic stochasticity. Note, however, that this fails to meet any specific short-term conservation goals such as being able to predict the probability of extinction by a given generation. Unlike when we considered only demographic stochasticity, we can here, at best, only approximate the time to extinction or cumulative extinction probabilities for a certain generation.

We turn our attention briefly to some results in the literature on approximations to the asymptotic value of the probability of extinction, as well as the rate of decline of the probability of survival in different scenarios. Wilkinson (1969) has shown that

the ultimate extinction probabilities of a BPRE with initial population of size z form a moment sequence, and using this, has found an approximation to the extinction probabilities for any finite initial population. This work laid the foundations for many of the simpler approximation approaches which followed [118]. For example, Agresti (1975) found bounds on the extinction time of a BPRE in which the environmental random variables are independent but not necessarily identically distributed.

In the event that the dynamics are supercritical, with a long time extinction probability strictly less than one, we can obtain the order of the long time extinction probability through the methods of Grey (1991). Using Laplace transforms on the distribution of the expected reproductive rates in a BPRE, Grey found that under certain regularity conditions, there exists a parameter $\theta_0 > 0$ such that the probability of extinction $d(z)$ for a population initially of size z is asymptotically (in z) of order not less than $z^{-\theta_0}$ and is of smaller order than z^{θ} for any $\theta < \theta_0$.

In a later paper, Grey et al. (1993) have shown that as z tends to infinity, the rate of convergence of $d(z)$ to zero is similar to either z^{θ}, $exp(c\sqrt{z})$, or $x^z z^{-\alpha}$, depending on whether there is at least one subcritical state in the random environment space, if there is at least one critical state in the random environment space and the others are supercritical, or if there are only supercritical states in random environment space, where θ, α, c, and x are constants determined by the process [34].

If, instead, we have dynamics that are critical and extinction is certain, Geiger and Kerstin (2001) have shown that the asymptotic extinction probability as time n goes to infinity is proportional to $n^{(-1/2)}$ for iid offspring and iid environments. In the subcritical case, Geiger et al. (2003) have shown that the probability of survival at time n decays exponentially fast, with the rate of decay dependent on whether $\mathbb{E}[\xi \ln \xi]$ is less

than, equal to, or greater than zero. Under suitable integrability assumptions, they determine the asymptotic behaviour of the survival probability for all three cases. If there are a finite number of possible environments, Dekking (1987) has shown that in the case of a strongly subcritical branching process, when $\mathbb{E}(\xi \ln(\xi)) \leq 0$, the BPRE behaves as an ordinary subcritical branching process (i.e. the rate of decay is simply $\mathbb{E}(\xi)$). If $\mathbb{E}(\xi \ln(\xi)) > 0$, the rate of decay is strictly less than $\mathbb{E}(\xi)$ [19]. This work was later expanded by D'Souza and Hambly (1997) to a broader class of environmental state spaces. Thus there are a variety of approximations in place if we wish to determine the probability of extinction of a population by a given generation.

3.5 Discussion and conclusions about environmental stochasticity

In the latter part of this chapter, we have looked at environmental variability and its effect on the critical domain size problem. Following the same progression as in the case of only demographic stochasticity, we first created an IBM, where each individual reproduced and dispersed independently, with the probability distributions of reproduction influenced by the environment for a given generation. The IBM was, however, computationally costly due to the explicit spatial dependence, results were difficult to compare, and little understanding could be gained of the importance of the mechanisms at work. We again developed two spatially implicit approximations in order to speed up simulations and gain new insights as to the driving mechanisms of population persistence or decline on a finite domain. The first again used the Central Limit Theorem to scale up to the population level, and resulted in much shorter simulation times for very similar results on the probability of extinction. The second modified a branching process to implicitly include space, but this time also incorpo-

rated random environments into a BPRE framework. Unlike when we only considered demographic variability, the results on BPRE do not allow us to determine the long time probability of extinction, or the probability of extinction by a given generation, but rather we must rely on the criticality condition which separates the cases where extinction is certain from those where the population goes extinct with a probability less than one, tending asymptotically to zero for large initial populations.

The branching process approximations we have used here have many benefits in addition to providing a good approximation to our IBM interpretation of a stochastic IDE. For one, so long as empirical predictions as to the proportion of larvae lost outside a reserve area are obtainable, it is just as easy to have our branching process model represent a reserve in two dimensions, rather than along a one-dimensional coastline as has been considered here. It is also a relatively simple model to parameterize with empirical data, which is important in marine systems where the mechanistic underpinnings are often unknown. For our modified BPRE, it is sufficient if experimental information can be obtained regarding reproductive rates in a range of environments and the proportion of larvae retained within a given area.

By observing the consistency with which the modified dispersal success approximation mimics the behaviour of the IDE, we gain understanding of the original IDE formulation. Much of the behaviour of the IDE is determined by the proportion of individuals which are successfully retained within the reserve area after a dispersal period, and it is for this reason that the approximation performs so well.

Incorporating environmental variability in addition to demographic stochasticity confirmed the generally accepted theory that the more types of stochasticity are incorporated, the higher the probability of extinction. We have here only started to develop

a stochastic framework for analyzing our target populations, and possible extensions to this work are outlined in the next chapter.

Chapter 4

Discussion

It is widely accepted that current fishing practices threaten the viability of marine species worldwide [42, 119]. Many of the populations of conservation and fisheries interest have similar life histories, with a pelagic larval period followed by a comparatively sedentary adult existence. Integrodifference equations provide a good framework from which to determine the critical domain size required for the effective implementation of marine reserves. Marine reserves are an effective management tool for species with these life history traits, as the adults within the reserve area may reproduce several times and with increasing fecundity as they are permitted to grow in size (typically, larger marine species are more fecund than their smaller counterparts). The larvae then disperse outside the reserve area and so, ideally, fishermen in the surrounding waters will also be able to continue their harvesting without significant financial loss.

Unfortunately, for many dispersal kernels and growth functions, the critical domain size of an IDE can only be found via numerical integration and thus it is difficult to compare the differences between populations with different assumed growth or dispersal behaviour. In this work, we have developed a novel spatial approximation

to the proportion of individuals lost to fishing pressure outside the reserve area in order to aid the ease of these comparisons. We then go on to use this approximation in a variety of spatially implicit approximations to the IDE framework in order to determine the critical domain size required for population persistence.

The standard approximation of dispersal success has typically been that of Van Kirk and Lewis (1997). Their approximation assumes that the population is evenly distributed through the reserve area, but this is not generally the case. One way to approximate the distribution of the individuals inside the reserve area is by using the dispersal success function at each point in the domain [113]. By accounting for this non-homogeneous population distribution, the new approximation consistently outperforms the standard one.

We compare the results on the critical domain size obtained using this new approximation first on a single reserve, then on an idealized network of evenly spaced reserves of equal size. We consider the case when the population is subject to advection and gain insight into the necessity of capturing the "wash-out" behaviour of the IDE into any approximations. We then turn to incorporate stage- or size-structure, which is more biologically relevant for many of our populations of interest. For all of these cases, this modified dispersal success approximation mimics the results of an IDE better than that of the standard dispersal success approximation, and requires far less computation than the IDE. From the consistency of the results, we gain an important insight as to what is important in determining the critical domain size of an IDE. By assuming the population density can be approximated by the dispersal success function at each point, we observe that it is not the shape of the kernel which matters, but the proportion of individuals which settle inside the reserve area.

We can use the modified dispersal success approximation to obtain an expression for L^*, unlike in most IDE formulations, and from this we can observe the dependence of the critical domain size on the demographic and dispersal parameters. This novel approximation thus allows for quick comparisons between IDES using different dispersal kernels and growth functions.

Following this, we turn our attention to a stochastic analogue to an IDE, choosing an IBM to represent a population of individuals independently reproducing and dispersing. We first consider only demographic stochasticity, and then go on to also look at environmental variability by allowing for a random environmental variable. In both of these cases, we create two spatially implicit approximations; first scaling the IBM up to the population level using the Central Limit Theorem, and then modifying a Galton-Watson branching process to implicitly include space. In both of the spatially implicit approximations, the modified dispersal success function first proposed in the deterministic work provides results on the critical domain size which closely approximate those of the IBM.

While we have here considered some of the possible uses of a stochastic analogue to an IDE model, as well as possible ways to approximate a detailed IBM in order to obtain analytic results, we have neglected many important areas. For simplicity, we have assumed density independent growth, regardless of population size, but real populations often experience some form of density dependence, whether this be a general decrease in growth rates as a population increases or, more relevant for marine populations at risk, this could take the form of an Allee effect. We have not looked at this in this work, as incorporating density dependence often results in the model becoming more difficult to analyze, and our understanding of density dependent stochastic models is still quite incomplete [50]. In general, a density independent

model may be used as a conservative assessment, as density dependent models tend to have less variability [1]. Density dependence is, however, a natural extension to this chapter and it is important to note that a failure to include density dependence is often found to change survival estimates substantially [27].

The second area in which the stochastic framework of Chapter 3 could be expanded was briefly explored in the deterministic models of Chapters 1 and 2, and it is the possibility of including size or age structure into our model. The populations we are interested in have very different dispersal behaviour throughout their life histories, and allowing for stage or age structure would allow for closer examination of the possible effects of an initial age distribution. Branching processes for structured populations such as these have been considered (see e.g. [33, 53, 121]) but it is difficult to derive general quantitative results about extinction probabilities since the results are sensitive to the variability in dispersal, births, and deaths for each stage. An excellent review of population viability analyses for stage-structured populations has been performed by Akçakaya (2000), though their models include space only in the form of a metapopulation structure.

In Chapter 2, we also considered the persistence of a population over a reserve network, and the stochastic models should extend without complication to different domain structures. We also looked at populations subject to alongshore currents, and advection could be incorporated in a similar way into the dispersal behaviour of the stochastic models. A further area for consideration and one of biological interest could be variability in currents. We could consider the advection strength as a random variable, or incorporate advection speed into our environmental variables. We have not looked at this further here, but this would be a natural extension to the work in Chapter 3.

There are three further types of possible variability which may also need to be considered, namely genetic stochasticity, variable sex ratios of offspring, and random catastrophes [70]. Shaffer (1987) has concluded that random catastrophes are more important than environmental stochasticity and demographic stochasticity when determining persistence of populations, and several later authors have agreed [52]. Catastrophes could most simply be modelled as a more extreme form of environmental stochasticity, with very large possible fluctuations that occur with very low probability. Alternatively, others have modelled catastrophes by reducing the population by a fixed proportion at random times [23, 38, 52]. Melbourne and Hastings (2008) derived a family of stochastic Ricker models in which different combinations of stochastic factors could be incorporated. They have shown that extinction risk depends strongly on the combination of these factors, and that only by including all possible mechanistic sources of stochasticity can the true relative extinction risks be assessed. In addition, they find that current estimates of extinction risk may be underestimated, as variability has often erroneously been attributed to environmental variability rather than to demographic factors, which result in a much higher extinction risk for the same level of variability [70].

Unfortunately, even with the relatively few parameters required by the stochastic models we have presented here, it is often very difficult to measure variability in demographic rates, or to tease out the dependence of fluctuating reproductive rates on environmental variation. In order for models to accurately capture levels of variability, it takes many years of careful data gathering to be able to separate the effects of demographic and environmental stochasticity. Complex interactions between individual life histories, environmental context, and anthropogenic factors all affect the threat of extinction of a given population and are difficult to detect from noisy or incomplete

data [27]. In order to be able to distinguish between models and find a model with the best fit, it is necessary to use likelihood approaches and information criteria, both of which require extensive data sets over many generations [70]. We direct the reader to two examples in Saether (1998, 1998a) of where both demographic and environmental variance were estimated based on long-term data. A concise review of this topic can be found in Engen (1998). In spite of these difficulties, including uncertainty in conservation studies is critical if we wish to avoid biased expectations and most effectively direct often scarce resources. Population viability analyses using models such as these can help to formalize our understanding of biological processes, expose gaps in our knowledge, and serve as a focus for both scientists and policy-makers [27]. However, models such as the above cannot hope to include every possible source of variability affecting a population, but rather provide a method of comparing relative extinction risks, and they should be used in this fashion rather than be expected to provide explicit guidelines.

Another important area for marine conservation which we have neglected throughout this work is that of community structure. While fisheries managers may be concerned with a single species of economic interest, conservationists will often be interested in maintaining a certain level of biodiversity. The introduction of a reserve area will necessarily alter the balance of various trophic levels and predator-prey or more symbiotic relationships will be affected in ways which we have not explored here. Determining how large a reserve needs to be in order to maintain biodiversity requires even more knowledge of the ecosystem than single species management strategies, as well as the establishment of a list of priorities - whether that be to preserve the greatest number of species, certain species of specific interest, or environments which are critical for certain life history stages such as nursery grounds. Moffitt et al. (2011) have created an indexing system using combinations of larval dispersal distances and adult home

range values to help determine the number of species that a network of protected areas could help to protect, and further work in this direction is necessary for the maintenance of biodiversity and ecosystem structures.

The work presented here is clearly an idealized and theoretical modelling framework for marine systems which, in reality, are subject to much uncertainty and complexity beyond what we have considered here. Many of the assumptions we are forced to make are difficult to test empirically, and experimental evidence is costly and difficult to acquire [99]. Calculating levels of recruitment, which have considerable inter-annual variability [16], or determining the dispersal patterns of larvae and how they are influenced by regional hydrodynamics [87] requires technology which is only beginning to be developed (see [85] and [111] for examples). Much of the life history information required to parameterize models such as those presented here is not available, and many of these values are often not even known to within several orders of magnitude. Movement of marine organisms is difficult to track, especially when those organisms are abundant and very small, like the pelagic larvae we have considered. In order for theoretical models like those proposed here to be developed further and more accurately, they will have to develop alongside other branches of marine science.

Furthermore, in order for spatial management to be effective, it is not simply a matter of further developing marine science. Conservation and management decisions are, to a large extent, the purview not of science but of society, which must determine which risks are worth taking [27]. There are socio-economic implications in any management strategy and interests between environmental groups, governments, industry, and individuals are often conflicting. Thus any theory such as that presented here must be incorporated into a larger, more comprehensive understanding of marine conservation which is beyond the scope of this work but is nonetheless of the utmost importance

[5, 25].

In this work, we have found that the modified dispersal success approximation provides close estimates to the behaviour of a population modelled using an IDE framework. This new approximation allows for a range of methods, both deterministic and stochastic, for determining the reserve size necessary for population persistence, based on and closely mimicking the more complicated IDE framework. This framework is suitable for many species of conservation and fisheries interest, and an easily usable approximation such as the one we have presented allows for insight into marine population persistence in a variety of environments and for populations with different dispersal or reproductive behaviour.

Appendix A

Growth functions

One of the simplest and most widely used discrete-time growth functions is the logistic map [68, 69]

$$N_{t+1} = rN_t\left(1 - \frac{N_t}{K}\right), \qquad N_t \leq K \tag{A.0.1}$$

with growth rate r and environmental carrying capacity K. This function can exhibit a wide variety of dynamical behaviours as the intrinsic growth rate, r, varies, ranging from stable equilibria to period doubling bifurcations, to chaotic fluctuations [113]. It is a model of overcompensatory growth, as is the Ricker model [94], which displays a similar startling array of behaviour. Proposed in 1954 to describe population dynamics in fisheries in the context of stock and recruitment, the Ricker model,

$$N_{t+1} = N_t \exp\left\{r\left(1 - \frac{N_t}{K}\right)\right\}, \tag{A.0.2}$$

is appropriate if recruitment is severely limited at very high population densities. Note that unlike the logistic map, the Ricker model will never obtain negative values and is thus sometimes more biologically appropriate. It is very common in the fisheries literature, as it is simple to work with and yet generally captures the most important features of marine population dynamics [71]. Another growth model designed with

fisheries in mind is the Beverton-Holt mapping [9],

$$N_{t+1} = \frac{rN_t}{1 + N_t(r-1)/K}. \tag{A.0.3}$$

This growth function displays compensatory behaviour rather than overcompensatory, with K as a globally stable non-trivial steady state [113]. All of the above models have density dependent declines in growth rate corresponding to population growth. For the present purposes, we will not consider growth functions displaying Allee effects, as Myers et al. performed a survey showing that of the 128 marine species considered, only three showed significant depensation (i.e. a decline in growth rates corresponding to a decline in population density) [77]. The above growth functions can be seen in Figure A.1.

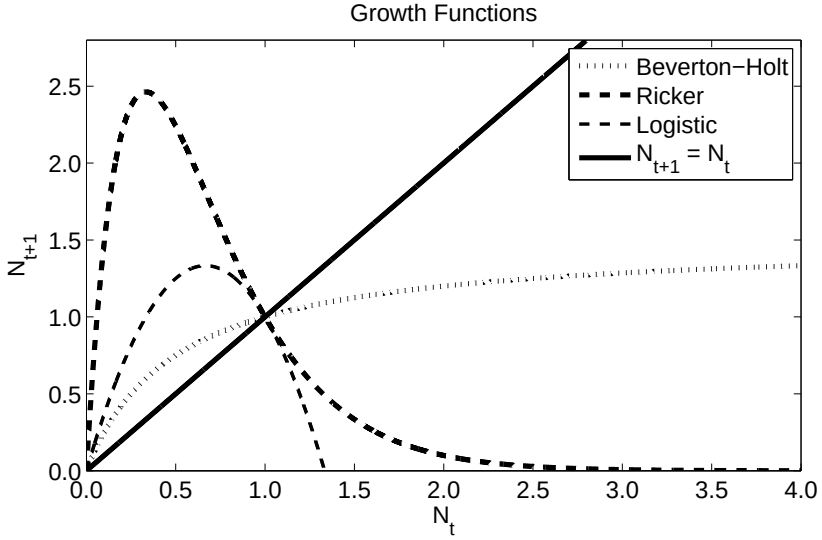

Figure A.1: Growth functions (A.0.1) - (A.0.3). In all of the plots, $r = 3$ and $K = 1$. Observe that all of the functions have a steady-state solution at $N^* = 1 = K$.

Appendix B

Summary of kernel derivation

We will now briefly summarize the kernel derivation procedure of Lutscher et al. (2005) who mechanistically derived dispersal kernels, first without unidirectional currents, and then incorporating advection to derive shifted and asymmetric kernels (see [62, 81] for full details). They start by supposing $\omega(t, x; y)$ is the PDF for the location of a pelagic individual with initial location $x = y$ over a change in time of length t. They assume that the individual moves for a random length of time T taken from a given PDF, $p(t)$, and after time T the individual settles. The dispersal kernel is then the PDF of settling points from the given initial location, i.e.,

$$k(x, y) = \int_0^\infty p(t)\omega(t, x; y)dt. \tag{B.0.1}$$

For example, if the individuals are moving via Brownian motion (i.e. simple diffusion) then $\omega(t, x; y)$ is the normal, or Gaussian PDF. If dispersers can jump long distances in short time intervals, $\omega(t, x; y)$ is the Cauchy distribution (see Appendix A in [62] for detailed derivations). Since we are also interested in deriving kernels for populations subject to advection, we next incorporate a unidirectional current with an effective drift rate v into these equations. Then $\omega(t, x; y)$ is as above, but with x replaced by $x - vt$ [84].

Turning now to the stopping time T, Lutscher et al. (2005) have considered two different possibilities. The simplest one would be to assume that all individuals disperse for the same, fixed length of time t_0, in which case

$$p(t) = \delta(t - t_0). \tag{B.0.2}$$

In this case, (B.0.1) becomes $k(x, y) = \omega(t_0, x; y)$, and the dispersal kernel is simply the chosen PDF, with a shift if $v \neq 0$. This results in the Gaussian and shifted Gaussian kernels (for $v = 0$ and $v \neq 0$, respectively)

$$k(x, y) = \frac{\exp\left(\frac{-(x - vt_0 - y)^2}{4Dt_0}\right)}{\sqrt{4\pi D t_0}}, \tag{B.0.3}$$

and the Cauchy and shifted Cauchy kernels (again, for $v = 0$ and $v \neq 0$, respectively)

$$k(x, y) = \frac{t_0}{\rho\pi}\left[\left(\frac{x - vt_0 - y}{\rho}\right)^2 + t_0^2\right]^{-1}. \tag{B.0.4}$$

Another possible choice of stopping time comes if $\alpha(t)$ is defined as the *settling rate*, so that $\alpha(t)dt$ is the probability that an individual settles during $[t, t + dt)$. Then if we assume dispersal via simple diffusion, the kernel becomes the Laplace distribution

$$k(x, y) = \sqrt{\frac{\alpha}{4D}} \exp\left(-|x - y|\sqrt{\frac{\alpha}{D}}\right) \tag{B.0.5}$$

and if using the Cauchy PDF for $\omega(t, x; y)$, we obtain the fat-tailed kernel

$$\begin{aligned} k(x, y) &= \theta\Re\left\{\mathrm{E}_1(\imath\theta(x - y)) \exp\left(\imath\theta(x - y)\right\}/\pi\right. \\ &= -\theta(\cos\left(\theta(x - y)\right)\mathrm{ci}(\theta(x - y)) + \sin\left(\theta(x - y)\right)\mathrm{si}(\theta(x - y))/\pi \end{aligned} \tag{B.0.6}$$

where $\theta = \alpha/\rho$ and the functions E_1, ci, and si are the exponential, cosine, and sine integrals, respectively [62]:

$$\mathrm{E}_1(x) = \int_1^\infty \frac{\exp(xz)}{z} dz, \quad \mathrm{ci}(x) = -\int_1^\infty \frac{\cos(xz)}{z} dz, \quad \mathrm{si}(x) = -\int_1^\infty \frac{\sin(xz)}{z} dz.$$

Unlike in the case where all individuals settled simultaneously, if we now incorporate advection into these derivations, it creates asymmetric kernels rather than merely shifted ones. Beginning with the assumption of a Gaussian PDF subject to advection results in the asymmetric Laplace kernel,

$$k(x,y) = \begin{cases} A\exp(a_1(x-y)), & (x-y) \leq 0 \\ A\exp(a_2(x-y)), & (x-y) \geq 0 \end{cases} \tag{B.0.7}$$

with the constant A

$$A = \frac{a_1 a_2}{a_2 - a_1} = \frac{\alpha}{\sqrt{v^2 + 4\alpha D}} \tag{B.0.8}$$

for

$$a_{1,2} = \frac{v}{2D} \pm \sqrt{\frac{v^2}{4D^2} + \frac{\alpha}{D}}, \tag{B.0.9}$$

which can be seen in Figure B.1 for different strengths of advection.

In general, when deriving dispersal kernels, all else being equal, the greater the diffusion coefficient, the fatter the tails of the kernel. Similarly, the lower the settling rate (i.e. the more time individuals spend in a pelagic phase), the fatter the tails of the kernel.

Lutscher et al. (2005) next looked at fat-tailed kernels, whose tails are not exponentially bounded. They derived a fat-tailed kernel by integrating the Cauchy distribution with x replaced by $x - vt$, multiplied with the probability of stopping times

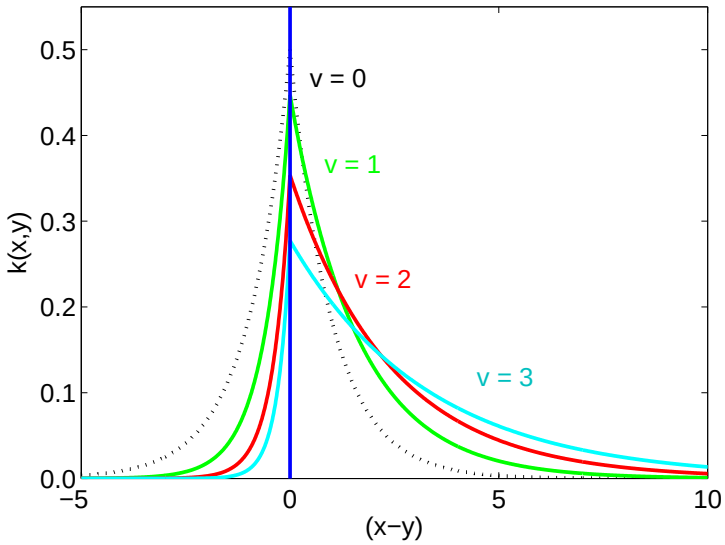

Figure B.1: Asymmetric Laplace kernel (1.7.4a) derived by Lutscher et al. (2005), with $D = 1$, $\alpha = 1$, and $v = 0, 1, 2, 3$ in decreasing height of the peaks (note: $v = 0$ produces the symmetric Laplace kernel).

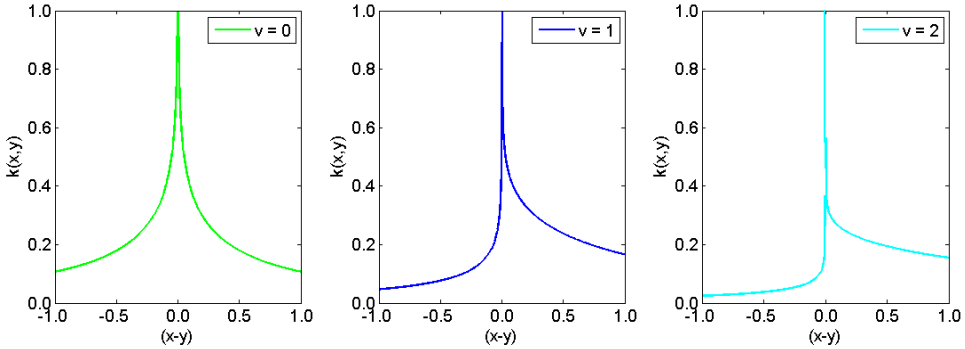

Figure B.2: Fat-tailed dispersal kernel (B.0.10) with $\mu = 1$ and $\alpha = 0.5$ for varying values of the advection velocity v [62].

$p(t)$ appropriate for a constant settling rate, according to (B.0.1), which yields the asymmetric fat-tailed kernel seen in Figure B.2 for different strengths of advection,

$$k(x,y) = \frac{\alpha}{(\mu^2+v^2)\pi}\Re\left((\mu+vi)\mathrm{E}_1\left(-\frac{\alpha(v-\mu i)(x-y)}{\mu^2+v^2}\right)\exp\left(-\frac{\alpha(v-\mu i)(x-y)}{\mu^2+v^2}\right)\right). \tag{B.0.10}$$

All of these kernels, and their mechanistic assumptions, are listed in Table B.1.

	Fixed dispersal length $T = t_0$		Constant settling rate α	
	No advection	With advection, v	No advection	With advection, v
Gaussian probability density for location of a mobile individual	Gaussian (B.0.3) ($v = 0$)	Shifted Gaussian (B.0.3)	Laplace (B.0.5)	Asymmetric Laplace (B.0.7)
Cauchy probability density for location of a mobile individual	Cauchy (B.0.4) ($v = 0$)	Shifted Cauchy (B.0.4)	Fat-tailed (B.0.6)	Asymmetric Fat-tailed (B.0.10)

Table B.1: Kernels derived from the mechanistic movement models of Lutscher et al. (2005). See Figure 1.7 for a plot of these dispersal kernels in addition to a few other phenomenological and mechanistic kernels.

Bibliography

[1] H. R. Akçakaya. Population viability analyses with demographically and spatially structured models. *Ecological Bulletins*, 48:23–38, 2000.

[2] G. W. Allison, J. Lubchenco, and M. H. Carr. Marine reserves are necessary but not sufficient for marine conservation. *Ecological Applications*, 8(1):S79–S92, 1998.

[3] M. Andersen. Properties of some density-dependent integrodifference equation population models. *Mathematical Biosciences*, 104(1):135–157, 1991.

[4] K. B. Athreya and S. Karlin. On branching processes with random environments: I: Extinction probabilities. *The Annals of Mathematical Statistics*, 42(5):1499–1520, 1971.

[5] S. A. Banks and G. A. Skilleter. Implementing marine reserve networks: A comparison of approaches in New South Wales (Australia) and New Zealand. *Marine Policy*, 34(2):197–207, 2010.

[6] M. S. Bartlett. *Stochastic population models in ecology and epidemiology*. Monographs on Applied Probability and Statistics. Methuen London, 1960.

[7] L. Berezansky, L. Idels, and M. Kipnis. Mathematical model of marine protected areas. *IMA Journal of Applied Mathematics*, 76:312–325, 2011.

[8] R. Beverton. Fish, fact and fantasy: a long view. *Reviews in Fish Biology and Fisheries*, 8:229–249, 1998.

[9] R. J. H. Beverton and S. J. Holt. *On the dynamics of exploited fish populations*. Her Majesty's Stationery Office, 1957.

[10] L. Botsford, D. Brumbaugh, C. Grimes, J. Kellner, J. Largier, M. O. Farrell, S. Ralston, E. Soulanille, and V. Wespestad. Connectivity, sustainability, and yield: bridging the gap between conventional fisheries management and marine protected areas. *Reviews in Fish Biology and Fisheries*, 19:69–95, 2009.

[11] L. W. Botsford, A. Hastings, and S. D. Gaines. Dependence of sustainability on the configuration of marine reserves and larval dispersal distance. *Ecology Letters*, 4:144–150, 2001.

[12] L. W. Botsford, C. L. Moloney, J. L. Largier, and A. Hastings. Metapopulation dynamics of meroplanktonic invertebrates: The dungeness crab (cancer magister) as an example. *Canadian Special Publication of Fisheries and Aquatic Sciences*, 125:295–306, 1998.

[13] J. M. Bullock, S. M. White, C. Prudhomme, C. Tansey, R. Perea, and D. A. P. Hooftman. Modelling spread of British wind-dispersed plants under future wind speeds in a changing climate. *Journal of Ecology*, 100(1):104–115, 2012.

[14] K. P. Burnham and D. R. Anderson. *Model selection and multi-model inference: a practical information-theoretic approach*. Springer, 2002.

[15] J. E. Byers and J. M. Pringle. Going against the flow: retention, range limits and invasions in advective environments. *Marine Ecology Progress Series*, 313:27–41, 2006.

[16] M. Caley, M. Carr, M. Hixon, T. Hughes, G. Jones, and B. Menge. Recruitment and the local dynamics of open marine populations. *Annual Review of Ecology and Systematics*, 27:477–500, 1996.

[17] H. Caswell. *Matrix population models*. Wiley Online Library, 2006.

[18] J. Conway. *A Course in Functional Analysis*. Springer-Verlag, New York, 1990.

[19] F. M. Dekking. On the survival probability of a branching process in a finite state iid environment. *Stochastic processes and their applications*, 27:151–157, 1987.

[20] S. Dewhirst and F. Lutscher. Dispersal in heterogeneous habitats: Thresholds, spatial scales, and approximate rates of spread. *Ecology*, 90(5):1338–1345, 2009.

[21] EcoWorld. Sverdrups and brine, July 2007.

[22] S. Engen and B. E. Sæther. Stochastic population models: some concepts, definitions and results. *Oikos*, pages 345–352, 1998.

[23] W. J. Ewens, P. J. Brockwell, J. M. Gani, and S. I. Resnick. Minimum viable population size in the presence of catastrophes. *Viable populations for conservation*, pages 59–68, 1987.

[24] W. Feller. Diffusion processes in genetics. In *Proc. Second Berkeley Symp. Math. Statist. Prob*, volume 227, page 246, 1951.

[25] L. Fernandes, J. Day, A. Lewis, S. Slegers, B. Kerrigan, D. Breen, D. Cameron, B. Jago, J. Hall, and D. Lowe. Establishing representative no-take areas in the Great Barrier Reef: Large-scale implementation of theory on marine protected areas. *Conservation Biology*, 19(6):1733–1744, 2005.

[26] R. A. Fisher. The wave of advance of advantageous genes. *Annals of Eugenics*, 7:355–369, 1937.

[27] C. H. Flather, G. D. Hayward, S. R. Beissinger, and P. A. Stephens. Minimum viable populations: is there a "magic number" for conservation practitioners? *Trends in Ecology & Evolution*, 26:307–316, 2011.

[28] S. D. Gaines, B. Gaylord, and J. L. Largier. Avoiding current oversights in marine reserve design. *Ecological Applications*, 13(1):S32–S46, 2003.

[29] S. D. Gaines, C. White, M. H. Carr, and S. R. Palumbi. Designing marine reserve networks for both conservation and fisheries management. *Proceedings of the National Academy of Sciences of the United States of America*, 107:18286–18293, 2012.

[30] B. Gaylord and S. D. Gaines. Temperature or transport? Range limits in marine species mediated solely by flow. *The American Naturalist*, 155(6):769–789, 2000.

[31] L. R. Gerber, L. W. Botsford, A. Hastings, H. P. Possingham, S. D. Gaines, S. R. Palumbi, and S. Andelman. Population models for marine reserve design: A retrospective and prospective synthesis. *Ecological Applications*, 13(1):S47–S64, 2003.

[32] L. R. Ginzburg, L. B. Slobodkin, K. Johnson, and A. G. Bindman. Quasiextinction probabilities as a measure of impact on population growth. *Risk Analysis*, 2:171–181, 1982.

[33] L. A. Goodman. The probabilities of extinction for birth-and-death processes that are age-dependent or phase-dependent. *Biometrika*, 54(3-4):579–596, 1967.

[34] D. Grey and L. Zhunwei. The asymptotic behaviour of extinction probability in the Smith-Wilkinson branching process. *Advances in Applied Probability*, 25:263–289, 1993.

[35] F. Guichard, S. A. Levin, A. Hastings, and D. Siegel. Toward a dynamic metacommunity approach to marine reserve theory. *BioScience*, 54(11):1003–1011, 2004.

[36] B. Halpern and J. E. Duffy. The encyclopedia of earth: Marine reserves. *http://www.eoearth.org/article/Marine_reserves*, 2008.

[37] R. Hannesson. Marine reserves: What would they accomplish? *Marine Resouce Economics*, 13:159–170, 1998.

[38] F. B. Hanson and H. C. Tuckwell. Logistic growth with random density independent disasters. *Theoretical Population Biology*, 19(1):1–18, 1981.

[39] D. P. Hardin, P. Tak, and G. F. Webb. Dispersion population models discrete in time and continuous in space. *Journal of Mathematical Biology*, 28:1–20, 1990.

[40] D. Hiebeler. Stochastic spatial models: from simulations to mean field and local structure approximations. *Journal of Theoretical Biology*, 187:307–319, 1997.

[41] S. Hsu and X. Zhao. Spreading speeds and traveling waves for non-monotone integrodifference equations. *SIAM Journal on Mathematical Analysis*, 40:776–789, 2008.

[42] J. B. Jackson, M. X. Kirby, W. H. Berger, K. A. Bjorndal, L. W. Botsford, B. J. Bourque, R. H. Bradbury, R. Cooke, J. Erlandson, J. A. Estes, et al. Historical overfishing and the recent collapse of coastal ecosystems. *Science*, 293(5530):629–637, 2001.

[43] G. S. Jamieson and C. O. Levings. Marine protected areas in Canada: implications for both conservation and fisheries management. *Canadian Journal of Fisheries and Aquatic Sciences*, 58(1):138–156, 2001.

[44] Y. Jin and M. A. Lewis. Seasonal influences on population spread and persistence in streams: critical domain size. *SIAM Journal on Applied Mathematics*, 71(4):1241–1262, 2011.

[45] E. Jongejans, O. Skarpaas, and K. Shea. Dispersal, demography and spatial population models for conservation and control management. *Perspectives in Plant Ecology, Evolution and Systematics*, 9(3-4):153–170, 2008.

[46] N. Keiding. Extinction and exponential growth in random environments. *Theoretical Population Biology*, 8(1):49–63, 1975.

[47] H. Kierstead and L. B. Slobodkin. The size of water masses containing plankton blooms. *J. mar. Res*, 12(1):141–147, 1953.

[48] M. Kot. Discrete-time travelling waves: Ecological examples. *Journal of Mathematical Biology*, 30:413–436, 1992.

[49] M. Kot, M. A. Lewis, and P. V. D. Driessche. Dispersal data and the spread of invading organisms. *Ecology*, 77(7):2027–2042, 1996.

[50] M. Kot, J. Medlock, T. Reluga, and D. Brian Walton. Stochasticity, invasions, and branching random walks. *Theoretical Population Biology*, 66(3):175–184, 2004.

[51] M. Kot and W. M. Schaffer. Discrete-time growth-dispersal models. *Mathematical Biosciences*, 80:109–136, 1986.

[52] R. Lande. Risks of population extinction from demographic and environmental stochasticity and random catastrophes. *American Naturalist*, 142(6):911–927, 1993.

[53] R. Lande and S. H. Orzack. Extinction dynamics of age-structured populations in a fluctuating environment. *Proceedings of the National Academy of Sciences*, 85(19):7418–7421, 1988.

[54] G. Leigh Jr. The average lifetime of a population in a varying environment. *Journal of Theoretical Biology*, 90(2):213–239, 1981.

[55] L. A. Levin. Recent progress in understanding larval dispersal: new directions and digressions. *Integrative and Comparative Biology*, 46(3):282–297, 2006.

[56] D. R. Lockwood, A. Hastings, and L. W. Botsford. The effects of dispersal patterns on marine reserves: Does the tail wag the dog? *Theoretical Population Biology*, 61(3):297–309, 2002.

[57] J. Lubchenco, S. R. Palumbi, S. D. Gaines, and S. Andelman. Plugging a hole in the ocean: The emerging science of marine reserves. *Ecological Applications*, 13(1):S3–S7, 2003.

[58] F. Lutscher. Density-dependent dispersal in integrodifference equations. *Journal of Mathematical Biology*, 56:499–524, 2008.

[59] F. Lutscher, M. Lewis, and E. McCauley. Effects of heterogeneity on spread and persistence in rivers. *Bulletin of Mathematical Biology*, 68:2129–2160, 2006.

[60] F. Lutscher and M. A. Lewis. Spatially-explicit matrix models. *Journal of mathematical biology*, 48(3):293–324, 2004.

[61] F. Lutscher, R. Nisbet, and E. Pachepsky. Population persistence in the face of advection. *Theoretical Ecology*, 3:271–284, 2010.

[62] F. Lutscher, E. Pachepsky, and M. A. Lewis. The effect of dispersal patterns on stream populations. *SIAM Review*, 47(4):749–772, 2005.

[63] F. Lutscher and S. V. Petrovskii. The importance of census times in discrete-time growth-dispersal models. *Journal of Biological Dynamics*, 2(1):55–63, 2008.

[64] P. M. Mace and M. P. Sissenwine. How much spawning per recruit is enough? *Canadian Special Publication of Fisheries and Aquatic Sciences*, pages 101–118, 1993.

[65] A. Man, R. Law, and N. V. C. Polunin. Role of marine reserves in recruitment to reef fisheries: A metapopulation model. *Biological Conservation*, 71:197–204, 1995.

[66] K. Mangor. Coastal wiki: Currents in the nearshore zone. Technical report, http://www.coastalwiki.org/wiki/Currents, 2008.

[67] A. Manica. Filial cannibalism in teleost fish. *Biological Reviews*, 77(2):261–277, 2002.

[68] R. M. May. Simple mathematical models with very complicated dynamics. *Nature*, 261:459–467, 1976.

[69] J. Maynard Smith. *Mathematical ideas in biology*. London and New York: Cambridge University Press., 1968.

[70] B. A. Melbourne and A. Hastings. Extinction risk depends strongly on factors contributing to stochasticity. *Nature*, 454(7200):100–103, 2008.

[71] F. Micheli, P. Amarasekare, J. Bascompte, and L. R. Gerber. Including species interactions in the design and evaluation of marine reserves: Some insights from a predator-prey model. *Bulletin of Marine Science*, 74(3):653–669, 2004.

[72] T. Miethe, J. Pitchford, and C. Dytham. An individual-based model for reviewing marine reserves in the light of fisheries-induced evolution in mobility and size at maturation. *Journal of Northwest Atlantic Fisheries Science*, 41:151–162, 2009.

[73] D. Mollison. Spatial contact models for ecological and epidemic spread. *Journal of the Royal Statistical Society. Series B (Methodological)*, 39(3):283–326, 1977.

[74] K. Müller. Investigations on the organic drift in north swedish streams. *Institute of Freshwater Research, Drottningholm, Report*, 34:133–148, 1954.

[75] J. Murray. *Mathematical Biology*. Springer-Verlag, 1989.

[76] J. D. Murray. *Mathematical Biology I: An Introduction*. Springer, third edition, 2002.

[77] R. A. Myers, N. J. Barrowman, J. A. Hutchings, and A. A. Rosenberg. Population dynamics of exploited fish stocks at low population levels. *Science*, 269(5227):1106–1108, 1995.

[78] R. A. Myers, K. G. Bowen, and N. J. Barrowman. Maximum reproductive rate of fish at low population sizes. *Canadian Journal of Fisheries and Aquatic Sciences*, 56(12):2404–2419, 1999.

[79] R. A. Myers and B. Worm. Rapid worldwide depletion of predatory fish communities. *Nature*, 423:280–283, 2003.

[80] M. G. Neubert and H. Caswell. Demography and dispersal: Calculation and sensitivity analysis of invasion speed for structured populations. *Ecology*, 81(6):1613–1628, 2000.

[81] M. G. Neubert, M. Kot, and M. A. Lewis. Dispersal and pattern formation in a discrete-time predator-prey model. *Theoretical Population Biology*, 48(1):7–43, 1995.

[82] M. G. Neubert and I. M. Parker. Projecting rates of spread for invasive species. *Risk Analysis*, 24(4):817–831, 2004.

[83] J. S. Nowlis and C. M. Roberts. Fisheries benefits and optimal design of marine reserves. *Fishery Bulletin*, 97:604–616, 1999.

[84] E. Pachepsky, F. Lutscher, R. M. Nisbet, and M. A. Lewis. Persistence, spread and the drift paradox. *Theoretical Population Biology*, 67(1):61–73, 2005.

[85] S. Palumbi, S. Gaines, H. Leslie, and R. Warner. New wave: high-tech tools to help marine reserve research. *Frontiers in Ecology and the Environment*, 1(2):73–79, 2003.

[86] S. R. Palumbi. *The Ecology of Marine Protected Areas*, chapter 19, pages 509–530. Sinauer Associates, 2001.

[87] C. Paris, R. Cowen, K. Lwiza, D. Wang, and D. Olson. Multivariate objective analysis of the coastal circulation of Barbados, West Indies: implication for larval transport. *Deep Sea Research Part I: Oceanographic Research Papers*, 49(8):1363–1386, 2002.

[88] C. B. Paris. Larval transport pathways from cuban snapper (lutjanidae) spawning aggregations based on biophysical modeling. *Marine Ecology Progress Series*, 296:93–106, 2005.

[89] J. C. V. Pezzey, C. M. Roberts, and B. T. Urdal. A simple bioeconomic model of a marine reserve. *Ecological Economics*, 33:77–91, 2000.

[90] PISCO. What can science tell us about marine reserves?, March 2011.

[91] H. Possingham, I. Ball, and S. Andelman. *Mathematical Methods for Identifying Representative Reserve Networks*, chapter 17, pages 291–305. Springer-Verlag, New York, 2000.

[92] H. P. Possingham and J. Roughgarden. Spatial population dynamics of a marine organism with a complex life cycle. *Ecology*, 71(3):973–985, 1990.

[93] A. M. Reitzel, B. G. Miner, and L. R. McEdward. Relationships betwen spawning date and larval development time for benthic marine invertebrates: a modeling approach. *Marine Ecology Progress Series*, 280:13–23, 2004.

[94] W. E. Ricker. Stock and recruitment. *Journal of the Fisheries Research Board of Canada*, 11(5):559–623, 1954.

[95] C. M. Roberts, S. Andelman, G. Branch, R. H. Bustamante, J. C. Castilla, J. Dugan, B. S. Halpern, K. D. Lafferty, H. Leslie, J. Lubchenco, D. McArdle, H. P. Possingham, M. Ruckelshaus, and R. R. Warner. Ecological criteria for evaluating candidate sites for marine reserves. *Ecological Applications*, 13(1):S199–S214, 2003.

[96] C. M. Roberts, G. Branch, R. H. Bustamante, J. C. Castilla, J. Dugan, B. S. Halpern, K. D. Lafferty, H. Leslie, J. Lubchenco, D. McArdle, M. Ruckelshaus, and R. R. Warner. Application of ecological criteria in selecting marine reserves and developing reserve networks. *Ecological Applications*, 13(1):S215–S228, 2003.

[97] S. L. Robertson and J. M. Cushing. A bifurcation analysis of stage-structured density dependent integrodifference equations. *Journal of Mathematical Analysis and Applications*, 388:490–499, 2012.

[98] E. Sala, O. Aburto-Oropeza, G. Paredes, I. Parra, J. C. Barrera, and P. K. Dayton. A general model for designing networks of marine reserves. *Science*, 298(5600):1991–1993, 2002.

[99] P. Sale, R. Cowen, B. Danilowicz, G. Jones, J. Kritzer, K. Lindeman, S. Planes, N. Polunin, G. Russ, Y. Sadovy, et al. Critical science gaps impede use of no-take fishery reserves. *Trends in Ecology & Evolution*, 20(2):74–80, 2005.

[100] J. N. Sanchirico and J. E. Wilen. A bioeconomic model of marine reserve creation. *Journal of Environmental Economics and Management*, 42:257–276, 2001.

[101] M. L. Shaffer. Minimum population sizes for species conservation. *BioScience*, pages 131–134, 1981.

[102] A. L. Shanks, B. A. Grantham, and M. H. Carr. Propagule dispersal distance and the size and spacing of marine reserves. *Ecological Applications*, 13(1):S159–S169, 2003.

[103] N. Shigesada, K. Kawasaki, and E. Teramoto. Traveling periodic waves in heterogeneous environments. *Theoretical Population Biology*, 30(1):143–160, 1986.

[104] M. Slatkin. Gene flow and selection in a cline. *Genetics*, 75(4):733–756, 1973.

[105] M. Slatkin. Gene flow and selection in a two-locus system. *Genetics*, 81(4):787–802, 1975.

[106] D. H. Slone. Increasing accuracy of dispersal kernels in grid-based population models. *Ecological Modelling*, 222(3):573–579, 2011.

[107] M. D. Smith, J. Lynham, J. N. Sanchirico, and J. A. Wilson. Political economy of marine reserves: Understanding the role of opportunity costs. *Proceedings of the National Academy of Sciences of the United States of America*, 107:18300–18305, 2010.

[108] W. L. Smith and W. E. Wilkinson. On branching processes in random environments. *The Annals of Mathematical Statistics*, 40(3):814–827, 1969.

[109] E. E. Sotka and S. R. Palumbi. The use of genetic clines to estimate dispersal distances of marine larvae. *Ecology*, 87:1094–1103, 2006.

[110] D. C. Speirs and W. S. C. Gurney. Population persistence in rivers and estuaries. *Ecology*, 82(5):1219–1237, 2001.

[111] S. Thorrold, G. Jones, M. Hellberg, R. Burton, S. Swearer, J. Neigel, S. Morgan, and R. Warner. Quantifying larval retention and connectivity in marine populations with artificial and natural markers. *Bulletin of Marine Science*, 70(Supplement 1):291–308, 2002.

[112] L. W. Traill, B. W. Brook, R. R. Frankham, and C. J. A. Bradshaw. Pragmatic population viability targets in a rapidly changing world. *Biological Conservation*, 143:28–34, 2010.

[113] R. Van Kirk and M. Lewis. Integrodifference models for persistence in fragmented habitats. *Bulletin of Mathematical Biology*, 59(1):107–137, 1997.

[114] H. W. Watson and F. Galton. On the probability of the extinction of families. *The Journal of the Anthropological Institute of Great Britain and Ireland*, 4:138–144, 1875.

[115] J. R. Watson, D. A. Siegel, B. E. Kendall, S. Mitarai, A. Rassweiller, and S. D. Gaines. Identifying critical regions in small-world marine metapopulations. *Proceedings of the National Academy of Sciences of the United States of America*, 108:E907–E913, 2011.

[116] H. Weinberger, K. Kawasaki, and N. Shigesada. Spreading speeds of spatially periodic integro-difference models for populations with nonmonotone recruitment functions. *Journal of Mathematical Biology*, 57:387–411, 2008.

[117] H. F. Weinberger. Long-time behavior of a class of biological models. *SIAM J. Math. Anal.*, 13:353–396, 1982.

[118] W. E. Wilkinson. On calculating extinction probabilities for branching processes in random environments. *Journal of Applied Probability*, 6(3):478–492, 1969.

[119] B. Worm, E. B. Barbier, N. Beaumont, J. E. Duffy, C. Folke, B. S. Halpern, J. B. C. Jackson, H. K. Lotze, F. Micheli, S. R. Palumbi, E. Sala, K. A. Selkoe, J. J. Stachowicz, and R. Watson. Impacts of biodiversity loss on ocean ecosystem services. *Science*, 314(5800):787–790, 2006.

[120] Y. Zhou and M. Kot. Discrete-time growth-dispersal models with shifting species ranges. *Theoretical Ecology*, 4(1):13–25, 2011.

[121] L. Zhunwei and P. Jagers. A note on the asymptotic behaviour of the extinction probability in supercritical population-size-dependent branching processes with independent and identically distributed random environments. *Journal of applied probability*, 41(1):176–186, 2004.